Published for SISSA by Springer

Received: *December 1, 2025*
Accepted: *February 11, 2026*
Published: *April 14, 2026*

Measurement of the top-quark mass using decays with a J/ψ meson at $\sqrt{s}$ =13 TeV with the ATLAS detector

The ATLAS collaboration

Full author list at the end of the paper

E-mail: atlas.publications@cern.ch

Abstract: The top-quark mass is measured using top-quark decays producing an isolated lepton and J/ψ meson reconstructed in its $\mu^+\mu^-$ decay mode. The data sample was recorded with the ATLAS detector in proton-proton collisions at a centre-of-mass energy of $\sqrt{s} = 13$ TeV during Run 2 of the Large Hadron Collider, corresponding to an integrated luminosity of 140 fb^{-1}. The measurement is based on the invariant mass $m(\ell\mu^+\mu^-)$ of the system made of the isolated lepton ℓ from the W boson decay and the non-isolated $\mu^+\mu^-$ pair from a J/ψ decay of a b-hadron, exploiting its sensitivity to the top-quark mass. An unbinned maximum-likelihood fit to the $m(\ell\mu^+\mu^-)$ distribution is performed to extract the top-quark mass. The top-quark mass is measured to be $m_{\text{top}} = 172.17 \pm 0.80\,(\text{stat}) \pm 0.81\,(\text{syst}) \pm 1.07\,(\text{recoil})$ GeV, with a total uncertainty of 1.56 GeV. The third uncertainty arises from changing the dipole parton shower gluon-recoil scheme used in top-quark decays.

Keywords: Hadron-Hadron Scattering, Top Physics

ArXiv ePrint: 2511.23091

https://doi.org/10.1007/JHEP04(2026)099

JHEP04(2026)099

Contents

1 Introduction 1

2 ATLAS detector 2

3 Data and simulated event samples 3

4 Object definition 8

5 Event selection 9

6 Systematic uncertainties 12
- 6.1 Data and Monte Carlo samples 13
- 6.2 Modelling of $t\bar{t}$ and single-top-quark processes 13
- 6.3 Modelling of background processes 16
- 6.4 Modelling of the detector response 17

7 Template method and result 18

8 Conclusion 22

The ATLAS collaboration 33

1 Introduction

The top quark is the heaviest fundamental particle observed so far and precise knowledge of its mass (m_{top}) is crucial to test the consistency of the Standard Model (SM) of particle physics [1–5]. The top-quark mass is a renormalisation-scheme-dependent parameter in perturbative quantum field theory. The precise identification of the m_{top} parameter in Monte Carlo (MC) simulations within a field-theory mass scheme is the subject of theoretical studies [6–11]. Since the discovery of the top quark at the Tevatron [12, 13], the CDF and D0 collaborations have made multiple measurements of m_{top}, culminating in the 2016 combined result [14]. The two general-purpose experiments at the Large Hadron Collider (LHC) [15], ATLAS [16] and CMS [17], produced multiple measurements of m_{top} using data collected in proton-proton (pp) collisions at $\sqrt{s} = 7$ TeV and 8 TeV. The combination of these measurements is $m_{\text{top}} = 172.52 \pm 0.14\,(\text{stat}) \pm 0.30\,(\text{syst})$ GeV, with a total uncertainty of 0.33 GeV [18]. It includes measurements with top-quark pair events that exploit both the semileptonic and hadronic decays of the top quark, and a measurement using events enriched in single-top-quark production via the electroweak t-channel. The uncertainty is dominated by the contribution of the b-jet and light-jet energy scale uncertainties, respectively 0.18 and 0.11 GeV.

Using the large data sample provided by the LHC during Run 2 at $\sqrt{s} = 13$ TeV, the most recent ATLAS top-quark mass measurement was performed in the lepton-plus-jets channel with a high transverse momentum top quark, leading to $m_{\text{top}} = 172.95 \pm 0.27\,(\text{stat}) \pm 0.46\,(\text{syst})$ GeV [19], while the most precise single measurement to date is

JHEP04(2026)099

171.77 ± 0.37 GeV [20] from the CMS Collaboration. With a complementary approach, ATLAS performed a measurement using a partial invariant mass reconstruction of the top-quark decay products where one of the b-quarks hadronises into a b-hadron which decays semileptonically into a muon [21], leading to $m_{\text{top}} = 174.41 \pm 0.39\,(\text{stat}) \pm 0.66\,(\text{syst}) \pm 0.25\,(\text{recoil})$ GeV, where the third uncertainty arises from changing the dipole parton shower gluon-recoil scheme used in top-quark decays.

In this paper, a measurement of m_{top} is presented using a partial reconstruction of top quarks in final states that contain a J/ψ meson from a b-hadron decay. Both top-quark-antiquark pair ($t\bar{t}$) and single-top-quark production are considered to be signal in this study. The decay mode of interest is $t \to (W \to \ell\nu)(b \to J/\psi + X \to \mu^+\mu^- + X)$, the charge conjugation being implicit. This channel has been suggested by the CMS Collaboration in ref. [22] and refined in ref. [23] with a first measurement leading to $m_{\text{top}} = 173.5 \pm 3.0\,(\text{stat}) \pm 0.9\,(\text{syst})$ GeV [24]. The key motivation for using J/ψ events lies in their reduced dependence on jet reconstruction. An unbinned maximum-likelihood fit to an observable sensitive to m_{top} is performed. This method exploits the invariant mass $m(\ell\mu^+\mu^-)$, built from the isolated lepton ℓ (with $\ell = e, \mu$) from the W-boson decay and the $\mu^+\mu^-$ pair from the J/ψ candidate. As this observable consists entirely of leptons, it benefits from improved momentum resolution and a reduction of sensitivity to the systematic uncertainties related to jet energy calibration. However, this method presents some challenges: a small branching ratio of the signal process and sensitivity to the signal process modelling, especially parton shower and hadronisation, b-quark fragmentation, and radiation. Methods with different types of systematic uncertainties are important when combining measurements, and for testing the consistency of the theoretical interpretation of the top-quark mass.

2 ATLAS detector

The ATLAS detector [16] at the LHC covers nearly the entire solid angle around the collision point.[1] It consists of an inner tracking detector surrounded by a thin superconducting solenoid, electromagnetic and hadronic calorimeters, and a muon spectrometer incorporating three large superconducting air-core toroidal magnets. The inner-detector system (ID) is immersed in a 2 T axial magnetic field and provides charged-particle tracking in the range $|\eta| < 2.5$. The high-granularity silicon pixel detector covers the vertex region and typically provides four measurements per track, the first hit generally being in the insertable B-layer (IBL) installed before Run 2 [25, 26]. It is followed by the SemiConductor Tracker (SCT), which usually provides eight measurements per track. These silicon detectors are complemented by the transition radiation tracker (TRT), which enables radially extended track reconstruction up to $|\eta| = 2.0$. The TRT also provides electron identification information based on the fraction of hits (typically 30 in total) above a higher energy-deposit threshold corresponding

[1] ATLAS uses a right-handed coordinate system with its origin at the nominal interaction point (IP) in the centre of the detector and the z-axis along the beam pipe. The x-axis points from the IP to the centre of the LHC ring, and the y-axis points upwards. Polar coordinates (r, ϕ) are used in the transverse plane, ϕ being the azimuthal angle around the z-axis. The pseudorapidity is defined in terms of the polar angle θ as $\eta = -\ln\tan(\theta/2)$ and is equal to the rapidity $y = \frac{1}{2}\ln\left(\frac{E+p_z}{E-p_z}\right)$ in the relativistic limit. Angular distance is measured in units of $\Delta R \equiv \sqrt{(\Delta y)^2 + (\Delta\phi)^2}$.

JHEP04(2026)099

to transition radiation. The calorimeter system covers the pseudorapidity range $|\eta| < 4.9$. Within the region $|\eta| < 3.2$, electromagnetic calorimetry is provided by barrel and endcap high-granularity lead/liquid-argon (LAr) calorimeters, with an additional thin LAr presampler covering $|\eta| < 1.8$ to correct for energy loss in material upstream of the calorimeters. Hadronic calorimetry is provided by the steel/scintillator-tile calorimeter, segmented into three barrel structures within $|\eta| < 1.7$, and two copper/LAr hadronic endcap calorimeters. The solid angle coverage is completed with forward copper/LAr and tungsten/LAr calorimeter modules optimised for electromagnetic and hadronic energy measurements, respectively. The muon spectrometer (MS) comprises separate trigger and high-precision tracking chambers measuring the deflection of muons in a magnetic field generated by the superconducting air-core toroidal magnets. The field integral of the toroids ranges between 2.0 and 6.0 T m across most of the detector. Three layers of precision chambers, each consisting of layers of monitored drift tubes, cover the region $|\eta| < 2.7$, complemented by cathode-strip chambers in the forward region, where the background is highest. The muon trigger system covers the range $|\eta| < 2.4$ with resistive-plate chambers in the barrel, and thin-gap chambers in the endcap regions. The luminosity is measured mainly by the LUCID-2 [27] detector that records Cherenkov light produced in the quartz windows of photomultipliers located close to the beampipe. Events were selected by the first-level trigger system implemented in custom hardware, followed by selections made by algorithms implemented in software in the high-level trigger [28]. The first-level trigger accepted events from the 40 MHz bunch crossings at a rate close to 100 kHz, which the high-level trigger further reduced in order to record complete events to disk at about 1.25 kHz. A software suite [29] is used in data simulation, in the reconstruction and analysis of real and simulated data, in detector operations, and in the trigger and data acquisition systems of the experiment.

3 Data and simulated event samples

The data were recorded with the ATLAS detector during Run 2 of the LHC, which took place from 2015 to 2018, in pp collisions at a centre-of-mass energy of $\sqrt{s} = 13$ TeV, corresponding to an integrated luminosity of 140 fb^{-1}. Only events recorded under stable beam conditions with all detector subsystems operational [30] are used. MC simulated event samples are used in the analysis to model the $t\bar{t}$ and single-top-quark events and most of the other processes, except non-prompt-lepton and fake-lepton backgrounds, which are estimated by using data-driven methods. The MC samples were processed either through a full simulation of the detector response [31] with the GEANT4 toolkit [32], or using the Atlfast2 fast simulation with a parameterised response of the calorimeter. All simulated samples were overlaid with additional pp interactions (pile-up), generated with Pythia 8.186 [33] using the NNPDF2.3lo [34] set of parton distribution functions (PDF) and the A3 set of tuned parameters [35] (tune). The average number of interactions per bunch crossing is reweighted to match that in data. Events were processed using the same reconstruction algorithms as applied to data. An m_{top} value of 172.5 GeV was used in all simulated samples, unless stated otherwise.

The production of $t\bar{t}$ events was simulated using the Powheg Box v2 [36–39] generator, which provides matrix elements (ME) at next-to-leading order (NLO) in quantum chromodynamics (QCD), and the NNPDF3.0nnlo [40] set. The h_{damp} parameter, which effectively regulates the high transverse momentum (p_{T}) radiation against which the $t\bar{t}$ system recoils, was set to $1.5m_{\mathrm{top}}$ [41]. The functional form of the renormalisation (μ_{r}) and factorisation (μ_{f}) scales was set to $\mu_{\mathrm{r}} = \mu_{\mathrm{f}} = \sqrt{(m_{\mathrm{top}}^2 + p_{\mathrm{T},t}^2)}$, where the top-quark transverse momentum $p_{\mathrm{T},t}$ was evaluated before radiation [42]. Parton showering (PS) and hadronisation was modelled with the Pythia 8.230 [43] generator using the A14 tune [44] and the NNPDF2.3lo set. ME corrections that approximate NLO QCD were enabled in Pythia for all emissions, compensating for the leading-order (LO) precision used in Powheg-hvq to simulate the top-quark decay. The $p_{\mathrm{T}}^{\mathrm{hard}}$ parameter in Pythia that affects the matching of the PS to the ME calculation was set to zero. The recoil target for secondary gluon emissions from the b-quark in the $t \to Wb$ vertex, was assigned to the b-quark.[2]

The A14 tune of Pythia 8 is based on the Monash tune [45] of PS and multiple parton interactions (MPI) parameters that leaves the hadronisation parameters at their default values and uses the Lund-Bowler fragmentation model [46]:

$$f(z) = \frac{1}{z^{1+br_b m_b^2}}(1-z)^a \exp(-bm_{\mathrm{T}}^2/z)\,,$$

where a, b and r_b are the function parameters, m_b is the b-quark mass, $m_{\mathrm{T}} = \sqrt{m_B^2 + p_{\mathrm{T},B}^2}$ is the b-hadron transverse mass (m_B and $p_{\mathrm{T},B}$ being the b-hadron mass and transverse momentum, respectively) and z is the fraction of the longitudinal energy of the b-hadron relative to the b-quark, in the light cone reference frame. The values of a and b were fit to data sensitive to light-quark fragmentation such as charged-particle multiplicities, event shapes and scaled momentum distributions. They are assumed to be universal for light- and heavy-quarks, while the r_b parameter is specific to b-quark fragmentation. The A14 tune sets the value of the strong coupling constant in the final-state shower ($\alpha_{\mathrm{s}}^{\mathrm{FSR}}$) to 0.127, whereas the value of 0.1365 is used in Monash. However, both Monash and A14 set $r_b = 0.855$. In ref. [21], a more appropriate r_b value was fitted for a value of $\alpha_{\mathrm{s}}^{\mathrm{FSR}} = 0.127$. The fit used the A14 tune with e^+e^- collision data from LEP/SLD [47–50]. The distribution $x_B = 2p_B \cdot p_Z/m_Z^2$ from semileptonically decaying b-hadrons in $e^+e^- \to Z \to b\bar{b}$ events was used, where p_B and p_Z are the four-momenta of the b-hadron and the Z boson respectively. A value of $r_b = 1.05 \pm 0.02$ was found to be optimal and the central value defines the A14–r_b tune used by default in this analysis. This tune provides good agreement with collision data in a measurement of b-quark fragmentation in top-quark decays [51].

The single-top-quark events are split into three processes: s-channel, t-channel and tW associated production. These samples were simulated using the Powheg Box v2 generator at NLO in QCD using the four-flavour (five-flavour) scheme for the t-channel (s-channel and tW) with the NNPDF3.0nnlo set. For the t-and s-channels, the functional form of μ_{r} and μ_{f} was set to $\sqrt{(m_b^2 + p_{\mathrm{T},b}^2)}$, where $p_{\mathrm{T},b}$ is the b-quark transverse momentum. The interference between the $t\bar{t}$ and the tW final states was handled using the diagram removal scheme [52, 53]. Events were further processed with Pythia 8.230 using the A14–r_b tune and the NNPDF2.3lo set.

The production fractions of weakly decaying b-hadrons observed in Powheg+Pythia MC simulation were rescaled to those from the Heavy Flavour Averaging Group (HFLAV) [54]

[2]This corresponds to the setting *recoil-to-colour=ON* in the TimeShower in Pythia.

Hadron	PDG	Powheg+Pythia 8.2	Scale factor
B^0	0.408 ± 0.006	0.429	0.951
B^+	0.408 ± 0.006	0.429	0.951
B_s^0	0.100 ± 0.008	0.094	1.064
b-baryon	0.084 ± 0.011	0.047	1.787
B_c	0.0030 ± 0.0005	0.0002	14.941

Table 1. The production fraction values for b-hadrons in the PDG and in Powheg+Pythia 8.2. The relative scale factors applied to Powheg+Pythia 8.2 are also shown. The values in the PDG column are derived from ref. [55].

as reported by the Particle Data Group (PDG) [55] with the method described in ref. [56]. The production fractions and corresponding scale factors for Powheg+Pythia simulations are shown in table 1. These scale factors refer only to the first weakly decaying hadron produced in the hadronisation process of b-quarks. The scale factors were applied to each of these hadrons present in a MC simulated event, with the overall event weight given by the product of these scale factors. This procedure assumes that the production fractions of heavy-flavour hadrons can be regarded as universal in the kinematic phase space relevant to this analysis, within the uncertainties accounted for here, as supported by recent results [57–63] that are consistent with universality except for pp collisions with high charged-particle multiplicity at transverse momenta below 6 GeV. The assumption is that production fractions are the same in all experiments and that they sum up to one.

The EvtGen [64] program was used to simulate bottom and charm hadron mixing and decays. The branching ratios ($\mathcal{BR}$) of the decay of b-hadrons into J/ψ were also rescaled to the latest values from the PDG. The total branching ratio of the decay of b-hadrons into J/ψ is $\mathcal{BR}(b \to J/\psi + X) = (1.16 \pm 0.1) \times 10^{-2}$. The J/ψ can be produced directly with a $\mathcal{BR}(b \to J/\psi(\text{direct}) + X) = (7.8 \pm 0.4) \times 10^{-3}$. Indirect production appears through excited mesonic or baryonic states that first deexcite with the emission of a photon and then decay into a J/ψ. The main processes are through the production of a $\psi(2S)$ and a $\chi_{c1}(1P)$ with branching fractions of $(1.76 \pm 0.19) \times 10^{-3}$ and $(4.8 \pm 1.5) \times 10^{-3}$ respectively. The J/ψ can decay into a $\mu^+\mu^-$ pair with a $\mathcal{BR}(J/\psi \to \mu^+\mu^-) = (5.96 \pm 0.03) \times 10^{-2}$. Thus, the branching ratio of the decay of b-hadrons into $J/\psi \to \mu^+\mu^-$ is $\mathcal{BR}(b \to J/\psi(\to \mu^+\mu^-) + X) \sim 6.9 \times 10^{-4}$.

The $t\bar{t}$ and single-top-quark event samples were generated for different assumed values of the top-quark mass, $m_{\text{top}}^{\text{gen}}$, namely 169, 171, 172, 172.25, 172.5, 172.75, 173, 174 and 176 GeV.

Alternative $t\bar{t}$ and single-top-quark samples were simulated to estimate the systematic uncertainties in the signal processes production modelling. Several alternative samples varied just one of the parameters of the MC generators, allowing individual systematic effects to be investigated separately. The ambiguities in matching the ME calculation and the PS are tested with a sample where the $p_{\text{T}}^{\text{hard}}$ parameter was set to 1 [65]. The $t\bar{t}$ production threshold may be sensitive to the modelling of off-shell effects and top-quark decay. To estimate the uncertainty in the modelling of these effects, an alternative sample was used, where the top-quark decay was simulated with the MadSpin generator in the MadGraph framework [66] interfaced to Powheg Box v2. The effect of using a different PS and hadronisation model is evaluated using a $t\bar{t}$ sample produced with Powheg Box v2 interfaced to Herwig 7.1.3 [67, 68] using the H7-UE set of tuned parameters and the MMHT2014lo [69] set of PDFs. For single-top-quark events the t- and tW-channels samples were simulated using Herwig 7.2.1. To evaluate the uncertainty in the modelling of the b-quark fragmentation, two additional samples were produced with the value of the r_b parameter entering the Lund-Bowler parameterisation in the fragmentation function varied by its uncertainty of ± 0.02. Another set of $t\bar{t}$ and single-top-quark samples was produced with the h_{damp} parameter doubled to $3m_{\text{top}}$. To probe uncertainties in final-state QCD radiation (FSR), two sets of $t\bar{t}$ and single-top-quark samples were generated with the scale parameters explicitly[3] varied up and down by factors of $\sqrt{2}$ [70]. For these alternative settings, the appropriate r_b values were determined following the same fit procedure described above in order to still correctly model the x_B distribution for LEP/SLD data [21]. Uncertainties in the modelling of the underlying event in $t\bar{t}$ events are evaluated with two samples using the same algorithms for ME and PS as in the nominal one, but using the Var1 settings [44] from the A14 set of tuned parameters. The parameters varied for Var1 up and down were the α_{s} value in the MPI model and the colour reconnection (CR) 'range' parameter in Pythia, which steers the number of possible reconnections. Three $t\bar{t}$ samples were generated with alternative MPI and CR models and tunes, denoted by CR0, CR1 and CR2 [71]. CR0 denotes a tune that uses the 'MPI-based CR model' and is essentially the same as that used in the nominal sample, with the only difference being a retuning of the colour-reconnection probability. CR1 denotes a tune that uses a 'QCD-based model' while CR2 denotes a tune that uses a 'gluon-move model'. The ambiguity in the choice of the recoil particle for the secondary gluon emission from a b-quark produced in $t \to Wb$ is addressed by generating a sample where the top quark takes part in the recoil (Pythia parameter *recoil-to-top*).

Unless stated otherwise, all cross-section values are stated for pp collisions at $\sqrt{s} = 13$ TeV and for $m_{\text{top}} = 172.5$ GeV. All $t\bar{t}$ samples were normalised to the m_{top}-dependent cross-section prediction obtained from Top++ 2.0 [72] at next-to-next-to-leading order (NNLO) in QCD, including a resummation of next-to-next-to-leading logarithmic (NNLL) soft gluon terms [73–77]. The $t\bar{t}$ cross-section was calculated to be $\sigma(t\bar{t})_{\text{NNLO+NNLL}} = 832 \pm 51$ pb. The predicted cross-sections of single-top-quark and single-top-antiquark production in the t-channel are $\sigma(t, t\text{-chan})_{\text{NNLO}} = 134.2^{+2.6}_{-1.7}$ pb and $\sigma(\bar{t}, t\text{-chan})_{\text{NNLO}} = 80.0^{+1.8}_{-1.4}$ pb, respectively. The cross-sections were calculated with the MCFM program [78] at NNLO in QCD. The quoted uncertainties for the t-channel include the uncertainties due to the choice of the μ_{r} and μ_{f} scales, the uncertainty in the PDFs and in the value of the strong coupling constant α_{s}. The scale uncertainty is determined by varying μ_{r} and μ_{f} independently up and down by a factor of two, whilst never allowing them to differ by a factor greater than two from each other – the so-called independent restricted scale variations. The combined PDF and α_{s} uncertainties are determined at the 68% confidence level according to the Hessian representation of the PDF4LHC21 set [79]. The predicted cross-section of tW production

[3]With explicit scale variations, dedicated alternative MC samples were generated with the $\mu_{\text{r, f}}$ scales modified in the parton shower settings, as opposed to the automated parton shower variations discussed in ref. [70], where weights are applied to the MC sample to obtain the systematic shifts. Explicitly changing $\mu_{\text{r, f}}$ by a factor of $\sqrt{2}$ corresponds approximately to an automated variation of a factor of two, thanks to the implementation of the NLO compensation terms in the latter case.

is $\sigma(t, tW\text{-chan})_{\text{NNLO+NNLL}} = 79.3^{+2.9}_{-2.8}$ pb and was computed at NNLO in QCD with the addition of third-order corrections of soft-gluon emissions by resuming NNLL terms [80] using the PDF4LHC21 set. The quoted uncertainty for the tW channel includes the uncertainty due to the choice of μ_{r} and μ_{f} and the uncertainty in the PDFs. The uncertainty in the scale choice is determined by varying the scales simultaneously up and down by a factor of two. The PDF uncertainties are based on the Hessian method and include the uncertainty in α_{s}. The predicted cross-section of s-channel production is $\sigma(t, s\text{-chan})_{\text{NLO}} = 11.07^{+0.19}_{-0.18}$ pb and was computed at NNLO in QCD [81]. The PDF4LHC21 set was used. The quoted uncertainty for the s-channel includes the uncertainty due to the choice of μ_r and μ_f and the uncertainty in the PDFs. The uncertainty in the scale choice was determined by varying the scales simultaneously up and down by a factor of two. The PDF uncertainties are based on the replicas method.

The production of $t\bar{t}$ in association with one or two vector bosons ($t\bar{t}V$) or with a Higgs boson ($t\bar{t}H$) was simulated using MadGraph5_aMC@NLO (v2.3.3) [82]. The generator provides ME calculation at NLO in α_{s}, with the NNPDF3.0nnlo set. It was interfaced to Pythia 8.210 and used the A14 set of tuned parameters and the NNPDF2.3lo set [83]. Other background processes include production of pairs of vector bosons (diboson, WW, ZZ, WZ) or W and Z bosons in association with jets, as well as specifically W bosons in association with J/ψ. Sherpa v2.2.1 and v2.2.2 were used for diboson processes with two and three leptons in the final state, respectively. Sherpa v2.2.11 [84] was used to model W+jets and Drell-Yan Z/γ^*+jets production. For these processes, Sherpa calculates the ME at NLO for up to two partons and at leading order (LO) for up to five partons using the OpenLoops [85] and Comix [86] ME event generators. They were matched with the Sherpa PS [87] using the MEPSNLO prescription. It employs a dedicated set of tuned parameters developed by the Sherpa authors based on the NNPDF3.0nnlo set. The MadGraph5_aMC@NLO 2.6.5 program was used to generate alternative W/Z + jets samples with up to three additional partons in the final state at NLO accuracy. The showering and subsequent hadronisation were performed using Pythia 8.245 with the A14 tune and the NNPDF2.3lo set with $\alpha_{\text{s}} = 0.13$. The different jet multiplicities were merged using the FxFx NLO matrix-element and parton-shower merging prescription [88]. Pythia 8.245 was used to model the PS, hadronisation and underlying event. These samples are referred to as MGFxFx W/Z+jets samples in the following. Two simulated samples of associated prompt $W + J/\psi$ production are used for this analysis. MadOnia, a heavy quarkonia package [89] that runs on MadGraph 4, was used to generate colour-octet samples of single parton scattering (SPS) associated production. Les Houches Event Files (LHEF) [90] were generated using MG_ME_V4.5.2 with the CTEQ6L1 set of PDFs [91]. The hard scatter LHEF from MadGraph were then interfaced to Pythia 8.186 (using the AU2 tune [92]) for hadronisation and showering. It is possible for the W boson and J/ψ to originate from two different parton interactions in the same pp collision, in a double parton scattering process (DPS). Such a DPS sample was generated, hadronised, and showered with Pythia 8.186 using the AU2 tune and the CTEQ6L1 set. Production of $Z + J/\psi$ is expected to be negligible.

The non-prompt- and fake-lepton background corresponds to events originating from processes that do not involve isolated leptons produced by W, Z or Higgs boson decays. It is estimated by using the data-driven 'matrix-method' [93], where data events passing the full selection with looser identification and isolation requirements on leptons are used along with the measured probability of loose leptons to satisfy the nominal selection requirements.

4 Object definition

The primary vertex is defined as the vertex with the largest $\sum p_{\mathrm{T}}^2$ of the associated tracks among all the vertices with at least two tracks with $p_{\mathrm{T}} > 0.5$ GeV consistent with the beam-collision region in the x-y plane [94].

Electron candidates are reconstructed by matching energy deposits in the electromagnetic calorimeter with a corresponding track in the inner tracking detector [95]. Electrons are required to satisfy the TightLH identification criteria [95] and to lie within $|\eta| < 2.47$, excluding candidates within the calorimeter transition region $1.37 < |\eta| < 1.52$. Muon candidates are reconstructed by combining tracks from the inner detector with matching tracks reconstructed in the muon spectrometer [96]. They are required to have $|\eta| < 2.5$ and to satisfy the Medium requirements [96]. Both lepton flavours are required to have a transverse momentum p_{T} greater than 25 GeV (27 GeV for 2016–2018 data periods) to ensure high efficiency of the single-lepton triggers. Their tracks are matched to the primary vertex, by requiring that the transverse impact parameter divided by its estimated uncertainty be less than five (three) for electron (muon) candidates and the longitudinal impact parameter is required to satisfy $|z_0(\ell)| < 0.5$ mm.

Charged leptons originating from the W boson decay have to satisfy isolation requirements. Isolated electron candidates are required to satisfy the Tight isolation requirement [95] that removes fake and non-prompt electrons from heavy-flavour decays. Isolated muon candidates are required to satisfy the PflowTight_FixedRad isolation selection [96] to reduce background from heavy-flavour decays inside jets.

Soft-muons (referred to as soft-μ) are a special case of muons that are used to select J/ψ in the final state. They are reconstructed similarly to isolated muons but selected with a low transverse momentum threshold $p_{\mathrm{T}} > 3$ GeV. To remove muons not originating from pp collision events, the longitudinal impact parameter is required to satisfy $|z_0(\mu)| < 10$ mm. The soft-μ are required to satisfy the LowPt working point identification criterion [97] optimised to provide good muon reconstruction efficiency down to 3 GeV, while controlling the fake-μ rate. No isolation requirement is applied. Soft-μ are associated with jets whenever the angular separation ΔR is smaller than 0.4

Jet candidates are reconstructed from particle-flow objects [98] using the anti-k_t jet algorithm [99, 100] implemented in the FastJet package [101] with a radius parameter $R = 0.4$. Jets are accepted if they have $p_{\mathrm{T}} > 25$ GeV and $|\eta| < 2.5$. To reduce the contribution from pile-up jets, jets with $p_{\mathrm{T}} < 60$ GeV and $|\eta| < 2.4$ are required to satisfy a criterion of the jet-vertex tagger (JVT) output value, JVT > 0.59. The JVT is a multivariate quantity that combines information from several track-based variables [102]. Further corrections, derived from a calibration based on MC simulations and data [103], are applied to the jet energy leading to corrections of the jet four-momentum. Jets containing b-hadrons are identified ('b-tagged') using the multivariate algorithm DL1r [104], which combines information about the impact parameters of displaced tracks and the topological properties of secondary and tertiary decay vertices reconstructed within the jet. The algorithm is trained on simulated $t\bar{t}$ events to discriminate b-jets from a background consisting of light-flavour jets and c-jets. The working point used has an efficiency of 77% and a corresponding rejection factor of 5 and 200 for c-quark jets and light-quark originated jets.

The missing transverse momentum $\vec{p}_{\mathrm{T}}^{\mathrm{miss}}$ (with magnitude $E_{\mathrm{T}}^{\mathrm{miss}}$), is defined as the negative vector sum of the $\vec{p}_{\mathrm{T}}$ of all selected and calibrated objects in the event, including a term to account for the momenta of soft particles that are not associated with any of the selected objects [105]. This soft term is calculated from ID tracks matched to the primary vertex, which makes it more resilient to contamination from pile-up interactions.

To avoid double-counting, overlapping physics objects are rejected in the following order: electrons sharing a track with a muon; the closest jet within $\Delta R = 0.2$ of an electron; electrons within $\Delta R = 0.4$ of a jet; jets within $\Delta R = 0.4$ of a muon if they have at most two associated tracks; muons within $\Delta R = 0.4$ of a jet. Soft-μ candidates matching ($|\Delta\eta| < 0.001$ and $|\Delta\phi| < 0.001$) isolated muon candidates used to preselect the ttbar events are rejected.

5 Event selection

The event selection targets top-quark events in the final state $\ell\nu bqq'\bar{b}$, where $\ell = e$ or μ and qq' are the quarks from the W decay that is producing jets. At least one b-initiated jet is required, along with a $J/\psi \to \mu^+\mu^-$ decay originating from a b-hadron.

Events are required to have at least one primary vertex and to have satisfied a single-electron or single-muon trigger. Multiple triggers were used to increase the selection efficiency. The lowest-threshold triggers utilised isolation requirements to reduce the trigger rate. These had p_{T} thresholds of 20 GeV for muons and 24 GeV for electrons in 2015 data, and 26 GeV for both lepton types in 2016, 2017 and 2018 data [28, 106, 107]. Events are selected by requiring exactly one isolated lepton candidate matched to the trigger lepton and at least two jets with at least one of them being b-tagged. This loose requirement on jet multiplicity retains signal events even at the expense of a larger background level. Events containing additional isolated leptons with $p_{\mathrm{T}} > 25$ GeV are rejected. This analysis does not require the presence of missing transverse momentum. About 35 million events satisfy this selection.

J/ψ candidates are reconstructed using all pairs of oppositely charged soft-μ that are constrained to originate from a common vertex using ID track parameters. The properties of the J/ψ, such as its invariant mass, transverse momentum, and pseudorapidity are determined from the result of the vertex fit. The J/ψ candidates consist of genuine prompt and non-prompt decays, background decays produced by various combination of fake and real muons, and genuine muon pairs producing an invariant mass in the continuum under the peak. The various components can be separated using the pseudo-proper lifetime τ_0 of the J/ψ candidates defined by $\tau_0 = L_{xy} \times m_{J/\psi}^{\mathrm{PDG}}/p_{\mathrm{T}}^{J/\psi}$, with $L_{xy} = \vec{L} \cdot \vec{p_{\mathrm{T}}}^{J/\psi}/p_{\mathrm{T}}^{J/\psi}$, where $\vec{L}$ is the vector of the distance between the primary vertex and the extrapolated common vertex of the two muon candidates in the transverse plane, $m_{J/\psi}^{\mathrm{PDG}}$ is the mass of the J/ψ from the PDG, and $\vec{p_{\mathrm{T}}}^{J/\psi}$ is the reconstructed transverse momentum vector of the J/ψ candidate. The mass variable $m_{J/\psi}^{\mathrm{PDG}}$ is used instead of the reconstructed value in order to have uncorrelated mass and lifetime information. Prompt J/ψ decays have a pseudo-proper lifetime consistent with zero within resolution.

Further J/ψ selection criteria are applied:

- The invariant mass of the J/ψ candidate lies in the final range of 2.9–3.3 GeV. A total of 19 576 candidates remain in the data.

- The quality of the fit of the two soft-μ to a common vertex has a $\chi^2 < 10$, for the one degree of freedom. A total of 18 133 candidates remain.

- The J/ψ candidate has a transverse momentum $p_{\mathrm{T}} > 8$ GeV and rapidity $|y| < 2.1$. A total of 17 280 candidates remain.

- The angular distance between the two soft-μ is $\Delta R(\mu, \mu) < 0.6$. Both are inside the same jet and their angular distance to this jet is $\Delta R(\text{soft-}\mu, \text{jet}) < 0.4$. A total of 16 821 candidates remain.

- The proper lifetime of the candidates is $\tau_0 > 0.1$ ps. A total of 15 350 candidates remain.

Furthermore, the p_{T} of the system made of the isolated lepton and the J/ψ candidate is $p_{\mathrm{T}}(\ell\mu^+\mu^-) > 25$ GeV and the invariant mass of the system is restricted to $10 < m(\ell\mu^+\mu^-) < 160$ GeV, since the tail of this distribution is more sensitive to $t\bar{t}$ and single-top-quark modelling uncertainties. Finally, a total of 12 165 candidates remain.

Figures 1(a) and 1(b) show the distributions of the invariant mass $m(\mu^+\mu^-)$ of the J/ψ candidates for the selected events in an extended mass window 2–3.6 GeV and in the final range 2.9–3.3 GeV, respectively. Figures 1(c) and 1(d) present the invariant mass $m(\ell\mu^+\mu^-)$ and the transverse momentum $p_{\mathrm{T}}(\ell\mu^+\mu^-)$ of the selected isolated lepton ℓ and the J/ψ system. The prediction reproduces the $m(\mu^+\mu^-)$ distribution in data within the associated uncertainties, in particular the momentum resolution uncertainty of the soft-μ, although some differences between the shapes are observed. These differences have a negligible impact on the analysis. Table 2 shows the number of events in the full Run 2 data sample retained after the final selection. Also shown are the expected numbers of $t\bar{t}$ and single-top-quark events, assuming a top-quark mass of $m_{\mathrm{top}} = 172.5$ GeV, broken down into contributions with and without the $b \to J/\psi \to \mu^+\mu^-$ decay, and other background events, corresponding to the integrated luminosity of the data. The sum of the predicted number of events agrees within uncertainties with the observed number of events in the data.

About 73% of the selected events come from the signal samples, containing a $t\bar{t}$ pair or a single-top-quark with a true $J/\psi \to \mu^+\mu^-$ decay from b-quark fragmentation. Most of these signal events, 90.5% (7%), have the two (only one) soft-μ coming from the decay of a J/ψ produced by a b- or c-hadron that comes from a b-quark produced by a $t \to Wb$ decay. For about 2% of the signal events, one of the soft-μ originates from the prompt W decay, found near a jet, or radiates a near-collinear photon mimicking a jet. For 0.5% of the signal events, one of the soft-μ arises from light-hadron decays or detector background. These events are referred to as 'Fake soft-μ' events in the following. About 13% of all selected events contain a $t\bar{t}$ pair or a single-top-quark without a true $b \to J/\psi \to \mu^+\mu^-$. The random combination of two selected soft-μ produces an exponentially decreasing $m(\mu^+\mu^-)$ distribution. Almost all of these combinatorial background events have the two soft-μ originating from the decay of a b- or c-hadron while in 5% of the cases, one of them is a 'Fake soft-μ'.

JHEP04(2026)099

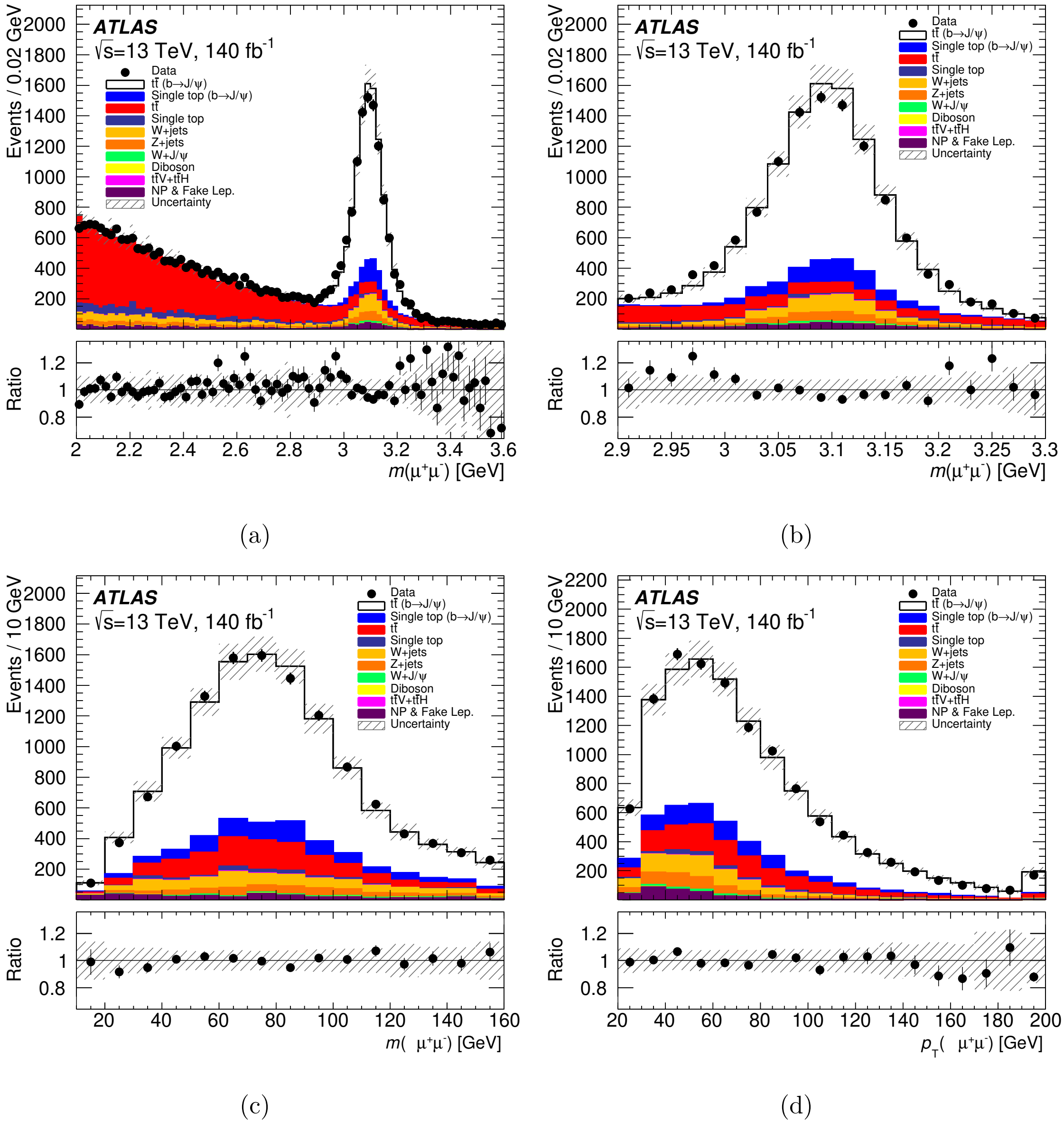

Figure 1. Distributions of the invariant mass $m(\mu^+\mu^-)$ of J/ψ candidates in (a) the 2–3.6 GeV and (b) the 2.9–3.3 GeV mass range, (c) the invariant mass $m(\ell\mu^+\mu^-)$ and (d) the transverse momentum $p_{\mathrm{T}}(\ell\mu^+\mu^-)$ of the system made of the selected isolated lepton and the two muons from the J/ψ candidate. The data is shown compared with the expectation from simulation, broken down into contributions from $t\bar{t}$ and single-top-quark with and without $b \to J/\psi \to \mu^+\mu^-$ decay, $t\bar{t}V + t\bar{t}H$, $W+$jets, $W + J/\psi$, $Z+$jets, dibosons and events with non-prompt and fake leptons (referred to as 'NP & Fake Lep.'). The data is represented as closed circles with statistical uncertainties. The predictions are shown as solid coloured histograms and are normalised to the same integrated luminosity as the data. The shaded area represents the combination of statistical and systematic uncertainties. The lower panels show the ratios of the data to the predictions.

JHEP04(2026)099

Data	12 165
$t\bar{t}$ ($b \to J/\psi \to \mu^+\mu^-$)	7941 ± 737
Single-top-quark ($b \to J/\psi \to \mu^+\mu^-$)	964 ± 109
$t\bar{t}$	1411 ± 145
Single-top-quark	164 ± 43
$t\bar{t}V + t\bar{t}H$	38 ± 8
W+ jets	777 ± 258
Z + jets	468 ± 138
$W + J/\psi$	78 ± 41
diboson	16 ± 9
Non-prompt and fake lepton	322 ± 99
Signal+background	$12\,180 \pm 821$
Expected background fraction	0.27 ± 0.01
Data/(Signal+background)	1.00 ± 0.07

Table 2. Number of selected events in data after the final selection. Also shown are the expected numbers of $t\bar{t}$ and single-top-quark events, assuming a top-quark mass of $m_{\text{top}} = 172.5$ GeV, broken down into contributions with and without the $b \to J/\psi \to \mu^+\mu^-$ decay, and other background events, corresponding to the integrated luminosity of the data. The last two rows show the expected background fraction and the ratio of observed to expected events. The total uncertainty includes both statistical and systematic components, combined in quadrature.

The contribution from other background processes accounts for approximately 14% of the total. These backgrounds produce a peak in the $m(\mu^+\mu^-)$ distribution under the signal peak. It is dominated by the production of W and Z boson in association with jets, for which in about two thirds of the cases a real J/ψ is produced, originating from a b- or a c-jet. Among $W + J/\psi$ selected events, about 70% originate from double parton scattering process (DPS) production. Background events containing non-prompt and fake leptons also lead to a peak around the J/ψ.

About half of the $t\bar{t}$ events have the isolated lepton and the J/ψ belonging to the decay of the same top quark, which is the signature providing the best sensitivity to the top-quark mass. Putting a requirement on the distance between the isolated lepton and the J/ψ could increase the fraction of such good pairings, but at the cost of a significant loss of events leading to an unacceptable increase in the statistical uncertainty.

6 Systematic uncertainties

The systematic uncertainties that affect the measurements of m_{top} are classified into four categories: those arising from the number of events in the data and Monte Carlo samples, from the modelling of $t\bar{t}$ and single-top-quark processes, estimated separately, from the modelling of the physics background processes, and from the effects of the ATLAS detector and reconstruction techniques. For sources that consist of two-sided variations, a symmetric

JHEP04(2026)099

uncertainty is estimated as half of the difference between the up and down variations, assuming that the impact on the measured m_{top} is symmetric around the nominal value. If both variations point in the same direction compared with the central result, the maximum is taken as the resulting uncertainty and the opposite-sign variation is assumed to be of identical size. In cases where the uncertainty is determined from two MC set-ups, e.g. for the evaluation of the uncertainty induced by the choice of signal MC generator, the full observed difference from the nominal result is used as a symmetric uncertainty.

Since the systematic uncertainties are evaluated based on MC samples of limited size, each systematic uncertainty has a corresponding statistical uncertainty, taking into account the statistical correlation of the samples [108]. Using the individual uncertainties $u_i \pm s_i$ the total uncertainty is calculated as $u \pm s$, where $u = \sqrt{\sum_i u_i^2}$ and $s = (1/u) \times \sqrt{\sum_i (u_i^2 \times s_i^2)}$. The statistical precision from a comparison of two samples σ_{12} is determined for each uncertainty source based on the correlation ρ_{12} of the underlying samples, using $\sigma_{12}^2 = \sigma_1^2 + \sigma_2^2 - 2\rho_{12}\sigma_1\sigma_2$. The statistical correlation is expressed as $\rho_{12} = w_{12}/(\sqrt{w_1}\sqrt{w_2})$ with $w_1 = \sum_{i,1} w_i^2$ and $w_2 = \sum_{i,2} w_i^2$ the sum of squared weights in the two samples, and $w_{12} = \sum_{i,12} w_i^2$ the sum of squared weights of events present in both samples.

6.1 Data and Monte Carlo samples

The limited size of the simulated samples as well as the non-prompt and fake-lepton background component impacts the construction of the m_{top}-dependent and independent templates. The corresponding uncertainty is estimated by using a bootstrap method [109]. The method calibration uncertainty is determined by repeating the mass extraction on MC samples generated with different values of $m_{\text{top}}^{\text{gen}}$ mass and estimating the residual bias of the measurement. A constant is fitted and its statistical uncertainty is assigned as the uncertainty. The uncertainty in the integrated luminosity is 0.83% [110] and is applied to all processes other than the non-prompt- and fake-lepton background. The reweighting of the simulation to match the pile-up distribution in data involves rescaling the average number of interactions per bunch crossing to achieve improved agreement between data and simulation for the observed number of primary vertices. The uncertainty in determining this rescaling is propagated to the reweighting factors to estimate the uncertainty due to pile-up.

6.2 Modelling of $t\bar{t}$ and single-top-quark processes

Uncertainties in $t\bar{t}$ and single-top-quark process modelling include sources that affect the kinematics of the lepton from the W boson decay, as well as the kinematics and fraction of events of different flavour of the b-hadron giving rise to the $J/\psi \to \mu^+\mu^-$. Uncertainties are assessed by either reweighting the nominal samples or by using the alternative simulation samples described in section 3. The full observed difference between the m_{top} measurements is quoted as the systematic uncertainty, unless where mentioned explicitly.

The impact on the measurement from the uncertainties in the $t\bar{t}$ and single-top-quark inclusive cross-sections is negligible, as the fit is performed using only the shape of the distributions and does not depend on yield variations arising from the assumed top-quark mass. The uncertainty related to the matching of the NLO calculation is evaluated using the $t\bar{t}$ and single-top-quark samples with the alternative $p_{\text{T}}^{\text{hard}}$ setting. An uncertainty is considered to account for the effect of $t\bar{t}$ NNLO corrections, which are known to be not fully covered by the scale uncertainties of the $t\bar{t}$ NLO+PS prediction [111, 112]. An iterative reweighting procedure is implemented to simulate NNLO+NLL QCD effects in the parton level p_{T}^{t}, $p_{\mathrm{T}}^{t\bar{t}}$ and $m_{t\bar{t}}$ distributions. The full observed difference using the nominal $t\bar{t}$ sample with and without this reweighting is quoted as the systematic uncertainty. The top-quark decay lineshape uncertainty accounts for the ambiguity in the models of the on-shell effects in production and compares the two existing implementations of the smearing and off-shell corrections: POWHEG and MADSPIN. The uncertainty in the interference between $t\bar{t}$ and tW production at NLO is assessed by comparing the default 'diagram removal' scheme with an alternative 'diagram subtraction' scheme [113]. The full observed difference is quoted as the systematic uncertainty. Uncertainties in the PS and hadronisation model are assessed by comparing the m_{top} values obtained from the sample generated with POWHEG+HERWIG 7.1.3 with the nominal $t\bar{t}$ sample and POWHEG+HERWIG 7.2.1 for the t- and tW-channels.

Uncertainties in the b-hadron production and decay branching fractions of the inclusive decays of b-hadrons into $J/\psi \to \mu^+\mu^-$ are derived from the uncertainties in the rescaling procedure described in section 3 and come entirely from the PDG values. These uncertainties are propagated through the analysis, taking into account the correlation coefficients between production fractions [55]: cor(B_s^0, b-baryon) = 0.064, cor(B_s^0, $B^\pm$=B^0) = −0.633 and cor(b-baryon, $B^\pm$=B^0) = −0.813. Initial- and final-state QCD radiation (ISR/FSR) lead to a higher jet multiplicity and different jet energies than the hard process, which affects the distributions of the observables used in this measurement. Several systematic variations are made to cover uncertainties in the amount of ISR radiation. One uncertainty component is obtained using alternative event weights in the nominal sample to mimic variations in the μ_{r} and μ_{f} scales in the matrix elements, varied by factors of 0.5 and 2.0, independently. For another component, additional sets of weights are used to reproduce the Var3c up/down variants of the A14 tune, altering the $\alpha_{\mathrm{s}}^{\mathrm{ISR}}$ scale [114]. Another uncertainty component is derived from the $t\bar{t}$ sample with the alternative value for the h_{damp} parameter. The effect of FSR is evaluated using alternative simulated $t\bar{t}$ samples generated with the scale parameters explicitly varied. The uncertainty from the underlying event is assessed by using the two samples generated with the Var1 eigentune variation. Uncertainties in the CR model are assessed by comparing the two alternative CR model samples (CR1 and CR2) with the CR0 sample. The largest difference relative to CR0 comes from the CR2 model and is taken as a symmetric uncertainty. The uncertainty originating from the PDFs is evaluated using the 30 eigenvectors of the PDF4LHC15 set [115].

Uncertainties in the modelling of the b-quark fragmentation are evaluated using samples generated with different r_b values, by comparing the m_{top} values obtained from the up (r_b = 1.07) and down (r_b = 1.03) variations for the A14–r_b tune described in section 3. To ensure that the estimate based on the r_b values adequately accounts for the modelling uncertainties in the b-quark fragmentation, two cross-checks are performed using different theoretical predictions of the fragmentation function. The first one concerns the variable x_B that is sensitive to the fraction of the b-quark energy taken by the b-hadron in the top-quark rest frame, when considering the top-quark decay $t \to Wb$:

$$x_B = \frac{1}{1 - m_W^2/m_{\mathrm{top}}^2 + m_b^2/m_{\mathrm{top}}^2} \frac{2p_B \cdot p_{\mathrm{top}}}{m_{\mathrm{top}}^2},$$

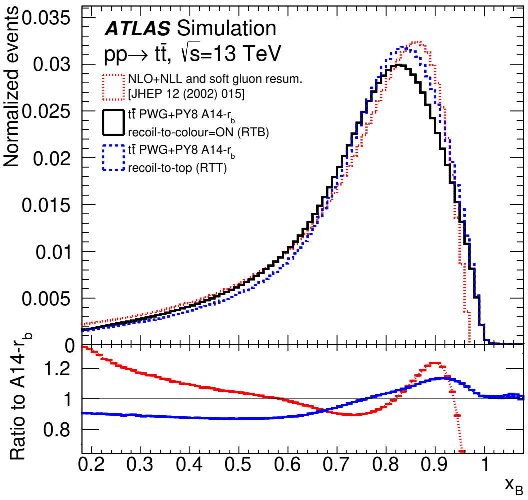

Figure 2. Distribution of x_B, the fraction of energy taken by the b-hadron in the top-quark rest frame, as obtained from theoretical prediction at NLO+NLL [116, 118], accounting for soft-gluon resummation with the hadronisation according to the Kartvelishvili model [119], and obtained at particle level using $t\bar{t}$ samples. The POWHEG+PYTHIA 8 A14–r_b MC samples are based on different recoil schemes using either the b-quark ('recoil-to-colour=ON') or the top quark ('recoil-to-top') as the recoil particle. The lower panel shows the ratios of the theoretical and 'recoil-to-top' predictions to the 'recoil-to-colour=ON' one.

where m_W and m_b are respectively the W-boson and the b-quark masses and p_B and p_{top} are the b-hadron and the top-quark four momenta [116, 117]. Figure 2 shows the x_B spectrum predicted at NLO+NLL [116, 118], accounting for soft-gluon resummation in top-quark decays, with the hadronisation according to the Kartvelishvili model [119]. This spectrum is compared with the one obtained at particle level in the $t\bar{t}$ PYTHIA 8 sample, controlled by the parameters of the fragmentation function and α_s^{FSR}, which are set in the A14–r_b tune. The observed differences between the shapes are used to define scale factors applied on $t\bar{t}$ events, which translate into variations of the observed $m(\ell\mu^+\mu^-)$ distribution. The second cross-check concerns the prediction of fragmentation functions at NNLO order accuracy, including NNLL soft gluon resummation of B-hadrons and J/ψ [120]. The differences in shape between the differential distributions of $m(\ell J/\psi)$ predicted at NLO and NNLO are used to define scale factors applied to the $t\bar{t}$ events, which translate into a variation of the observed $m(\ell\mu^+\mu^-)$ distribution. In both cases, the variations in measured m_{top} values are comparable in size to the uncertainty assigned to the b-quark fragmentation modelling. These variations are not included as dedicated systematic uncertainties in the final result.

In the simulation of the dipole QCD radiation scheme, there is an ambiguity in the choice of the recoil particle for the modelling of the second and subsequent gluon emission from quarks produced by coloured resonance decays, such as the b-quark in a $t \to Wb$ process. Practically this determines how the momentum is re-arranged between the W boson and the b-quark, but it has no impact, for example, on $Z \to b\bar{b}$ decays [121]. The default gluon recoil scheme in the nominal $t\bar{t}$ samples uses the b-quark as the recoil particle using the

JHEP04(2026)099

PYTHIA 8 parameter *recoil-to-colour=ON*, referred to as RTB. The uncertainty due to the ambiguity in the choice of recoil scheme is assessed by comparing with an alternative $t\bar{t}$ sample produced where the top quark is the recoil particle, using the PYTHIA 8 parameter *recoil-to-top*, referred to as RTT. A fully self-consistent variation of the recoil scheme would require a dedicated tuning of PYTHIA 8 parameters. This necessitates measurements in top-quark events with sufficient sensitivity to this aspect of the modelling that could be fed into existing measurements able to constrain α_s and b-quark fragmentation. Despite previous measurements showing sensitivity to the recoil scheme [19, 21], and indicating a preference of data for the recoil scheme used in the nominal simulation of this analysis [19], no such dedicated measurements yet exist. The full observed difference in m_{top} measurements between the RTB and RTT recoil schemes is 1.07 ± 0.22 GeV. The RTT set-up mildly changes the W-boson p_{T} and the angle between the W boson and the b-hadron resulting from the top-quark decay, but it hardens the b-hadron momentum and, as a consequence, modifies the distribution of x_B, as shown in figure 2. As in ref. [21], a reweighting procedure is tested in order to force the x_B spectrum derived with the RTT scheme to be the same as that for the RTB one. This would reduce the recoil systematic uncertainty down to 0.10 GeV with a statistical uncertainty in this uncertainty of 0.21 GeV. A fully consistent comparison of the fragmentation description in parton shower simulations with the available theoretical predictions at NLO+NLL [116, 118] and NNLO [120] is beyond the scope of the present paper. The full observed difference in m_{top} measurements between the RTB and RTT recoil schemes is therefore conservatively included in the final result, separately from other systematic modelling uncertainties.

6.3 Modelling of background processes

Several sources of uncertainties are considered for the normalisation and shape of background contributions. As seen in section 5, about 13% of the selected events originate from $t\bar{t}$ or single-top-quark events without a true $b \to J/\psi \to \mu^+\mu^-$ leading to a combinatorial background under the peak of the J/ψ. The normalisation and shape of the $m(\mu^+\mu^-)$ distributions of these contributions are checked with other selections where this component is enhanced, in particular by selecting events with three or four jets, at least one of them being b-tagged. In the $m(\mu^+\mu^-)$ sideband region [2–2.9] GeV where this background is dominant, the normalisation and shape of the $m(\ell\mu^+\mu^-)$ distribution is also checked. In all cases, the data is well reproduced by expectations, and the impact of this effect is found to be negligible. The fraction of the soft-μ component of $t\bar{t}$ events that arises from 'Fake soft-μ', as defined in section 5, is small, 4% in the sideband and only 0.5% in the signal region. A conservative uncertainty of 25% in the normalisation of this component is taken as a systematic uncertainty, supported by the comparison between data and prediction in the sidebands of the invariant mass distributions.

Processes like $t\bar{t}V$ and $t\bar{t}H$ represent only a small contribution to the oberved number of events and are included in the background component. The cross-sections of the $t\bar{t}V$ and $t\bar{t}H$ processes are known with a precision around 13% [122]. Still, some processes show discrepancies between data and MC in previous measurements [123, 124]. The inclusive cross-sections for diboson production are calculated using MCFM [125] and are known to a precision of better than 10% [126]. For all these processes, more conservative uncertainties of 50% are applied to also cover shape uncertainties and observed differences found in previous analyses [126]. Uncertainties related to the $W/Z+$jets processes are determined using two methods. The uncertainties related to the default SHERPA samples are determined by varying independently the μ_r and μ_f scales by factors of 0.5 and 2 as well as considering PDF and α_s variations [127]. The alternative MGFxFx generator to simulate W/Z+jet processes, described in section 3, which provides a different treatment of multi-jets multiplicity from the nominal samples, leads to generator-choice-induced differences in the normalisations and shapes of the distributions $m(\mu^+\mu^-)$ and $m(\ell\mu^+\mu^-)$, which in turn give rise to systematic uncertainties. The uncertainties obtained from the two methods are summed in quadrature to obtain the full uncertainty for the W/Z+jets background. For prompt $W + J/\psi$ production, a 50% normalisation uncertainty is used. The normalisation and shape of the $m(\mu^+\mu^-)$ distributions of the peaking backgrounds are checked in two validation regions, designed to enrich these components: a region with exactly one reconstructed jet to validate the $W+$jets and $W + J/\psi$ production; and one with exactly two jets and two isolated leptons to validate $Z+$jets production. It is verified that the uncertainty arising from differences observed between data and MC simulation in these validation regions is negligible.

For the data-driven estimate of the non-prompt and fake lepton background, a 30% systematic uncertainty in the predicted yields is assigned, uncorrelated between e+jets and μ+jets events. This uncertainty is supported by comparison of distributions at low E_T^{miss} values, enriched in non-prompt and fake lepton background events.

6.4 Modelling of the detector response

Uncertainties for isolated leptons arise from the efficiency of their reconstruction, identification and isolation requirements, all derived from studies using Z and J/ψ decays [95, 96]. A similar procedure is used to estimate the trigger efficiencies [106, 107]. The lepton energy/momentum scales and resolutions are obtained from Z and J/ψ decays [128, 129]. The uncertainties associated with the soft-μ are related in particular to the muon momentum scale, resolution and identification efficiencies at low p_T. Although the observable $m(\ell\mu^+\mu^-)$ does not involve jets, the various jet uncertainties impact the analysis through the event selection. Uncertainties in the jet energy scale (JES) are evaluated using 29 independent variations in the jet energies that parametrise the uncertainties in the JES of $R = 0.4$ particle-flow jets [103]. The JES comprises statistical subcomponents from in situ calibrations, detector related subcomponents such as energy scales and resolutions of electromagnetic objects and modelling subcomponents for γ+jets and $Z+$jets calibrations. The magnitude of the jet energy resolution (JER) uncertainty is parameterised in jet p_T and η [103], and the uncertainty is propagated by smearing the jet p_T in the simulation. The uncertainty in the efficiency to satisfy the JVT requirement is evaluated by varying the scale factors within their uncertainties [102]. The b-tagging efficiencies and mistag rates are measured in data, and scale factors are derived to correct the predicted tagging rates. Corresponding uncertainties are taken into account by varying these scale factors, which depend on jet p_T, η, and on the hadronic content of the jet. They include the uncertainties in the b-tagging [130] and mistagging scale factors [131, 132] with nine, four and five eigenvector variations for b, c/τ-lepton and light jets, respectively.

The uncertainty in m_{top} is derived by varying the scale factors within their uncertainties and adding the resulting fitted differences in quadrature. As $E_{\text{T}}^{\text{miss}}$ is not explicitly used in the selection, no uncertainty is assigned to it.

7 Template method and result

The analysis method employed in this paper is a template fit. Templates are simulated distributions of the invariant mass $m(\ell\mu^+\mu^-)$ of the system made of the selected isolated lepton ℓ and the two soft-μ associated with the J/ψ candidate. The templates are built from MC samples representing different m_{top} values, with added non-prompt and fake-lepton events. The templates are split into two components separating the contributions with a significant m_{top} dependence from contributions that do not depend on m_{top}.

The m_{top}-dependent templates are constructed from $t\bar{t}$ and single-top-quark MC samples produced for nine $m_{\text{top}}^{\text{gen}}$ values: 169, 171, 172, 172.25, 172.50, 172.75, 173, 174 and 176 GeV. This procedure is adopted, firstly, because $t\bar{t}$ and single-top-quark production without $b \to J/\psi \to \mu^+\mu^-$ decay, although formally a background process, still carries information about the top-quark mass and, secondly, by doing so an m_{top}-independent background template can be used. A parameterisation of these distributions is performed using the sum of a Gaussian and a LogNormal function, the latter having the form:

$$f(x|m_0,k) = \frac{1}{\sqrt{2\pi} \cdot \ln(k) \cdot x} \exp\left(\frac{-\ln^2(x/m_0)}{2\ln^2(k)}\right),$$

where m_0 is the median and $k = \exp(\sigma)$ with σ a shape parameter. The parameterisation is chosen to represent the Gaussian part of the distribution, coming mostly from $t\bar{t}$ and single-top-quark events where the J/ψ and the prompt lepton come from the same top quark, and a contribution with a larger tail coming from the cases where the J/ψ and the isolated lepton do not come from the same top quark or the J/ψ candidate does not come from a b-quark produced by a $t \to Wb$ decay. This approach assumes that each fit parameter has a linear dependence on the top-quark mass, which has been verified. The m_{top}-dependent templates are shown in figure 3(a) for three different $m_{\text{top}}^{\text{gen}}$ values: 169, 172.5 and 176 GeV. The m_{top}-independent template is constructed from the $t\bar{t}V$ and $t\bar{t}H$ processes (neglecting their m_{top} dependence due to their small contributions), from the $W+$jets, $W+J/\psi$, $Z+$jets and dibosons processes, and from events with non-prompt and fake leptons. A Chebyshev polynomial function [133] is fitted to this m_{top}-independent template as shown in figure 3(b). These functions are shown to provide an adequate parameterisation for the m_{top}-dependent and m_{top}-independent templates. Other choices for the templates fit functions give compatible results.

The templates are normalised to unity to build m_{top}-dependent and m_{top}-independent probability density functions, respectively $P^{m_{\text{top}}\text{-dep.}}$ and $P^{m_{\text{top}}\text{-indep.}}$. They are summed in an unbinned likelihood that is maximised to give the value of m_{top} that best describes the data:

$$\mathcal{L}(m_{\text{top}}) = \prod_{i=1}^{N} f_{m_{\text{top}}\text{-dep.}} P^{m_{\text{top}}\text{-dep.}}(m^i(\ell\mu^+\mu^-)|m_{\text{top}}) + (1 - f_{m_{\text{top}}\text{-dep.}}) P^{m_{\text{top}}\text{-indep.}}(m^i(\ell\mu^+\mu^-)),$$

where N is the number of events and $f_{m_{\text{top}}\text{-dep.}}$ is the fraction of events from the m_{top}-dependent component.

JHEP04(2026)099

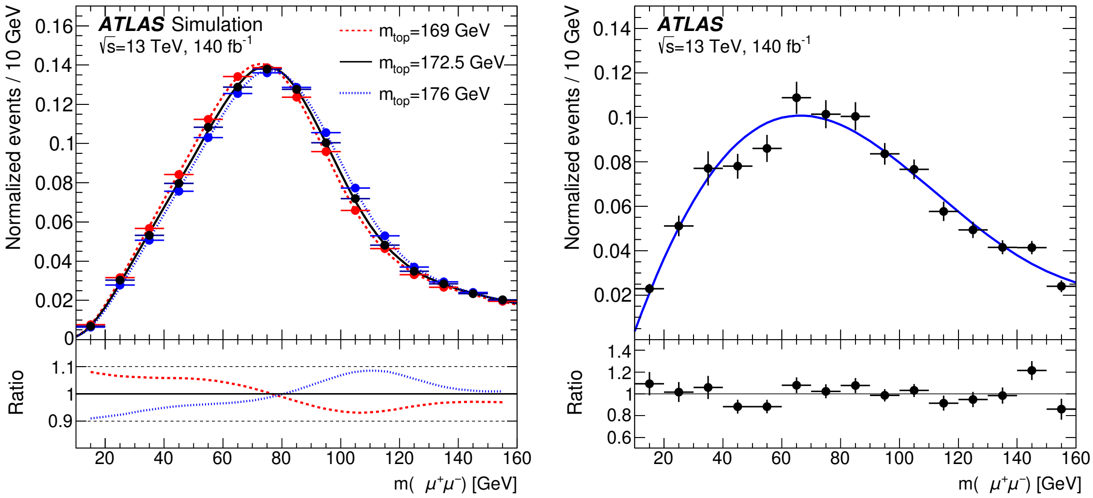

(a) (b)

Figure 3. Template fit functions for (a) the m_{top}-dependent sample shown for $m_{\text{top}}^{\text{gen}}$ values of 169, 172.5 and 176 GeV and (b) the m_{top}-independent samples compared with the histograms used in the parameterisation. The lower panel of the m_{top}-dependent template plot shows the ratios of the fit functions obtained with other $m_{\text{top}}^{\text{gen}}$ values to the one obtained with $m_{\text{top}}^{\text{gen}} = 172.5$ GeV. The lower panel of the m_{top}-independent template plot shows the ratios of the histogram to the fit function.

Figure 4(a) shows the calibration curve, i.e. the reconstructed m_{top} as a function of the generated one $m_{\text{top}}^{\text{gen}}$. A linear function is fitted to all mass points and gives the following parameters: $m_{\text{top}} = (172.56 \pm 0.10) + (0.98 \pm 0.06) \times (m_{\text{top}}^{\text{gen}} - 172.5)$. The determination of m_{top} from these fits is found to be linear and unbiased relative to the input top-quark mass hypothesis by means of pseudo experiments [109]. No evidence for a significant bias or non-closure has been found and the method calibration uncertainty, described in section 6, is assigned to cover for any bias below the sensitivity of the tests performed.

The value of m_{top} obtained from the fit to data and the corresponding statistical and systematic uncertainties are:

$$m_{\text{top}} = 172.17 \pm 0.80\,(\text{stat}) \pm 0.81\,(\text{syst}) \pm 1.07\,(\text{recoil})\ \text{GeV}\,,$$

with a total uncertainty of 1.56 GeV. The third uncertainty arises from changing the dipole parton shower gluon-recoil scheme used in top-quark decays. The data distribution is shown in figure 4(b) where it is compared with the predicted distribution and the uncertainty band corresponding to the total uncertainty reported above. The uncertainty band is constructed by varying the template fit function within the statistical and systematic uncertainties. The individual uncertainties and their sum in quadrature are given in table 3. Uncertainties related to $t\bar{t}$ and single-top-quark processes are shown separately and are considered uncorrelated to obtain the total uncertainty. The statistical and systematic uncertainties, excluding recoil, are at the same level. Apart from the dominant recoil uncertainty, the main sources of systematic uncertainties are due to the parton shower and hadronisation modelling, final-state radiation modelling, b-quark fragmentation and also large uncertainties from background

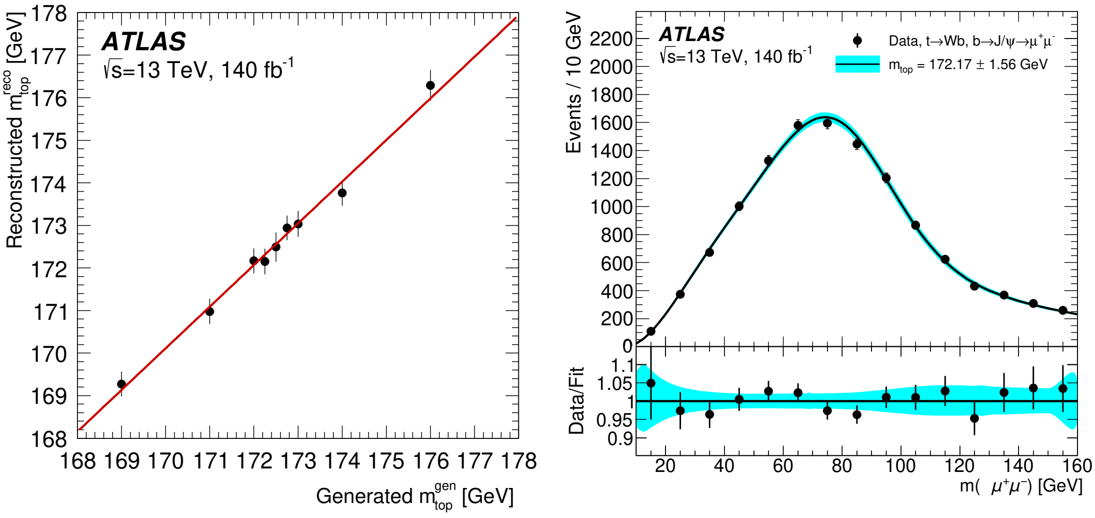

(a) (b)

Figure 4. (a) Calibration curve obtained showing the reconstructed m_{top} as a function of the generated one $m_{\mathrm{top}}^{\mathrm{gen}}$. The fitted values are represented as closed circles with statistical uncertainties. A linear function is fitted to the mass points. (b) The $m(\ell\mu^+\mu^-)$ distribution in data compared with the predicted distribution. The shaded uncertainty band is constructed by varying the template fit function within the statistical and systematic uncertainties of the measurement. The lower panel shows the ratio of data to the template fit function.

modelling in particular from the $W+$jets modelling. The detector uncertainties are on the contrary much smaller; in particular the uncertainty due to the calibration of the jet energies is below 100 MeV.

A comparison of this result with other m_{top} measurements is shown in figure 5. This new measurement is found to be in good agreement with previous ATLAS measurements, the ATLAS+CMS Run 1 combination [18] and the CMS measurement using the same final state [24]. Precisely quantifying the level of agreement between the results displayed in figure 5 requires a detailed estimate of the correlation between each pair of measurements, which is beyond the scope of this paper.

JHEP04(2026)099

Source of uncertainty	Unc. in m_{top} [GeV]	Stat. precision [GeV]
Data and Monte Carlo samples		
Statistical error in data	0.80	
Statistical error in signal and background model	0.27	±0.06
Method	0.06	±0.10
Luminosity	0.01	$< \pm0.005$
Pile-up	0.11	±0.02
Modelling of $t\bar{t}$ process		
Matrix element matching	0.14	±0.20
NNLO reweighting	0.01	±0.02
Top-quark decay lineshape	0.07	±0.02
Parton shower and hadronisation	0.40	±0.19
b-hadron production fractions	0.04	±0.02
b-hadron decay BR	0.08	±0.02
Initial-state QCD radiation	0.10	±0.07
Final-state QCD radiation	0.21	±0.05
Underlying event	0.20	±0.12
Colour reconnection	0.04	±0.28
Parton distribution function	0.03	$< \pm0.005$
b-quark fragmentation r_b	0.15	±0.04
Modelling of single-top-quark process		
Matrix element matching	0.02	±0.11
$t\bar{t}$–tW interference	0.15	±0.07
Parton shower and hadronisation	0.09	±0.11
b-hadron production fractions	0.09	±0.07
b-hadron decay BR	0.02	$< \pm0.005$
Initial-state QCD radiation	0.05	±0.04
Final-state QCD radiation	0.06	±0.04
Parton distribution function	0.01	$< \pm0.005$
b-quark fragmentation r_b	0.05	±0.07
Modelling of background processes		
$t\bar{t}V + t\bar{t}H$, diboson	0.02	±0.01
$W/Z+$jets	0.40	±0.12
$W + J/\psi$	0.04	$< \pm0.005$
Non-prompt and fake lepton	0.15	±0.01
Fake soft-μ	0.01	$< \pm0.005$
Detector response		
Isolated leptons	0.08	±0.01
Soft-μ	0.12	±0.01
Light jet energy scale	0.07	±0.01
b-jet energy scale	0.04	±0.01
Jet energy resolution	0.02	±0.01
Flavour tagging	0.02	$< \pm0.005$
Total systematic uncertainty (excluding recoil)	0.81	±0.15
Total stat. and syst. uncertainty (excluding recoil)	1.14	±0.15
Recoil uncertainty	1.07	±0.22
Total uncertainty	1.56	±0.18

Table 3. Impact of sources of uncertainty in m_{top}. Each row of the table corresponds to a group of individual systematic variations. Uncertainties related to $t\bar{t}$ and single-top-quark processes are shown separately and are considered uncorrelated. For each systematic uncertainty listed, the first value corresponds to the uncertainty in m_{top}, and the second to the statistical precision of this uncertainty. The total systematic uncertainty and the corresponding statistical precision are calculated as discussed in section 6. The total uncertainty is the sum in quadrature of the statistical and systematic uncertainties.

JHEP04(2026)099

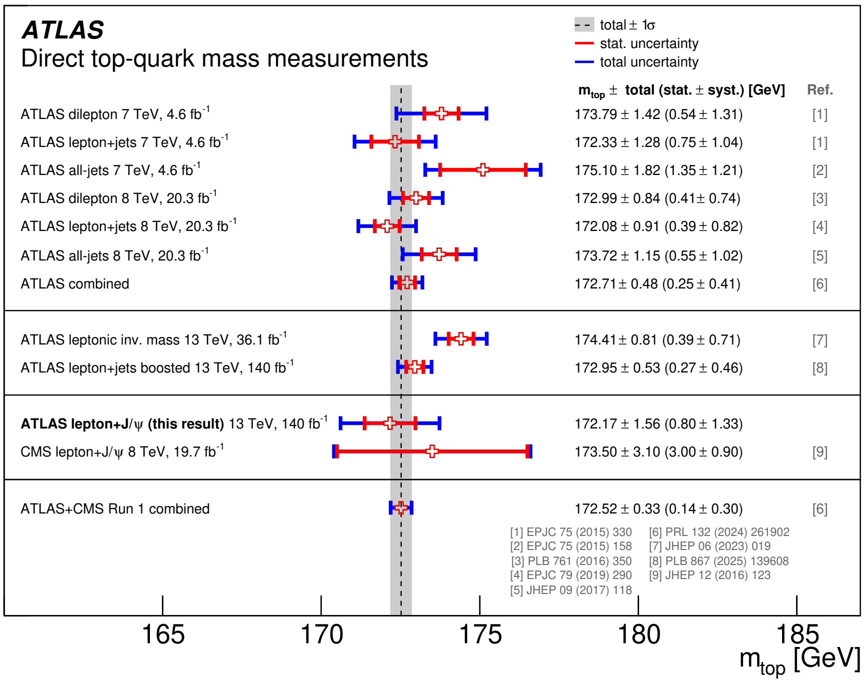

Figure 5. This measurement of the top-quark mass m_{top} compared with earlier ATLAS measurements, in particular at 13 TeV [19, 21], the ATLAS and CMS Run 1 combination [18], and a CMS measurement in the same lepton+J/ψ channel [24]. The dashed line and shaded band represent the central value and uncertainty of the ATLAS+CMS Run 1 combination.

8 Conclusion

The top-quark mass is measured in top-quark events with a b-quark decaying into $J/\psi + X \to \mu^+\mu^- + X$. The analysis uses 140 fb^{-1} of proton-proton collision data recorded during Run 2 of the LHC at a centre-of-mass of $\sqrt{s} = 13$ TeV with the ATLAS detector. The measurement is based on the invariant mass $m(\ell\mu^+\mu^-)$ of the system constructed from the isolated lepton ℓ from the W-boson decay and the non-isolated $\mu^+\mu^-$ pair from a J/ψ decay of a b-hadron. An unbinned maximum-likelihood fit to the $m(\ell\mu^+\mu^-)$ distribution is performed to determine the most probable top-quark mass value. The top-quark mass is measured to be $m_{\text{top}} = 172.17 \pm 0.80\,(\text{stat}) \pm 0.81\,(\text{syst}) \pm 1.07\,(\text{recoil})$ GeV, with a total uncertainty of 1.56 GeV. The third uncertainty arises from changing the dipole parton shower gluon-recoil scheme used in top-quark decays. The main sources of systematic uncertainties are due to the recoil, parton-shower and hadronisation, b-quark fragmentation, final-state radiation modelling with uncertainties from background modelling and soft-μ reconstruction also being significant. The uncertainty due to the calibration of the jet energies is smaller and is below 100 MeV, which is advantageous for future combinations of this result with those from the other reconstructions of the top-quark decay products. The measurement has a large statistical uncertainty, which indicates that future measurements with larger LHC data samples could reach an improved precision.

JHEP04(2026)099

Acknowledgments

We thank CERN for the very successful operation of the LHC and its injectors, as well as the support staff at CERN and at our institutions worldwide without whom ATLAS could not be operated efficiently.

The crucial computing support from all WLCG partners is acknowledged gratefully, in particular from CERN, the ATLAS Tier-1 facilities at TRIUMF/SFU (Canada), NDGF (Denmark, Norway, Sweden), CC-IN2P3 (France), KIT/GridKA (Germany), INFN-CNAF (Italy), NL-T1 (Netherlands), PIC (Spain), RAL (U.K.) and BNL (U.S.A.), the Tier-2 facilities worldwide and large non-WLCG resource providers. Major contributors of computing resources are listed in ref. [134].

We gratefully acknowledge the support of ANPCyT, Argentina; YerPhI, Armenia; ARC, Australia; BMWFW and FWF, Austria; ANAS, Azerbaijan; CNPq and FAPESP, Brazil; NSERC, NRC and CFI, Canada; CERN; ANID, Chile; CAS, MOST and NSFC, China; Minciencias, Colombia; MEYS CR, Czech Republic; DNRF and DNSRC, Denmark; IN2P3-CNRS and CEA-DRF/IRFU, France; SRNSFG, Georgia; BMFTR, HGF and MPG, Germany; GSRI, Greece; RGC and Hong Kong SAR, China; ICHEP and Academy of Sciences and Humanities, Israel; INFN, Italy; MEXT and JSPS, Japan; CNRST, Morocco; NWO, Netherlands; RCN, Norway; MNiSW, Poland; FCT, Portugal; MNE/IFA, Romania; MSTDI, Serbia; MSSR, Slovakia; ARIS and MVZI, Slovenia; DSI/NRF, South Africa; MICIU/AEI, Spain; SRC and Wallenberg Foundation, Sweden; SERI, SNSF and Cantons of Bern and Geneva, Switzerland; NSTC, Taipei; TENMAK, Türkiye; STFC/UKRI, United Kingdom; DOE and NSF, United States of America.

Individual groups and members have received support from BCKDF, CANARIE, CRC and DRAC, Canada; CERN-CZ, FORTE and PRIMUS, Czech Republic; COST, ERC, ERDF, Horizon 2020, ICSC-NextGenerationEU and Marie Skłodowska-Curie Actions, European Union; Investissements d'Avenir Labex, Investissements d'Avenir Idex and ANR, France; DFG and AvH Foundation, Germany; Herakleitos, Thales and Aristeia programmes co-financed by EU-ESF and the Greek NSRF, Greece; BSF-NSF and MINERVA, Israel; NCN and NAWA, Poland; La Caixa Banking Foundation, CERCA Programme Generalitat de Catalunya and PROMETEO and GenT Programmes Generalitat Valenciana, Spain; Göran Gustafssons Stiftelse, Sweden; The Royal Society and Leverhulme Trust, United Kingdom; United States of America.

In addition, individual members wish to acknowledge support from CERN: European Organization for Nuclear Research (CERN DOCT); Chile: Agencia Nacional de Investigación y Desarrollo (FONDECYT 1230812, FONDECYT 1240864, Fondecyt 3240661, Fondecyt Regular 1240721); China: Chinese Ministry of Science and Technology (MOST-2023YFA1605700, MOST-2023YFA1609300), National Natural Science Foundation of China (NSFC – 12175119, NSFC 12275265); Czech Republic: Czech Science Foundation (GACR – 24-11373S), Ministry of Education Youth and Sports (ERC-CZ-LL2327, FORTE CZ.02.01.01/00/22_008/0004632), PRIMUS Research Programme (PRIMUS/21/SCI/017); EU: H2020 European Research Council (ERC – 101002463); European Union: European Research Council (BARD No. 101116429, ERC – 948254, ERC 101089007), European Regional Development Fund (HE COFUND GA No.101081355, ERDF), European Union, Future Artificial Intelligence Research (FAIR-

JHEP04(2026)099

NextGenerationEU PE00000013), Italian Center for High Performance Computing, Big Data and Quantum Computing (ICSC, NextGenerationEU); France: Agence Nationale de la Recherche (ANR-21-CE31-0013, ANR-21-CE31-0022, ANR-22-EDIR-0002, ANR-24-CE31-0504-01); Germany: Deutsche Forschungsgemeinschaft (DFG – 469666862, DFG – CR 312/5-2); China: Research Grants Council (GRF); Italy: Istituto Nazionale di Fisica Nucleare (ICSC, NextGenerationEU), Ministero dell'Università e della Ricerca (NextGenEU 153D23001490006 M4C2.1.1, NextGenEU I53D23000820006 M4C2.1.1, NextGenEU I53D23001490006 M4C2.1.1, SOE2024_0000023); Japan: Japan Society for the Promotion of Science (JSPS KAKENHI JP22H01227, JSPS KAKENHI JP22H04944, JSPS KAKENHI JP22KK0227, JSPS KAKENHI JP24K23939, JSPS KAKENHI JP24KK0251, JSPS KAKENHI JP25H00650, JSPS KAKENHI JP25H01291, JSPS KAKENHI JP25K01023); Norway: Research Council of Norway (RCN-314472); Poland: Ministry of Science and Higher Education (IDUB AGH, POB8, D4 no 9722), Polish National Science Centre (NCN 2021/42/E/ST2/00350, NCN OPUS 2023/51/B/ST2/02507, NCN OPUS nr 2022/47/B/ST2/03059, NCN UMO-2019/34/E/ST2/00393, UMO-2022/47/O/ST2/00148, UMO-2023/49/B/ST2/04085, UMO-2023/51/B/ST2/00920, UMO-2024/53/N/ST2/00869); Portugal: Foundation for Science and Technology (FCT); Spain: Agencia de Gestión de Ayudas Universitarias y de Investigación (AGAUR – 2023 BP 00141), Generalitat Valenciana (ASFAE/2022/008), Ministry of Science and Innovation (MCIN & NextGenEU PCI2022-135018-2, MICIN & FEDER PID2021-125273NB, RYC2019-028510-I, RYC2020-030254-I, RYC2021-031273-I, RYC2022-038164-I), Ministerio de Ciencia, Innovación y Universidades/Agencia Estatal de Investigación (PID2022-142604OB-C22); Sweden: Carl Trygger Foundation (Carl Trygger Foundation CTS 22:2312), Swedish Research Council (Swedish Research Council 2023-04654, VR 2021-03651, VR 2022-03845, VR 2022-04683, VR 2023-03403, VR 2024-05451), Knut and Alice Wallenberg Foundation (KAW 2018.0458, KAW 2022.0358, KAW 2023.0366); Switzerland: Swiss National Science Foundation (SNSF – PCEFP2_194658); United Kingdom: Royal Society (NIF-R1-231091); United States of America: U.S. Department of Energy (ECA DE-AC02-76SF00515), Neubauer Family Foundation.

Data Availability Statement. This article has no associated data or the data will not be deposited.

Code Availability Statement. This article has no associated code or the code will not be deposited.

References

[1] ALEPH et al. collaborations, *Precision Electroweak Measurements and Constraints on the Standard Model*, arXiv:1012.2367 [INSPIRE].

[2] G. Degrassi et al., *Higgs mass and vacuum stability in the Standard Model at NNLO*, *JHEP* **08** (2012) 098 [arXiv:1205.6497] [INSPIRE].

[3] F.L. Bezrukov and M. Shaposhnikov, *The Standard Model Higgs boson as the inflaton*, *Phys. Lett. B* **659** (2008) 703 [arXiv:0710.3755] [INSPIRE].

[4] A. De Simone, M.P. Hertzberg and F. Wilczek, *Running Inflation in the Standard Model*, *Phys. Lett. B* **678** (2009) 1 [arXiv:0812.4946] [INSPIRE].

[5] F. Bezrukov, M.Y. Kalmykov, B.A. Kniehl and M. Shaposhnikov, *Higgs Boson Mass and New Physics*, *JHEP* **10** (2012) 140 [arXiv:1205.2893] [INSPIRE].

[6] A.H. Hoang, S. Plätzer and D. Samitz, *On the Cutoff Dependence of the Quark Mass Parameter in Angular Ordered Parton Showers*, *JHEP* **10** (2018) 200 [arXiv:1807.06617] [INSPIRE].

[7] P. Nason, *The Top Mass in Hadronic Collisions*, arXiv:1712.02796.

[8] G. Corcella, *The top-quark mass: challenges in definition and determination*, *Front. in Phys.* **7** (2019) 54 [arXiv:1903.06574] [INSPIRE].

[9] P. Azzi et al., *Standard Model Physics at the HL-LHC and HE-LHC*, *CERN Yellow Rep. Monogr.* **7** (2019) 1 [arXiv:1902.04070] [INSPIRE].

[10] A.H. Hoang, *What is the Top Quark Mass?*, *Ann. Rev. Nucl. Part. Sci.* **70** (2020) 225 [arXiv:2004.12915] [INSPIRE].

[11] B. Dehnadi, A.H. Hoang, O.L. Jin and V. Mateu, *Top quark mass calibration for Monte Carlo event generators — an update*, *JHEP* **12** (2023) 065 [arXiv:2309.00547] [INSPIRE].

[12] CDF collaboration, *Observation of top quark production in $\bar{p}p$ collisions with the Collider Detector at Fermilab*, *Phys. Rev. Lett.* **74** (1995) 2626 [hep-ex/9503002] [INSPIRE].

[13] D0 collaboration, *Observation of the top quark*, *Phys. Rev. Lett.* **74** (1995) 2632 [hep-ex/9503003] [INSPIRE].

[14] CDF and D0 collaborations, *Combination of CDF and D0 results on the mass of the top quark using up $9.7\,fb^{-1}$ at the Tevatron*, arXiv:1608.01881 [INSPIRE].

[15] L. Evans and P. Bryant, *LHC Machine*, 2008 *JINST* **3** S08001 [INSPIRE].

[16] ATLAS collaboration, *The ATLAS Experiment at the CERN Large Hadron Collider*, 2008 *JINST* **3** S08003 [INSPIRE].

[17] CMS collaboration, *The CMS Experiment at the CERN LHC*, 2008 *JINST* **3** S08004 [INSPIRE].

JHEP04(2026)099

[18] ATLAS and CMS collaborations, *Combination of Measurements of the Top Quark Mass from Data Collected by the ATLAS and CMS Experiments at $\sqrt{s} = 7$ and 8 TeV*, Phys. Rev. Lett. **132** (2024) 261902 [arXiv:2402.08713] [INSPIRE].

[19] ATLAS collaboration, *Measurement of the top quark mass with the ATLAS detector using $t\bar{t}$ events with a high transverse momentum top quark*, Phys. Lett. B **867** (2025) 139608 [arXiv:2502.18216] [INSPIRE].

[20] CMS collaboration, *Measurement of the top quark mass using a profile likelihood approach with the lepton+jets final states in proton-proton collisions at $\sqrt{s} = 13$ TeV*, Eur. Phys. J. C **83** (2023) 963 [arXiv:2302.01967] [INSPIRE].

[21] ATLAS collaboration, *Measurement of the top-quark mass using a leptonic invariant mass in pp collisions at $\sqrt{s} = 13$ TeV with the ATLAS detector*, JHEP **06** (2023) 019 [arXiv:2209.00583] [INSPIRE].

[22] CMS collaboration, *Letter of intent: by the CMS Collaboration for a general purpose detector at LHC*, CERN-LHCC 92-003, (1992).

[23] A. Kharchilava, *Top mass determination in leptonic final states with J/ψ*, Phys. Lett. B **476** (2000) 73 [hep-ph/9912320] [INSPIRE].

[24] CMS collaboration, *Measurement of the mass of the top quark in decays with a J/ψ meson in pp collisions at 8 TeV*, JHEP **12** (2016) 123 [arXiv:1608.03560] [INSPIRE].

[25] ATLAS collaboration, *ATLAS Insertable B-Layer Technical Design Report*, CERN-LHCC-2010-013 (2010) [INSPIRE].

[26] ATLAS IBL collaboration, *Production and Integration of the ATLAS Insertable B-Layer*, 2018 *JINST* **13** T05008 [arXiv:1803.00844] [INSPIRE].

[27] G. Avoni et al., *The new LUCID-2 detector for luminosity measurement and monitoring in ATLAS*, 2018 *JINST* **13** P07017 [INSPIRE].

[28] ATLAS collaboration, *Performance of the ATLAS Trigger System in 2015*, Eur. Phys. J. C **77** (2017) 317 [arXiv:1611.09661] [INSPIRE].

[29] ATLAS collaboration, *Software and computing for Run 3 of the ATLAS experiment at the LHC*, Eur. Phys. J. C **85** (2025) 234 [arXiv:2404.06335] [INSPIRE].

[30] ATLAS collaboration, *ATLAS data quality operations and performance for 2015–2018 data-taking*, 2020 *JINST* **15** P04003 [arXiv:1911.04632] [INSPIRE].

[31] ATLAS collaboration, *The ATLAS Simulation Infrastructure*, Eur. Phys. J. C **70** (2010) 823 [arXiv:1005.4568] [INSPIRE].

[32] GEANT4 collaboration, *Geant4 — a simulation toolkit*, Nucl. Instrum. Meth. A **506** (2003) 250 [INSPIRE].

[33] T. Sjöstrand, S. Mrenna and P.Z. Skands, *A brief introduction to PYTHIA 8.1*, Comput. Phys. Commun. **178** (2008) 852 [arXiv:0710.3820] [INSPIRE].

[34] R.D. Ball et al., *Parton distributions with LHC data*, Nucl. Phys. B **867** (2013) 244 [arXiv:1207.1303] [INSPIRE].

[35] ATLAS collaboration, *The Pythia 8 A3 tune description of ATLAS minimum bias and inelastic measurements incorporating the Donnachie-Landshoff diffractive model*, ATL-PHYS-PUB-2016-017 (2016) [INSPIRE].

[36] P. Nason, *A new method for combining NLO QCD with shower Monte Carlo algorithms*, JHEP **11** (2004) 040 [hep-ph/0409146] [INSPIRE].

[37] S. Frixione, P. Nason and C. Oleari, *Matching NLO QCD computations with Parton Shower simulations: the POWHEG method*, *JHEP* **11** (2007) 070 [arXiv:0709.2092] [INSPIRE].

[38] S. Alioli, P. Nason, C. Oleari and E. Re, *A general framework for implementing NLO calculations in shower Monte Carlo programs: the POWHEG BOX*, *JHEP* **06** (2010) 043 [arXiv:1002.2581] [INSPIRE].

[39] S. Frixione, P. Nason and G. Ridolfi, *A Positive-weight next-to-leading-order Monte Carlo for heavy flavour hadroproduction*, *JHEP* **09** (2007) 126 [arXiv:0707.3088] [INSPIRE].

[40] NNPDF collaboration, *Parton distributions for the LHC Run II*, *JHEP* **04** (2015) 040 [arXiv:1410.8849] [INSPIRE].

[41] ATLAS collaboration, *Studies on top-quark Monte Carlo modelling for Top2016*, ATL-PHYS-PUB-2016-020 (2016) [INSPIRE].

[42] ATLAS collaboration, *Simulation of top-quark production for the ATLAS experiment at* $\sqrt{s} = 13$ *TeV*, ATL-PHYS-PUB-2016-004 (2016) [INSPIRE].

[43] T. Sjöstrand et al., *An introduction to PYTHIA 8.2*, *Comput. Phys. Commun.* **191** (2015) 159 [arXiv:1410.3012] [INSPIRE].

[44] ATLAS collaboration, *ATLAS Pythia 8 tunes to 7 TeV data*, ATL-PHYS-PUB-2014-021 (2014) [INSPIRE].

[45] P. Skands, S. Carrazza and J. Rojo, *Tuning PYTHIA 8.1: the Monash 2013 Tune*, *Eur. Phys. J. C* **74** (2014) 3024 [arXiv:1404.5630] [INSPIRE].

[46] M.G. Bowler, e^+e^- *Production of Heavy Quarks in the String Model*, *Z. Phys. C* **11** (1981) 169 [INSPIRE].

[47] ALEPH collaboration, *Study of the fragmentation of b quarks into B mesons at the Z peak*, *Phys. Lett. B* **512** (2001) 30 [hep-ex/0106051] [INSPIRE].

[48] DELPHI collaboration, *A study of the b-quark fragmentation function with the DELPHI detector at LEP I and an averaged distribution obtained at the Z Pole*, *Eur. Phys. J. C* **71** (2011) 1557 [arXiv:1102.4748] [INSPIRE].

[49] OPAL collaboration, *Inclusive analysis of the b quark fragmentation function in Z decays at LEP*, *Eur. Phys. J. C* **29** (2003) 463 [hep-ex/0210031] [INSPIRE].

[50] SLD collaboration, *Precise measurement of the b quark fragmentation function in Z0 boson decays*, *Phys. Rev. Lett.* **84** (2000) 4300 [hep-ex/9912058] [INSPIRE].

[51] ATLAS collaboration, *Measurements of jet observables sensitive to b-quark fragmentation in* $t\bar{t}$ *events at the LHC with the ATLAS detector*, *Phys. Rev. D* **106** (2022) 032008 [arXiv:2202.13901] [INSPIRE].

[52] S. Frixione, E. Laenen, P. Motylinski and B.R. Webber, *Single-top production in MC@NLO*, *JHEP* **03** (2006) 092 [hep-ph/0512250] [INSPIRE].

[53] R. Frederix, E. Re and P. Torrielli, *Single-top t-channel hadroproduction in the four-flavour scheme with POWHEG and aMC@NLO*, *JHEP* **09** (2012) 130 [arXiv:1207.5391] [INSPIRE].

[54] HFLAV collaboration, *Averages of b-hadron, c-hadron, and* τ*-lepton properties as of 2018*, *Eur. Phys. J. C* **81** (2021) 226 [arXiv:1909.12524] [INSPIRE].

[55] Particle Data Group collaboration, *Review of Particle Physics*, *PTEP* **2020** (2020) 083C01 [INSPIRE].

[56] ATLAS collaboration, *Reweighting heavy-flavor production fractions to reduce flavor modelling uncertainties for ATLAS*, ATL-PHYS-PUB-2022-035 (2022) [INSPIRE].

[57] LHCb collaboration, *Evidence for modification of b quark hadronization in high-multiplicity pp collisions at* $\sqrt{s} = 13$ *TeV*, Phys. Rev. Lett. **131** (2023) 061901 [arXiv:2204.13042] [INSPIRE].

[58] LHCb collaboration, *Measurement of the fragmentation fraction ratio* f_s/f_d *and its dependence on B meson kinematics*, JHEP **04** (2013) 001 [arXiv:1301.5286] [INSPIRE].

[59] LHCb collaboration, *Measurement of* f_s/f_u *Variation with Proton-Proton Collision Energy and B-Meson Kinematics*, Phys. Rev. Lett. **124** (2020) 122002 [arXiv:1910.09934] [INSPIRE].

[60] LHCb collaboration, *Precise measurement of the* f_s/f_d *ratio of fragmentation fractions and of* B_s^0 *decay branching fractions*, Phys. Rev. D **104** (2021) 032005 [arXiv:2103.06810] [INSPIRE].

[61] LHCb collaboration, *Measurement of b-hadron production fractions in* 7 TeV *pp collisions*, Phys. Rev. D **85** (2012) 032008 [arXiv:1111.2357] [INSPIRE].

[62] LHCb collaboration, *Measurement of b hadron fractions in 13 TeV pp collisions*, Phys. Rev. D **100** (2019) 031102 [arXiv:1902.06794] [INSPIRE].

[63] ALICE collaboration, *Charm-quark fragmentation fractions and production cross section at midrapidity in pp collisions at the LHC*, Phys. Rev. D **105** (2022) L011103 [arXiv:2105.06335] [INSPIRE].

[64] D.J. Lange, *The EvtGen particle decay simulation package*, Nucl. Instrum. Meth. A **462** (2001) 152 [INSPIRE].

[65] ATLAS collaboration, *Studies on the improvement of the matching uncertainty definition in top-quark processes simulated with Powheg+Pythia8*, ATL-PHYS-PUB-2023-029 (2023) [INSPIRE].

[66] P. Artoisenet, R. Frederix, O. Mattelaer and R. Rietkerk, *Automatic spin-entangled decays of heavy resonances in Monte Carlo simulations*, JHEP **03** (2013) 015 [arXiv:1212.3460] [INSPIRE].

[67] M. Bähr et al., *Herwig++ Physics and Manual*, Eur. Phys. J. C **58** (2008) 639 [arXiv:0803.0883] [INSPIRE].

[68] J. Bellm et al., *Herwig 7.0/Herwig++ 3.0 release note*, Eur. Phys. J. C **76** (2016) 196 [arXiv:1512.01178] [INSPIRE].

[69] L.A. Harland-Lang, A.D. Martin, P. Motylinski and R.S. Thorne, *Parton distributions in the LHC era: MMHT 2014 PDFs*, Eur. Phys. J. C **75** (2015) 204 [arXiv:1412.3989] [INSPIRE].

[70] S. Mrenna and P. Skands, *Automated Parton-Shower Variations in Pythia 8*, Phys. Rev. D **94** (2016) 074005 [arXiv:1605.08352] [INSPIRE].

[71] ATLAS collaboration, *A study of different colour reconnection settings for Pythia8 generator using underlying event observables*, ATL-PHYS-PUB-2017-008 (2017) [INSPIRE].

[72] M. Czakon and A. Mitov, *Top++: A Program for the Calculation of the Top-Pair Cross-Section at Hadron Colliders*, Comput. Phys. Commun. **185** (2014) 2930 [arXiv:1112.5675] [INSPIRE].

[73] M. Cacciari et al., *Top-pair production at hadron colliders with next-to-next-to-leading logarithmic soft-gluon resummation*, Phys. Lett. B **710** (2012) 612 [arXiv:1111.5869] [INSPIRE].

[74] P. Bärnreuther, M. Czakon and A. Mitov, *Percent-Level-Precision Physics at the Tevatron: Next-to-Next-to-Leading Order QCD Corrections to* $q\bar{q} \to t\bar{t} + X$, Phys. Rev. Lett. **109** (2012) 132001 [arXiv:1204.5201] [INSPIRE].

JHEP04(2026)099

[75] M. Czakon and A. Mitov, *NNLO corrections to top pair production at hadron colliders: the quark-gluon reaction*, *JHEP* **01** (2013) 080 [arXiv:1210.6832] [INSPIRE].

[76] M. Czakon and A. Mitov, *NNLO corrections to top-pair production at hadron colliders: the all-fermionic scattering channels*, *JHEP* **12** (2012) 054 [arXiv:1207.0236] [INSPIRE].

[77] M. Czakon, P. Fiedler and A. Mitov, *Total Top-Quark Pair-Production Cross Section at Hadron Colliders Through* $\mathcal{O}(\alpha_S^4)$, *Phys. Rev. Lett.* **110** (2013) 252004 [arXiv:1303.6254] [INSPIRE].

[78] J. Campbell, T. Neumann and Z. Sullivan, *Single-top-quark production in the t-channel at NNLO*, *JHEP* **02** (2021) 040 [arXiv:2012.01574] [INSPIRE].

[79] PDF4LHC Working Group collaboration, *The PDF4LHC21 combination of global PDF fits for the LHC Run III*, *J. Phys. G* **49** (2022) 080501 [arXiv:2203.05506] [INSPIRE].

[80] N. Kidonakis and N. Yamanaka, *Higher-order corrections for tW production at high-energy hadron colliders*, *JHEP* **05** (2021) 278 [arXiv:2102.11300] [INSPIRE].

[81] Z.L. Liu and J. Gao, *s -channel single top quark production and decay at next-to-next-to-leading-order in QCD*, *Phys. Rev. D* **98** (2018) 071501 [arXiv:1807.03835] [INSPIRE].

[82] J. Alwall et al., *The automated computation of tree-level and next-to-leading order differential cross sections, and their matching to parton shower simulations*, *JHEP* **07** (2014) 079 [arXiv:1405.0301] [INSPIRE].

[83] ATLAS collaboration, *Modelling of the* $t\bar{t}H$ *and* $t\bar{t}V$ $(V = W, Z)$ *processes for* $\sqrt{s} = 13$ *TeV ATLAS analyses*, ATL-PHYS-PUB-2016-005 (2016) [INSPIRE].

[84] Sherpa collaboration, *Event Generation with Sherpa 2.2*, *SciPost Phys.* **7** (2019) 034 [arXiv:1905.09127] [INSPIRE].

[85] F. Cascioli, P. Maierhöfer and S. Pozzorini, *Scattering Amplitudes with Open Loops*, *Phys. Rev. Lett.* **108** (2012) 111601 [arXiv:1111.5206] [INSPIRE].

[86] T. Gleisberg and S. Hoeche, *Comix, a new matrix element generator*, *JHEP* **12** (2008) 039 [arXiv:0808.3674] [INSPIRE].

[87] S. Schumann and F. Krauss, *A parton shower algorithm based on Catani-Seymour dipole factorisation*, *JHEP* **03** (2008) 038 [arXiv:0709.1027] [INSPIRE].

[88] R. Frederix and S. Frixione, *Merging meets matching in MC@NLO*, *JHEP* **12** (2012) 061 [arXiv:1209.6215] [INSPIRE].

[89] P. Artoisenet, F. Maltoni and T. Stelzer, *Automatic generation of quarkonium amplitudes in NRQCD*, *JHEP* **02** (2008) 102 [arXiv:0712.2770] [INSPIRE].

[90] J. Alwall et al., *A standard format for Les Houches event files*, *Comput. Phys. Commun.* **176** (2007) 300 [hep-ph/0609017] [INSPIRE].

[91] E. Boos et al., *Generic User Process Interface for Event Generators*, in the proceedings of the *2nd Les Houches Workshop on Physics at TeV Colliders*, Les Houches, France, May 21 – June 01 (2001) [hep-ph/0109068] [INSPIRE].

[92] ATLAS collaboration, *Summary of ATLAS Pythia 8 tunes*, ATL-PHYS-PUB-2012-003 (2012) [INSPIRE].

[93] ATLAS collaboration, *Tools for estimating fake/non-prompt lepton backgrounds with the ATLAS detector at the LHC*, 2023 *JINST* **18** T11004 [arXiv:2211.16178] [INSPIRE].

[94] ATLAS collaboration, *Vertex Reconstruction Performance of the ATLAS Detector at $\sqrt{s} = 13$ TeV*, ATL-PHYS-PUB-2015-026 (2015) [INSPIRE].

[95] ATLAS collaboration, *Electron and photon performance measurements with the ATLAS detector using the 2015–2017 LHC proton-proton collision data*, 2019 *JINST* **14** P12006 [arXiv:1908.00005] [INSPIRE].

[96] ATLAS collaboration, *Muon reconstruction and identification efficiency in ATLAS using the full Run 2 pp collision data set at $\sqrt{s} = 13$ TeV*, *Eur. Phys. J. C* **81** (2021) 578 [arXiv:2012.00578] [INSPIRE].

[97] ATLAS collaboration, *Identification of very-low transverse momentum muons in the ATLAS experiment*, ATL-PHYS-PUB-2020-002 (2020) [INSPIRE].

[98] ATLAS collaboration, *Jet reconstruction and performance using particle flow with the ATLAS Detector*, *Eur. Phys. J. C* **77** (2017) 466 [arXiv:1703.10485] [INSPIRE].

[99] M. Cacciari and G.P. Salam, *Dispelling the N^3 myth for the k_t jet-finder*, *Phys. Lett. B* **641** (2006) 57 [hep-ph/0512210] [INSPIRE].

[100] M. Cacciari, G.P. Salam and G. Soyez, *The anti-k_t jet clustering algorithm*, *JHEP* **04** (2008) 063 [arXiv:0802.1189] [INSPIRE].

[101] M. Cacciari, G.P. Salam and G. Soyez, *FastJet User Manual*, *Eur. Phys. J. C* **72** (2012) 1896 [arXiv:1111.6097] [INSPIRE].

[102] ATLAS collaboration, *Performance of pile-up mitigation techniques for jets in pp collisions at $\sqrt{s} = 8$ TeV using the ATLAS detector*, *Eur. Phys. J. C* **76** (2016) 581 [arXiv:1510.03823] [INSPIRE].

[103] ATLAS collaboration, *Jet energy scale and resolution measured in proton-proton collisions at $\sqrt{s} = 13$ TeV with the ATLAS detector*, *Eur. Phys. J. C* **81** (2021) 689 [arXiv:2007.02645] [INSPIRE].

[104] ATLAS collaboration, *ATLAS flavour-tagging algorithms for the LHC Run 2 pp collision dataset*, *Eur. Phys. J. C* **83** (2023) 681 [arXiv:2211.16345] [INSPIRE].

[105] ATLAS collaboration, *The performance of missing transverse momentum reconstruction and its significance with the ATLAS detector using 140 fb^{-1} of $\sqrt{s} = 13$ TeV pp collisions*, *Eur. Phys. J. C* **85** (2025) 606 [arXiv:2402.05858] [INSPIRE].

[106] ATLAS collaboration, *Performance of the ATLAS muon triggers in Run 2*, 2020 *JINST* **15** P09015 [arXiv:2004.13447] [INSPIRE].

[107] ATLAS collaboration, *Performance of electron and photon triggers in ATLAS during LHC Run 2*, *Eur. Phys. J. C* **80** (2020) 47 [arXiv:1909.00761] [INSPIRE].

[108] ATLAS collaboration, *Measurement of the top quark mass in the $t\bar{t} \to$ lepton+jets channel from $\sqrt{s} = 8$ TeV ATLAS data and combination with previous results*, *Eur. Phys. J. C* **79** (2019) 290 [arXiv:1810.01772] [INSPIRE].

[109] ATLAS collaboration, *Evaluating statistical uncertainties and correlations using the bootstrap method*, ATL-PHYS-PUB-2021-011 (2021) [INSPIRE].

[110] ATLAS collaboration, *Luminosity determination in pp collisions at $\sqrt{s} = 13$ TeV using the ATLAS detector at the LHC*, *Eur. Phys. J. C* **83** (2023) 982 [arXiv:2212.09379] [INSPIRE].

[111] M. Czakon, D. Heymes and A. Mitov, *High-precision differential predictions for top-quark pairs at the LHC*, *Phys. Rev. Lett.* **116** (2016) 082003 [arXiv:1511.00549] [INSPIRE].

[112] M. Czakon et al., *Top-pair production at the LHC through NNLO QCD and NLO EW*, *JHEP* **10** (2017) 186 [arXiv:1705.04105] [INSPIRE].

[113] S. Frixione et al., *Single-top hadroproduction in association with a W boson*, *JHEP* **07** (2008) 029 [arXiv:0805.3067] [INSPIRE].

[114] ATLAS collaboration, *Studies on top-quark Monte Carlo modelling with Sherpa and MG5_aMC@NLO*, ATL-PHYS-PUB-2017-007 (2017) [INSPIRE].

[115] J. Butterworth et al., *PDF4LHC recommendations for LHC Run II*, *J. Phys. G* **43** (2016) 023001 [arXiv:1510.03865] [INSPIRE].

[116] G. Corcella and V. Drollinger, *Bottom-quark fragmentation: Comparing results from tuned event generators and resummed calculations*, *Nucl. Phys. B* **730** (2005) 82 [hep-ph/0508013] [INSPIRE].

[117] G. Corcella and F. Mescia, *A Phenomenological Study of Bottom Quark Fragmentation in Top Quark Decay*, *Eur. Phys. J. C* **65** (2010) 171 [arXiv:0907.5158] [INSPIRE].

[118] M. Cacciari, G. Corcella and A.D. Mitov, *Soft gluon resummation for bottom fragmentation in top quark decay*, *JHEP* **12** (2002) 015 [hep-ph/0209204] [INSPIRE].

[119] V.G. Kartvelishvili, A.K. Likhoded and V.A. Petrov, *On the Fragmentation Functions of Heavy Quarks Into Hadrons*, *Phys. Lett. B* **78** (1978) 615 [INSPIRE].

[120] M. Czakon, T. Generet, A. Mitov and R. Poncelet, *NNLO B-fragmentation fits and their application to $t\bar{t}$ production and decay at the LHC*, *JHEP* **03** (2023) 251 [arXiv:2210.06078] [INSPIRE].

[121] H. Brooks and P. Skands, *Coherent showers in decays of colored resonances*, *Phys. Rev. D* **100** (2019) 076006 [arXiv:1907.08980] [INSPIRE].

[122] LHC Higgs Cross Section Working Group collaboration, *Handbook of LHC Higgs Cross Sections: 4. Deciphering the Nature of the Higgs Sector*, *CERN Yellow Rep. Monogr.* **2** (2017) 1 [arXiv:1610.07922] [INSPIRE].

[123] ATLAS collaboration, *Measurement of the total and differential cross-sections of $t\bar{t}W$ production in pp collisions at $\sqrt{s} = 13$ TeV with the ATLAS detector*, *JHEP* **05** (2024) 131 [*Erratum ibid.* **11** (2025) 127] [arXiv:2401.05299] [INSPIRE].

[124] ATLAS collaboration, *Inclusive and differential cross-section measurements of $t\bar{t}Z$ production in pp collisions at $\sqrt{s} = 13$ TeV with the ATLAS detector, including EFT and spin-correlation interpretations*, *JHEP* **07** (2024) 163 [arXiv:2312.04450] [INSPIRE].

[125] J.M. Campbell and R.K. Ellis, *MCFM for the Tevatron and the LHC*, *Nucl. Phys. B Proc. Suppl.* **205-206** (2010) 10 [arXiv:1007.3492] [INSPIRE].

[126] ATLAS collaboration, *Multi-Boson Simulation for 13 TeV ATLAS Analyses*, ATL-PHYS-PUB-2016-002 (2016) [INSPIRE].

[127] ATLAS collaboration, *ATLAS simulation of boson plus jets processes in Run 2*, ATL-PHYS-PUB-2017-006 (2017) [INSPIRE].

[128] ATLAS collaboration, *Electron and photon energy calibration with the ATLAS detector using LHC Run 2 data*, 2024 *JINST* **19** P02009 [arXiv:2309.05471] [INSPIRE].

[129] ATLAS collaboration, *Studies of the muon momentum calibration and performance of the ATLAS detector with pp collisions at $\sqrt{s} = 13$ TeV*, *Eur. Phys. J. C* **83** (2023) 686 [arXiv:2212.07338] [INSPIRE].

[130] ATLAS collaboration, *ATLAS b-jet identification performance and efficiency measurement with $t\bar{t}$ events in pp collisions at $\sqrt{s} = 13$ TeV*, Eur. Phys. J. C **79** (2019) 970 [arXiv:1907.05120] [INSPIRE].

[131] ATLAS collaboration, *Measurement of the c-jet mistagging efficiency in $t\bar{t}$ events using pp collision data at $\sqrt{s} = 13$ TeV collected with the ATLAS detector*, Eur. Phys. J. C **82** (2022) 95 [arXiv:2109.10627] [INSPIRE].

[132] ATLAS collaboration, *Calibration of the light-flavour jet mistagging efficiency of the b-tagging algorithms with Z+jets events using 139 fb^{-1} of ATLAS proton-proton collision data at $\sqrt{s} = 13$ TeV*, Eur. Phys. J. C **83** (2023) 728 [arXiv:2301.06319] [INSPIRE].

[133] M. Abramowitz and I. Stegun, eds., *Handbook of Mathematical Functions with Formulas, Graphs, and Mathematical Tables*, Dover Publications, New York, U.S.A. (1965).

[134] ATLAS collaboration, *ATLAS Computing Acknowledgements*, ATL-SOFT-PUB-2026-001, (2026).

The ATLAS collaboration

G. Aad[104], E. Aakvaag[17], B. Abbott[123], S. Abdelhameed[119a], K. Abeling[55], N.J. Abicht[49], S.H. Abidi[30], M. Aboelela[45], A. Aboulhorma[36e], H. Abramowicz[157], Y. Abulaiti[120], B.S. Acharya[69a,69b,a], A. Ackermann[63a], C. Adam Bourdarios[4], L. Adamczyk[87a], S.V. Addepalli[149], M. J. Addison[103], J. Adelman[118], A. Adiguzel[22c], T. Adye[137], A.A. Affolder[139], Y. Afik[40], M.N. Agaras[13], A. Aggarwal[102], C. Agheorghiesei[28c], F. Ahmadov[39,b], S. Ahuja[97], S. Ahuja[169], X. Ai[143b], G. Aielli[76a,76b], A. Aikot[169], M. Ait Tamlihat[36e], B. Aitbenchikh[36a], M. Akbiyik[102], T.P.A. Åkesson[100], A.V. Akimov[151], D. Akiyama[174], N.N. Akolkar[25], S. Aktas[172], G.L. Alberghi[24b], J. Albert[171], U. Alberti[20], P. Albicocco[53], G.L. Albouy[60], S. Alderweireldt[52], Z.L. Alegria[124], M. Aleksa[37], C. Alexa[28b], I.N. Aleksandrov[39], T. Alexopoulos[10], F. Alfonsi[24b], M. Algren[56], M. Alhroob[173], B. Ali[135], H. M. J. Ali[93,c], S. Ali[32], S.W. Alibocus[94], M. Aliev[34c], G. Alimonti[71a], W. Alkakhi[55], C. Allaire[66], B.M.M. Allbrooke[152], D. R. Allen[124], J. S. Allen[103], J.F. Allen[52], P.P. Allport[21], A. Aloisio[72a,72b], F. Alonso[92], C. Alpigiani[142], Z.M.K. Alsolami[93], A. Alvarez Fernandez[102], M. Alves Cardoso[56], M.G. Alviggi[72a,72b], M. Aly[103], A. Ambler[106], C. Amelung[37], M. Amerl[103], C.G. Ames[111], T. Amezza[130], D. Amidei[108], B. Amini[54], K. Amirie[161], A. Amirkhanov[39], S.P. Amor Dos Santos[133a], K.R. Amos[169], D. Amperiadou[158], S. An[84], C. Anastopoulos[145], T. Andeen[11], J.K. Anders[94], A. C. Anderson[59], A. Andreazza[71a,71b], S. Angelidakis[9], A. Angerami[42], A.V. Anisenkov[39], A. Annovi[74a], C. Antel[37], E. Antipov[151], M. Antonelli[53], F. Anulli[75a], M. Aoki[84], T. Aoki[159], M.A. Aparo[152], L. Aperio Bella[48], M. Apicella[31], C. Appelt[157], A. Apyan[27], M. Arampatzi[10], S. J. Arbiol Val[88], C. Arcangeletti[53], A.T.H. Arce[51], J-F. Arguin[110], S. Argyropoulos[158], J.-H. Arling[48], O. Arnaez[4], H. Arnold[151], G. Artoni[75a,75b], H. Asada[113], K. Asai[121], S. Asatryan[179], N.A. Asbah[37], R. A. Ashby Pickering[173], A. M. Aslam[97], K. Assamagan[30], R. Astalos[29a], K. S. V. Astrand[100], S. Atashi[165], R.J. Atkin[34a], H. Atmani[36f], P.A. Atmasiddha[131], K. Augsten[135], A.D. Auriol[41], V.A. Austrup[103], A.S. Avad[96], G. Avolio[37], K. Axiotis[56], A. Azzam[13], D. Babal[29b], H. Bachacou[138], K. Bachas[158,d], A. Bachiu[35], E. Bachmann[50], M. J. Backes[63a], A. Badea[40], T.M. Baer[108], P. Bagnaia[75a,75b], M. Bahmani[19], D. Bahner[54], K. Bai[126], J.T. Baines[137], L. Baines[96], O.K. Baker[178], E. Bakos[16], D. Bakshi Gupta[8], L.E. Balabram Filho[83b], V. Balakrishnan[123], R. Balasubramanian[4], E.M. Baldin[38], P. Balek[87a], E. Ballabene[24b,24a], F. Balli[138], L.M. Baltes[63a], W.K. Balunas[33], J. Balz[102], I. Bamwidhi[119b], E. Banas[88], M. Bandieramonte[132], A. Bandyopadhyay[25], S. Bansal[25], L. Barak[157], M. Barakat[48], E.L. Barberio[107], D. Barberis[18b], M. Barbero[104], M. Z. Barel[117], K.N. Barends[34a], T. Barillari[112], M-S. Barisits[37], T. Barklow[149], P. Baron[136], D.A. Baron Moreno[103], A. Baroncelli[62], A.J. Barr[129], J.D. Barr[98], F. Barreiro[101], J. Barreiro Guimarães da Costa[14], M.G. Barros Teixeira[133a], R.F. Coelho Barrue[133a], S. Barsov[38], F. Bartels[63a], R. Bartoldus[149], A.E. Barton[93], P. Bartos[29a], M. Baselga[49], S. Bashiri[88], A. Bassalat[66,e], M.J. Basso[162a], S. Bataju[45], R. Bate[170], R.L. Bates[59], S. Batlamous[101], M. Battaglia[139], D. Battulga[19], M. Bauce[75a,75b], M. Bauer[79], P. Bauer[25], L. T. Bayer[48], L.T. Bazzano Hurrell[31], J.B. Beacham[112], T. Beau[130], J.Y. Beaucamp[92], P.H. Beauchemin[164], P. Bechtle[25], H.P. Beck[20,f], K. Becker[173], A.J. Beddall[82], V.A. Bednyakov[39], C.P. Bee[151], L.J. Beemster[16], M. Begalli[83d], M. Begel[30], J.K. Behr[48], J.F. Beirer[37], F. Beisiegel[25], M. Belfkir[119b], G. Bella[157], L. Bellagamba[24b], A. Bellerive[35], C.D. Bellgraph[68], P. Bellos[21], K. Beloborodov[38], I. Benaoumeur[21], D. Benchekroun[36a], F. Bendebba[36a], Y. Benhammou[157], K.C. Benkendorfer[61], L. Beresford[48], M. Beretta[53], E. Bergeaas Kuutmann[167], N. Berger[4], B. Bergmann[135], J. Beringer[18a], G. Bernardi[5], C. Bernius[149], F.U. Bernlochner[25], A. Berrocal Guardia[13], T. Berry[97], P. Berta[136], A. Berthold[50], A. Berti[133a], R. Bertrand[104], S. Bethke[112], A. Betti[75a,75b], A.J. Bevan[96], L. Bezio[56], N.K. Bhalla[54], S. Bharthuar[112], S. Bhatta[151], P. Bhattarai[149], Z.M. Bhatti[120], K. D. Bhide[54], V.S. Bhopatkar[124], R.M. Bianchi[132], G. Bianco[24b,24a], O. Biebel[111], M. Biglietti[77a], C. S. Billingsley[45], Y. Bimgdi[36f], M. Bindi[55], A. Bingham[177], A. Bingul[22b], C. Bini[75a,75b], G.A. Bird[33], M. Birman[175], M. Biros[136], S. Biryukov[152], T. Bisanz[49], E. Bisceglie[24b,24a], J.P. Biswal[137], D. Biswas[147], I. Bloch[48], A. Blue[59], U. Blumenschein[96], V.S. Bobrovnikov[39], L. Boccardo[57b,57a], M. Boehler[54], D. Bogavac[13], A.G. Bogdanchikov[38], L. S. Boggia[130], B. Boehm[172], V. Boisvert[97], P. Bokan[37], T. Bold[87a], M. Bomben[5], M. Bona[96], M. Boonekamp[138], A.G. Borbély[59], I.S. Bordulev[38], G. Borissov[93], D. Bortoletto[129], D. Boscherini[24b], K. Bouaouda[36a], N. Bouchhar[169], L. Boudet[4], J. Boudreau[132], E.V. Bouhova-Thacker[93], D. Boumediene[41], R. Bouquet[57b,57a], A. Boveia[122], J. Boyd[37], D. Boye[30], I.R. Boyko[39], L. Bozianu[56], J. Bracinik[21], N. Brahimi[4], G. Brandt[177], O. Brandt[33], B. Brau[105], J.E. Brau[126], L. Brenner[117], R. Brenner[167], S. Bressler[175], G. Brianti[78a,78b], D. Britton[59], D. Britzger[112], I. Brock[25], R. Brock[109], G. Brooijmans[42], A.J. Brooks[68], E. M. Brooks[162b], E. Brost[30], L.M. Brown[171,162a], L.E. Bruce[61], T.L. Bruckler[129], P.A. Bruckman de Renstrom[88], B. Brüers[48], A. Bruni[24b], G. Bruni[24b], D. Brunner[47a,47b], M. Bruschi[24b], N. Bruscino[75a,75b], T. Buanes[17], Q. Buat[142], D. Buchin[112], A.G. Buckley[59], V. Büscher[102], O. Bulekov[82], B.A. Bullard[149], S. Burdin[94], C.D. Burgard[49], A.M. Burger[91], B. Burghgrave[8], O. Burlayenko[54], J. Burleson[168], J.C. Burzynski[148], E.L. Busch[42], P.J. Bussey[59], O. But[25], J.M. Butler[26], C.M. Buttar[59], J.M. Butterworth[98], W. Buttinger[137], C.J. Buxo Vazquez[109], A.R. Buzykaev[39], S. Cabrera Urbán[169], L. Cadamuro[66], H. Cai[37], Y. Cai[24b,114c,24a], Y. Cai[114a], V.M.M. Cairo[37], O. Cakir[3a], N. Calace[37], P. Calafiura[18a], G. Calderini[130], P. Calfayan[35], L. Calic[100], G. Callea[59], L.P. Caloba[83b], D. Calvet[41], S. Calvet[41], R. Camacho Toro[130], S. Camarda[37], D. Camarero Munoz[27], P. Camarri[76a,76b], C. Camincher[171], M. Campanelli[98], A. Camplani[43], V. Canale[72a,72b], A.C. Canbay[3a], E. Canonero[97], J. Cantero[169], Y. Cao[168], F. Capocasa[27], M. Capua[44b,44a], A. Carbone[71a,71b], R. Cardarelli[76a], J.C.J. Cardenas[8], M. P. Cardiff[27], J.M. Silva[52], G. Carducci[44b,44a], T. Carli[37], G. Carlino[72a], J.I. Carlotto[13], B.T. Carlson[132,g], E.M. Carlson[171], J. Carmignani[94], L. Carminati[71a,71b], A. Carnelli[4], M. Carnesale[37], S. Caron[116], E. Carquin[140g], I.B. Carr[107], S. Carrá[73a,73b], G. Carratta[24b,24a], C. Carrion Martinez[169], A.M. Carroll[126], M.P. Casado[13,h], P. Casolaro[72a,72b], M. Caspar[48], W.R. Castiglioni[40], F.L. Castillo[4], L. Castillo Garcia[13], V. Castillo Gimenez[169], N.F. Castro[133a,133e], M.C.N. Fiolhais[133a,133c,i], A. Catinaccio[37], J.R. Catmore[128], T. Cavaliere[4], V. Cavaliere[30], L.J. Caviedes Betancourt[23b], E. Celebi[82], S. Cella[37], V. Cepaitis[56], K. Cerny[125], A. Cerri[74a,j], L. Cerrito[76a,76b], F. Cerutti[18a],

B. Cervato[71a,71b], A. Cervelli[24b], G. Cesarini[53], S.A. Cetin[82], P.M. Chabrillat[130], R. Chakkappai[66], S. Chakraborty[173], A. Chambers[61], J. Chan[18a], W.Y. Chan[159], J.D. Chapman[33], E. Chapon[138], B. Chargeishvili[155b], D.G. Charlton[21], C. Chauhan[136], Y. Che[114a], S. Chekanov[6], B. Chen[157], B. Chen[171], H. Chen[114a], H. Chen[30], J. Chen[144a], J. Chen[148], M. Chen[129], S. Chen[89], S.J. Chen[114a], X. Chen[144a], X. Chen[15,k], Z. Chen[62], C.L. Cheng[176], H.C. Cheng[64a], S. Cheong[149], A. Cheplakov[39], E. Cherepanova[117], R. Cherkaoui El Moursli[36e], E. Cheu[7], K. Cheung[65], L. Chevalier[138], V. Chiarella[53], G. Chiarelli[74a], G. Chiodini[70a], A.S. Chisholm[21], A. Chitan[28b], M. Chitishvili[169], M.V. Chizhov[39,l], K. Choi[11], Y. Chou[142], E.Y.S. Chow[116], V.A. Schegelsky[38], K.L. Chu[175], M.C. Chu[64a], X. Chu[14,114c], Z. Chubinidze[53], J. Chudoba[134], J.J. Chwastowski[88], D. Cieri[112], K.M. Ciesla[87a], V. Cindro[95], A. Ciocio[18a], F. Cirotto[72a,72b], Z.H. Citron[175], M. Citterio[71a], D.A. Ciubotaru[28b], A. Clark[56], P.J. Clark[52], N. Clarke Hall[98], C. Clarry[161], S.E. Clawson[48], C. Clement[47a,47b], L. Clissa[24b,24a], Y. Coadou[104], M. Cobal[69a,69c], A. Coccaro[57b], R. Coelho Lopes De Sa[105], S. Coelli[71a], M.M. Cohen[131], L. S. Colangeli[161], B. Cole[42], P. Collado Soto[101], J. Collot[60], M.R. Coluccia[70a], P. Conde Muiño[133a,133g], M.P. Connell[34c], S.H. Connell[34c], E.I. Conroy[129], M. Contreras Cossio[11], F. Conventi[72a,m], L. Corazzina[75a,75b], F. A. Corchia[24b,24a], A. Cordeiro Oudot Choi[142], L.D. Corpe[41], M. Corradi[75a,75b], F. Corriveau[106,n], A. Cortes-Gonzalez[159], M.J. Costa[169], F. Costanza[4], D. Costanzo[145], J. Couthures[4], G. Cowan[97], K. Cranmer[176], L. Cremer[49], D. Cremonini[24b,24a], S. Crépé-Renaudin[60], F. Crescioli[130], T. Cresta[73a,73b], M. Cristinziani[147], M. Cristoforetti[78a,78b], E. Critelli[98], V. Croft[117], G. Crosetti[44b,44a], A. Cueto[101], H. Cui[98], Z. Cui[7], B.M. Cunnett[152], W.R. Cunningham[59], F. Curcio[169], J. R. Curran[52], G. D'amen[30], V. D'Amico[111], M. D'Andrea[57b,57a], G. D'anniballe[74a,74b], S. D'Auria[71a,71b], A. D'Avanzo[72a,72b], L. D'Eramo[41], A. D'Onofrio[72a,72b], M. D'Onofrio[94], M. D'uffizi[103], J.V. Da Fonseca Pinto[83b], A. Gomes[133a,133b], C. Da Via[103], W. Dabrowski[87a], T. Dado[37], S. Dahbi[154], T. Dai[108], D. Dal Santo[20], C. Dallapiccola[105], M. Dam[43], J.R. Dandoy[35], D. Dannheim[37], M. Danninger[148], V. Dao[151], G. Darbo[57b], S.J. Das[30], F. Dattola[48], T. Davidek[136], J. Davidson[173], I. Dawson[96], K. De[8], F.A. Dias[117], C. De Almeida Rossi[161], R. De Asmundis[72a], N. De Biase[48], S. De Castro[24b,24a], N. De Groot[116], P. de Jong[117], H. De la Torre[118], A. De Maria[114a], A. De Salvo[75a], U. De Sanctis[76a,76b], F. De Santis[70a,70b], A. De Santo[152], J.B. De Vivie De Regie[60], J. Debevc[95], D.V. Dedovich[39], J. Degens[94], A.M. Deiana[45], J. Del Peso[101], L. Delagrange[130], F. Deliot[138], C.M. Delitzsch[49], A. Dell'Acqua[37], L. Dell'Asta[71a,71b], M. Della Pietra[72a,72b], D. Della Volpe[56], M. Delmastro[4], C.C. Delogu[57b,57a], P.A. Delsart[60], S. Demers[178], M. Demichev[39], S.P. Denisov[38], H. Denizli[22a,o], D. Derendarz[88], F. Derue[130], P. Dervan[94,†], A. M. Desai[1], K. Desch[25], F.A. Di Bello[57b,57a], A. Di Ciaccio[76a,76b], L. Di Ciaccio[4], A. Di Domenico[75a,75b], C. Di Donato[72a,72b], A. Di Girolamo[37], G. Di Gregorio[62], A. Di Luca[78a,78b], B. Di Micco[77a,77b], R. Di Nardo[77a,77b], K.F. Di Petrillo[40], M. Diamantopoulou[35], M.A. Diaz[140a,140b], A. R. Didenko[39], M. Didenko[169], S.D. Diefenbacher[18a], E.B. Diehl[108], S. Díez Cornell[48], C. Diez Pardos[147], C. Dimitriadi[150], A. Dimitrievska[21], A. Dimri[151], Y. Ding[62], J. Dingfelder[25], T. Dingley[129], I-M. Dinu[28b], S.J. Dittmeier[63b], F. Dittus[37],

M. Divisek[136], B. Dixit[94], F. Djama[104], T. Djobava[155b], Y. Amaral Coutinho[83b], C. Doglioni[103,100], A. Dohnalova[29a], Z. Dolezal[136], K. Domijan[87a], K.M. Dona[40], M. Donadelli[83d], B. Dong[109], D. Qichen[129], J. Donini[41], J. Dopke[137], A. Doria[72a], N. Dos Santos Fernandes[133a], I.A. Dos Santos Luz[83e], P. Dougan[103], M.T. Dova[92], A.T. Doyle[59], M.P. Drescher[55], E. Dreyer[175], I. Drivas-koulouris[10], M. Drnevich[120], D. Du[62], T.A. du Pree[117], Z. Duan[114a], M. Dubau[4], F. Dubinin[39], M. Dubovsky[29a], E. Duchovni[175], G. Duckeck[111], P. K. Duckett[98], O.A. Ducu[28b], D. Duda[52], A. Dudarev[37], M.M. Dudek[88], E. R. Duden[27], M. Dührssen[37], L. Duflot[66], I. Duminica[28g], A.E. Dumitriu[28b], M. Dunford[63a], K. Dunne[47a,47b], A. Duperrin[104], A. Durglishvili[155b], G.I. Dyckes[18a], M. Dyndal[87a], B.S. Dziedzic[37], Z.O. Earnshaw[152], G.H. Eberwein[129], B. Eckerova[29a], S. Eggebrecht[55], G. Eigen[17], K. Einsweiler[18a], T. Ekelof[167], P.A. Ekman[100], S. El Farkh[36b], Y. El Ghazali[62], H. El Jarrari[34j], A. El Moussaouy[36a], D. Elitez[37], M. Ellert[167], F. Ellinghaus[177], T.A. Elliot[97], N. Ellis[37], J. Elmsheuser[30], M. Elsawy[119a], M. Elsing[37], D. Emeliyanov[137], Y. Enari[84], S. Epari[110], D. Ernani Martins Neto[88], F. Ernst[37], M. Escalier[66], C. Escobar[169], E. Etzion[157], H. Evans[68], L.S. Evans[48], A. Ezhilov[38], S. Ezzarqtouni[36a], F. Fabbri[24b,24a], L. Fabbri[24b,24a], G. Facini[98], V. Fadeyev[139], R.M. Fakhrutdinov[38], D. Fakoudis[102], S. Falciano[75a], L.F. Falda Ulhoa Coelho[133a], F. Fallavollita[112], G. Falsetti[44b,44a], J. Faltova[136], C. Fan[168], K. Y. Fan[64b], Y. Fan[14], Y. Fang[14,114c], M. Fanti[71a,71b], M. Faraj[69a,69b], Z. Farazpay[99], A. Farbin[8], A. Farilla[77a], K. Farman[154], T. Farooque[109], J. N. Farr[178], M. S. Farrington[61], S.M. Farrington[137,52], F. Fassi[36e], D. Fassouliotis[9], L. Fayard[66], P. Federic[136], P. Federicova[134], O.L. Fedin[38,p], M. Feickert[176], L. Feligioni[104], D.E. Fellers[18a], C. Feng[143a], Y. Feng[14], Z. Feng[117], M.J. Fenton[165], L. Ferencz[48], B. Fernandez Barbadillo[93], P. Fernandez Martinez[67], M. Bosman[13], M.J.V. Fernoux[104], J. Ferrando[93], A. Ferrari[167], P. Ferrari[117,116], R. Ferrari[73a], D. Ferrere[56], C. Ferretti[108], M. P. Fewell[1], D. Fiacco[75a,75b], F. Fiedler[102], P. Fiedler[135], S. Filimonov[39], M.S. Filip[28b,q], A. Filipčič[95], E.K. Filmer[162a], F. Filthaut[116], L. Fiorini[169], W.C. Fisher[109], T. Fitschen[103], P. M. Fitzhugh[138], I. Fleck[147], P. Fleischmann[108], T. Flick[177], M. Flores[34d,r], L.R. Flores Castillo[64a], L. Flores Sanz De Acedo[37], F.M. Follega[78a,78b], N. Fomin[33], J.H. Foo[161], A. Formica[138], A.C. Forti[103], E. Fortin[37], A.W. Fortman[18a], L. Foster[18a], L. Fountas[9,s], D. Fournier[66], H. Fox[93], P. Francavilla[74a,74b], S. Francescato[61], S. Franchellucci[56], M. Franchini[24b,24a], S. Franchino[63a], D. Francis[37], L. Franco[116], L. Franconi[48], M. Franklin[61], G. Frattari[27], Y.Y. Frid[157], J. Friend[59], N. Fritzsche[37], A. Froch[56], D. Froidevaux[37], J.A. Frost[137], Y. Fu[109], S. Fuenzalida Garrido[140g], M. Fujimoto[151], K. Y. Fung[64a], M. Furukawa[159], M. Fuste Costa[48], J. Fuster[169], A. Gaa[55], A. Gabrielli[24b,24a], A. Gabrielli[161], P. Gadow[37], G. Gagliardi[57b,57a], L.G. Gagnon[18a], S. Gaid[85b], S. Galantzan[157], J. Gallagher[1], E.J. Gallas[129], A.L. Gallen[167], B.J. Gallop[137], K.K. Gan[122], S. Ganguly[159], Y. Gao[52], A. Garabaglu[142], F.M. Garay Walls[140a,140b], C. García[169], A. Garcia Alonso[117], A.G. Garcia Caffaro[178], J.E. García Navarro[169], M. A. Garcia Ruiz[23b], M. Garcia-Sciveres[18a], G.L. Gardner[131], R.W. Gardner[40], N. Garelli[164], R.B. Garg[149], J.M. Gargan[33], C.A. Garner[161], C.M. Garvey[34a], G. Evans[133a,133b], V. K. Gassmann[164], G. Gaudio[73a], V. Gautam[13], P. Gauzzi[75a,75b], J. Gavranovic[95], I.L. Gavrilenko[133a],

A. Gavrilyuk[38], C. Gay[170], G. Gaycken[126], E.N. Gazis[10], A. Gekow[122], C. Gemme[57b], M.H. Genest[60], A. D. Gentry[115], S. George[97], T. Geralis[46], A. A. Gerwin[123], P. Gessinger-Befurt[37], M.E. Geyik[177], M. Ghani[173], K. Ghorbanian[96], A. Ghosal[147], A. Ghosh[165], A. Ghosh[7], B. Giacobbe[24b], S. Giagu[75a,75b], T. Giani[117], A. Giannini[62], S.M. Gibson[97], M. Gignac[139], D.T. Gil[87b], A.K. Gilbert[87a], B.J. Gilbert[42], D. Gillberg[35], G. Gilles[117], D.M. Gingrich[2,t], M.P. Giordani[69a,69c], P.F. Giraud[138], G. Giugliarelli[69a,69c], D. Giugni[71a], F. Giuli[76a,76b], I. Gkialas[9,s], L.K. Gladilin[38], C. Glasman[101], M. Glazewska[20], R. M. Gleason[165], G. Glemža[48], M. Glisic[126], I. Gnesi[44b], Y. Go[30], M. Goblirsch-Kolb[37], B. Gocke[49], D. Godin[110], B. Gokturk[22a], S. Goldfarb[107], T. Golling[56], M.G.D. Gololo[34c], A. Golub[142], D. Golubkov[38], J.P. Gombas[109], G. Gomes Da Silva[147], A.J. Gomez Delegido[37], L. Gonella[21], A. Gongadze[155c], F. Gonnella[21], J.L. Gonski[149], R.Y. González Andana[52], S. González de la Hoz[169], M. V. Gonzalez Rodrigues[48], S. Gonzalez-Sevilla[56], R. Gonzalez Suarez[167], L. Goossens[37], B. Gorini[37], E. Gorini[70a,70b], A. Gorišek[95], T.C. Gosart[131], A.T. Goshaw[51], M.I. Gostkin[39], S. Goswami[124], C.A. Gottardo[37], S. A. Gotz[111], M. Gouighri[36b], A.G. Goussiou[142], N. Govender[34c], R. P. Grabarczyk[129], I. Grabowska-Bold[87a], K. Graham[35], E. Gramstad[128], S. Grancagnolo[70a,70b], C.M. Grant[1], P.M. Gravila[28f], F.G. Gravili[70a,70b], H.M. Gray[18a], M. Greco[112], M. J. Green[1], C. Grefe[25], A. S. Grefsrud[17], I.M. Gregor[48], R.R. Marcelo Gregorio[96], K.T. Greif[165], P. Grenier[149], S.G. Grewe[112], A.A. Grillo[139], K. Grimm[32], S. Grinstein[13,u], J.-F. Grivaz[66], E. Gross[175], J. Grosse-Knetter[55], L. Guan[108], G. Guerrieri[37], R. Guevara[128], R. Gugel[102], J.A.M. Guhit[108], A. Guida[19], E. Guilloton[173], S. Guindon[37], F. Guo[14,114c], J. Guo[144a], L. Guo[48], L. Guo[114b,v], Y. Guo[108], Y. Guo[42], A. Gupta[49], R. Gupta[132], S. Gupta[27], S. Gurbuz[25], S.S. Gurdasani[48], G. Gustavino[75a,75b], P. Gutierrez[123], L.F. Gutierrez Zagazeta[131], M. Gutsche[50], C. Gutschow[98], C. Gwenlan[129], C.B. Gwilliam[94], E.S. Haaland[128], A. Haas[120], M. Habedank[59], C. Haber[18a], H.K. Hadavand[8], A. Haddad[41], A. Hadef[50], A.I. Hagan[93], J. J. Hahn[147], E.H. Haines[98], M. Haleem[172], J. Haley[124], G.D. Hallewell[104], J.A. Hallford[48], K. Hamano[171], H. Hamdaoui[167], M. Hamer[25], S. E. D. Hammoud[66], E.J. Hampshire[97], J. Han[143a], L. Han[114a], L. Han[62], S. Han[14], K. Hanagaki[84], M. Hance[139], D.A. Hangal[42], H. Hanif[148], M.D. Hank[131], J.B. Hansen[43], P.H. Hansen[43], T. Harenberg[177], S. Harkusha[179], M.L. Harris[105], Y.T. Harris[25], J. Harrison[13], N.M. Harrison[122], P.F. Harrison[173], M. L. E. Hart[98], N.M. Hartman[112], R. Z. Hasan[97,137], Y. Hasegawa[146], F. Haslbeck[129], S. Hassan[17], R. Hauser[109], M. Haviernik[136], C.M. Hawkes[21], R.J. Hawkings[37], Y. Hayashi[159], D. Hayden[109], C. Hayes[108], R.L. Hayes[117], C.P. Hays[129], J.M. Hays[96], H.S. Hayward[94], M. He[14,114c], Y. He[48], Y. He[98], N.B. Heatley[96], V. Hedberg[100], J. Heilman[35], S. Heim[48], T. Heim[18a], J.J. Heinrich[126], L. Heinrich[112], J. Hejbal[134], M. Helbig[50], A. Held[176], S. Hellesund[17], C.M. Helling[170], S. Hellman[47a,47b], A.M. Henriques Correia[37], H. Herde[100], Y. Hernández Jiménez[151], L.M. Herrmann[25], T. Herrmann[50], G. Herten[54], R. Hertenberger[111], L. Hervas[37], M.E. Hesping[102], N.P. Hessey[162a], J. Hessler[112], M. Hidaoui[36b], N. Hidic[136], Y. Nakahama[84], E. Hill[161], T. S. Hillersoy[17], S.J. Hillier[21], J.R. Hinds[109], F. Hinterkeuser[25], M. Hirose[127], S. Hirose[163], D. Hirschbuehl[177], T.G. Hitchings[103],

B. Hiti[95], J. Hobbs[151], R. Hobincu[28e], A.M. Hodges[168], M.C. Hodgkinson[145], B.H. Hodkinson[129], A. Hoecker[37], D. D. Hofer[108], J. Hofer[169], J. Hofner[102], M. Holzbock[37], L.B.A.H. Hommels[33], V. Homsak[129], B.P. Honan[103], J. J. Hong[68], T.M. Hong[132], B.H. Hooberman[168], W.H. Hopkins[6], M. C. Hoppesch[168], Y. Horii[113], M. E. Horstmann[112], S. Hou[154], M. R. Housenga[168], J. Howarth[59], J. Hoya[6], M. Hrabovsky[125], T. Hryn'ova[4], P.J. Hsu[65], S.-C. Hsu[142], T. Hsu[66], M. Hu[18a], Q. Hu[62], S. Huang[33], X. Huang[14,114c], Y. Huang[136], Y. Huang[114b], Y. Huang[14], Z. Huang[66], Z. Hubacek[135], F. Huegging[25], T.B. Huffman[129], M. Hufnagel Maranha De Faria[83a], C. A. Hugli[48], M. Huhtinen[37], S.K. Huiberts[128], R. Hulsken[106], C. E. Hultquist[18a], D.L. Humphreys[105], N. Huseynov[12], J. Huston[109], B. Huth[37], J. Huth[61], L. Huth[48], R. Hyneman[7], G. Iacobucci[56], G. Iakovidis[30], L. Iconomidou-Fayard[66], J. P. Iddon[37], P. Iengo[72a,72b], Y. Iiyama[159], T. Iizawa[159], Y. Ikegami[84], D. Iliadis[158], N. Ilic[161], H. Imam[36a], G. Inacio Goncalves[83d], S. A. Infante Cabanas[140c], T. Ingebretsen Carlson[47a,47b], J. M. Inglis[96], G. Introzzi[73a,73b], M. Iodice[77a], V. Ippolito[75a,75b], R. K. Irwin[94], M. Ishino[159], W. Islam[176], C. Issever[19], S. Istin[22a,w], K. Itabashi[127], H. Ito[174], R. Iuppa[78a,78b], A. Ivina[175], V. Izzo[72a], P. Jacka[135], P. Jackson[1], P. Jain[48], K. Jakobs[54], T. Jakoubek[175], J. Jamieson[59], W. Jang[159], S. Jankovych[136], M. Javurkova[105], P. Jawahar[103], L. Jeanty[126], J. Jejelava[155a,x], P. Jenni[54,y], C.E. Jessiman[35], C. Jia[143a], H. Jia[170], J. Jia[151], X. Jia[112,114c], Z. Jia[114a], C. Jiang[52], Q. Jiang[64b], S. Jiggins[48], M. Jimenez Ortega[169], J. Jimenez Pena[13], S. Jin[114a], A. Jinaru[28b], O. Jinnouchi[141], P. Johansson[145], K.A. Johns[7], J.W. Johnson[139], F. A. Jolly[48], D.M. Jones[152], E. Jones[48], K.S. Jones[8], P. Jones[33], R.W.L. Jones[93], T.J. Jones[94], H.L. Joos[55], R. Joshi[122], J. Jovicevic[16], X. Ju[18a], J.J. Junggeburth[37], T. Junkermann[63a], A. Juste Rozas[13,u], M.K. Juzek[88], S. Kabana[140f], A. Kaczmarska[88], S. A. Kadir[149], M. Kado[112], H. Kagan[122], M. Kagan[149], A. Kahn[131], C. Kahra[102], T. Kaji[159], E. Kajomovitz[156], N. Kakati[175], N. Kakoty[13], I. Kalaitzidou[54], S. Kandel[8], N. Kanellos[10], N.J. Kang[139], D. Kar[34j,†], E. Karentzos[25], K. Karki[8], G. Martinovicova[136], O. Karkout[117], S.N. Karpov[39], Z.M. Karpova[39], V. Kartvelishvili[93,155b], A.N. Karyukhin[38], E. Kasimi[158], J. Katzy[48], S. Kaur[35], K. Kawade[146], M.P. Kawale[123], C. Kawamoto[89], T. Kawamoto[62], E.F. Kay[37], S. Kazakos[109], V.F. Kazanin[38], J.M. Keaveney[34a], R. Keeler[171], G.V. Kehris[61], J.S. Keller[35], J. M. Kelly[171], J.J. Kempster[152], O. Kepka[134], J. Kerr[162b], B.P. Kerridge[137], B.P. Kerševan[95], L. Keszeghova[29a], R. A. Khan[132], A. Khanov[124], A.G. Kharlamov[38], T. Kharlamova[38], E.E. Khoda[142], M. Kholodenko[133a], T.J. Khoo[19], G. Khoriauli[172], Y. Khoulaki[36a], Y.A.R. Khwaira[130], B. Kibirige[34j], D. Kim[6], D.W. Kim[18b], Y.K. Kim[40], N. Kimura[98], M.K. Kingston[55], A. Kirchhoff[55], C. Kirfel[25], F. Kirfel[25], J. Kirk[137], A.E. Kiryunin[112], S. Kita[163], O. Kivernyk[25], M. Klassen[164], C. Klein[35], L. Klein[172], M.H. Klein[45], S.B. Klein[56], U. Klein[94], A. Klimentov[30], T. Klioutchnikova[37], P. Kluit[117], S. Kluth[112], E. Kneringer[79], T.M. Knight[161], A. Knue[49], M. Kobel[50], D. Kobylianskii[175], S.F. Koch[129], M. Kocian[149], D.M. Koeck[126], P. Kodyš[136], K. Köneke[55], T. Koffas[35], O. Kolay[50], I. Koletsou[4], T. Komarek[88], A.X.Y. Kong[1], T. Kono[121], N. Konstantinidis[98], P. Kontaxakis[56], B. Konya[100], R. Kopeliansky[42], S. Koperny[87a], R. Koppenhofer[54], K. Korcyl[88], K. Kordas[158,z],

A. Korn[98], S. Korn[55], I. Korolkov[13], N. Korotkova[38], B. Kortman[117], O. Kortner[112], S. Kortner[112], W.H. Kostecka[118], M. Kostov[29a], V.V. Kostyukhin[147], A. Kotsokechagia[37], A. Kotwal[51], A. Koulouris[37], Y. Kulchitsky[39], A. Kourkoumeli-Charalampidi[73a,73b], C. Kourkoumelis[9], E. Kourlitis[112], O. Kovanda[126], R. Kowalewski[171], W. Kozanecki[126], A.S. Kozhin[38], V.A. Kramarenko[38], G. Kramberger[95], P. Kramer[25], M.W. Krasny[130], A. Krasznahorkay[105], A. C. Kraus[118], J.W. Kraus[177], J.A. Kremer[48], N. B. Krengel[147], T. Kresse[50], L. Kretschmann[177], J. Kretzschmar[94], P. Krieger[161], K. Krizka[21], K. Kroeninger[49], H. Kroha[112], J. Kroll[134], J. Kroll[131], K.S. Krowpman[109], U. Kruchonak[39], H. Krüger[25], N.M. Hartmann[111], N. Krumnack[81], M.C. Kruse[51], O. Kuchinskaia[39], S. Kuday[3a], S. Kuehn[37], T. Kuhl[48], V. Kukhtin[39], S. Kuleshov[140d,140b], J. Kull[1], E. V. Kumar[111], M. Kumar[34j], N. Kumari[48], P. Kumari[162b], A. Kupco[134], A. Kupich[38], O. Kuprash[54], H. Kurashige[86], L.L. Kurchaninov[162a], O. Kurdysh[4], A. Kurova[38], R. Kuesters[54], M. Kuze[141], A.K. Kvam[105], J. Kvita[125], N.G. Kyriacou[142], M. Laassiri[30], C. Lacasta[169], F. Lacava[75a,75b], H. Lacker[19], D. Lacour[130], N.N. Lad[98], E. Ladygin[39], A. Lafarge[41], B. Laforge[130], T. Lagouri[178], F.Z. Lahbabi[36a], S. Lai[55,37], W. S. Lai[98], I.K. Lakomiec[55], J.E. Lambert[171], S. Lammers[68], W. Lampl[7], C. Lampoudis[158,z], G. Lamprinoudis[172], A.N. Lancaster[118], E. Lançon[30], U. Landgraf[54], M.P.J. Landon[96], V.S. Lang[54], A.J. Lankford[165], F. Lanni[37], K. Lantzsch[25], A. Lanza[73a], M. Lanzac Berrocal[169], J.F. Laporte[138], T. Lari[71a], D. Larsen[17], L. Larson[11], F. Lasagni Manghi[24b], M. Lassnig[37], S.D. Lawlor[145], R. Lazaridou[165], M. Lazzaroni[71a,71b], E. T. T. Le[165], H. D. M. Le[109], E.M. Le Boulicaut[178], L.T. Le Pottier[18a], B. Leban[24b,24a], F. Ledroit-Guillon[60], T.F. Lee[162b], L.L. Leeuw[34c], M. Lefebvre[171], C. Leggett[18a], G. Lehmann Miotto[37], M. Leigh[56], W.A. Leight[105], W. Leinonen[116], A. Leisos[158,aa], C.E. Leitgeb[19], R. Leitner[136], K.J.C. Leney[45], T. Lenz[25], S. Leone[74a], C. Leonidopoulos[52], A. Leopold[150], J. LePage-Bourbonnais[35], R. Les[109], C.G. Lester[33], M. Levchenko[38], J. Levêque[4], L.J. Levinson[175], G. Levrini[24b,24a], M.P. Lewicki[88], C. Lewis[142], D.J. Lewis[4], L. Lewitt[145], A. Li[30], B. Li[143a], C. Li[108], C-Q. Li[112], H. Li[143a], H. Li[103], H. Li[15], H. Li[62], H. Li[143a], J. Li[144a], K. Li[14], L. Li[144a], R. Li[178], S. Li[14,114c], S. Li[144b,144a], T. Li[5], X. Li[106], Y. Li[14], Z. Li[159], Z. Li[14,114c], Z. Li[62], S. Liang[14,114c], Z. Liang[14], M. Liberatore[138], B. Liberti[76a], G. B. Libotte[83d], K. Lie[64c], J. Lieber Marin[83e], H. Lien[68], H. Lin[108], S. F. Lin[151], L. Linden[111], R.E. Lindley[7], J.H. Lindon[37], J. Ling[61], E. Lipeles[131], A. Lipniacka[17], M.A.L. Leite[83c], A. Lister[170], J.D. Little[68], B. Liu[14], B.X. Liu[114b], D. Liu[144b], D. Liu[139], E. H. L. Liu[21], J.K.K. Liu[120], K. Liu[144b], K. Liu[144b,144a], M. Liu[62], M.Y. Liu[62], P. Liu[14], Q. Liu[149], S. Liu[151], X. Liu[62], X. Liu[143a], Y. Liu[114b,114c], Y. Liu[168], Y.L. Liu[143a], Y.W. Liu[62], Z. Liu[66,ab], S.L. Lloyd[96], E.M. Lobodzinska[48], P. Loch[7], E. Lodhi[161], G. Löschcke Centeno[4], K. Lohwasser[145], E. Loiacono[48], J. D. Lomas[21], J.D. Long[42], I. Longarini[165], R. Longo[168], A. Lopez Solis[13], N.A. Lopez-canelas[7], N. Lorenzo Martinez[4], A.M. Lory[111], M. Losada[119a], X. Lou[47a,47b], X. Lou[14,114c], A. Lounis[66], P.A. Love[93], M. Lu[66], S. Lu[131], Y.J. Lu[154], H.J. Lubatti[142], C. Luci[75a,75b], F.L. Lucio Alves[114a], F. Luehring[68], B. S. Lunday[131], O. Lundberg[150], J. Lunde[37], N.A. Luongo[6], M.S. Lutz[37], A.B. Lux[26], D. Lynn[30], R. Lysak[134], V. Lysenko[135], E. Lytken[100],

JHEP04(2026)099

V. Lyubushkin[39], T. Lyubushkina[39], M.M. Lyukova[151], H. Ma[30], K. Ma[62], L.L. Ma[143a], W. Ma[62], Y. Ma[124], J.C. MacDonald[102], B. Maček[95], P.C. Machado De Abreu Farias[83e], D. Macina[37], R. Madar[41], T. Madula[98], J. Maeda[86], T. Maeno[30], P.T. Mafa[34c,ac], H. Maguire[145], M. Maheshwari[33], V. Maiboroda[66], A. Maio[133a,133b,133d], K. Maj[87a], O. Majersky[48], S. Majewski[126], R. Makhmanazarov[38], N. Makovec[66], V. Maksimovic[16], B. Malaescu[130], J. Malamant[128], Pa. Malecki[88], V.P. Maleev[38], F. Malek[60,ad], M. Mali[95], D. Malito[97], U. Mallik[80,†], A. Maloizel[5], S. Maltezos[10], A. Malvezzi Lopes[83d], S. Malyukov[39], J. Mamuzic[95], G. Mancini[53], M. N. Mancini[27], G. Manco[73a,73b], J.P. Mandalia[96], S.S. Mandarry[152], I. Mandić[95], L. Manhaes de Andrade Filho[83a], I.M. Maniatis[175], J. Manjarres Ramos[91], D.C. Mankad[175], A. Mann[111], T. Manoussos[37], M.N. Mantinan[40], S. Manzoni[37], L. Mao[144a], X. Mapekula[34c], A. Marantis[158], G. Marchiori[5], C. Marcon[71a], E. Maricic[16], M. Marinescu[48], S. Marium[48], M. Marjanovic[123], A. Markhoos[54], M. Markovitch[66], M. K. Maroun[105], M. C. Marr[148], G. T. Marsden[103], E.J. Marshall[93], Z. Marshall[18a], S. Marti-Garcia[169], J. Martin[98], T.A. Martin[137], V.J. Martin[52], B. Martin dit Latour[17], S. Martin-Haugh[137], L. Martinelli[75a,75b], P. Martinez Agullo[169], V.I. Martinez Outschoorn[105], P. Martinez Suarez[37], M. Martinez[13,u], V.S. Martoiu[28b], A.C. Martyniuk[98], A. Marzin[37], D. Mascione[78a,78b], L. Masetti[102], J. Masik[103], A.L. Maslennikov[39], S.L. Mason[42], P. Massarotti[72a,72b], P. Mastrandrea[74a,74b], A. Mastroberardino[44b,44a], T. Masubuchi[127], T.T. Mathew[126], G. Pinheiro Matos[42], J. Matousek[136], D.M. Mattern[49], K. Mauer[48], J. Maurer[28b], T. Maurin[59], A.J. Maury[66], C. Mavungu Tsava[104], D.A. Maximov[38], A. E. May[103], E. Mayer[41], R. Mazini[34j], I. Maznas[118], S.M. Mazza[139], E. Mazzeo[37], R.P. McGovern[131], J.P. Mc Gowan[171], S.P. Mc Kee[108], C.C. McCracken[170], E.F. McDonald[107], A.E. McDougall[117], L. F. Mcelhinney[93], J.A. Mcfayden[152], R.P. Mckenzie[34j], T.C. Mclachlan[48], D.J. Mclaughlin[98], C.A. Mc Lean[6], S.J. McMahon[137], C.M. Mcpartland[94], R.A. McPherson[171,n], S. Mehlhase[111], A. Mehta[94], D. Melini[169], B.R. Mellado Garcia[34j], A.H. Melo[55], F. Meloni[48], A.M. Mendes Jacques Da Costa[103], J.G. Saraiva[133a,133d], L. Meng[93], S. Menke[112], M. Mentink[37], E. Meoni[44b,44a], G. Mercado[118], S. Merianos[158], C. Merlassino[69a,69c], C. Meroni[71a,71b], J. Metcalfe[6], A.S. Mete[6], E. Meuser[102], C. Meyer[68], J-P. Meyer[138], Y. Miao[114a], R.P. Middleton[137], M. Mihovilovic[66], K. Petukhova[37], L. Mijović[52], G. Mikenberg[175], M. Mikestikova[134], M. Mikuž[95], H. Mildner[102], A. Milic[37], D.W. Miller[40], E. H. Miller[149], A. Milov[175], D.A. Milstead[47a,47b], T. Min[114a], A.A. Minaenko[38], I.A. Minashvili[155b], A.I. Mincer[120], B. Mindur[87a], M. Mineev[39], Y. Mino[89], L.M. Mir[13], M. Miralles Lopez[59], M. Mironova[18a], M. Missio[41], A. Mitra[173], V.A. Mitsou[169], Y. Mitsumori[113], O. Miu[161], P.S. Miyagawa[96], T. Mkrtchyan[37], M. Mlinarevic[98], T. Mlinarevic[98], M. Mlynarikova[136], L. Mlynarska[87a], C. Mo[144a], S. Mobius[20], M. H. Mohamed Farook[115], S. Mohapatra[42], S. Mohiuddin[124], G. Mokgatitswane[34j], L. Moleri[175], U. Molinatti[129], L.G. Mollier[20], B. Mondal[134], S. Mondal[135], K. Mönig[48], E. Monnier[104], L. Monsonis Romero[169], J. Montejo Berlingen[13], A. Montella[47a,47b], M. Montella[122], F. Montereali[77a,77b], F. Monticelli[92], S. Monzani[69a,69c], R. Gonçalo[133a], A. Morancho Tarda[43], N. Morange[66], A.L. Moreira De Carvalho[48], M. Moreno Llácer[169], C. Moreno Martinez[56], J.M. Moreno Perez[23b], P. Morettini[57b], S. Morgenstern[37], M. Morii[61], M. Morinaga[159],

M. Moritsu[90], F. Morodei[75a,75b], P. Moschovakos[37], B. Moser[54], M. Mosidze[155b], T. Moskalets[45], P. Moskvitina[116], J. Moss[32], P. Moszkowicz[87a], T. Motta Quirino[83d], A. Moussa[36d], Y. Moyal[175], H. Moyano Gomez[13], E.J.W. Moyse[105], T.G. Mroz[88], S. Muanza[104], M. Mucha[25], J. Mueller[132], G.A. Mullier[167], A.J. Mullin[33], J.J. Mullin[51], A.C. Mullins[45], A.E. Mulski[61], D.P. Mungo[161], D. Munoz Perez[169], F.J. Munoz Sanchez[103], W.J. Murray[173,137], M. Muškinja[95], C. Mwewa[48], A.G. Myagkov[38,p], A.J. Myers[8], G. Myers[108], M. Myska[135], B.P. Nachman[149], K. Nagai[129], K. Nagano[84], R. Nagasaka[159], J.L. Nagle[30,ae], E. Nagy[104], A.M. Nairz[37], K. Nakamura[84], K. Nakkalil[5], A. Nandi[63b], H. Nanjo[127], E.A. Narayanan[45], Y. Narukawa[159], I. Naryshkin[38], L. Nasella[71a,71b], S. Nasri[119b], C. Nass[25], G. Navarro[23a], A. Nayaz[19], P.Y. Nechaeva[38], S. Nechaeva[24b,24a], F. Nechansky[134], L. Nedic[129], T.J. Neep[21], A. Negri[73a,73b], M. Negrini[24b], C. Nellist[117], C. Nelson[106], K. Nelson[108], S. Nemecek[134], M. Nessi[37,af], M.S. Neubauer[168], J. Newell[94], P.R. Newman[21], Y.W.Y. Ng[168], B. Ngair[119a], H.D.N. Nguyen[110], J.D. Nichols[123], R.B. Nickerson[129], J. Nielsen[139], M. Niemeyer[55], J. Niermann[37], N. Nikiforou[37], V. Nikolaenko[38,p], R. Nicolaidou[138], I. Nikolic-Audit[130], P. Nilsson[30], I. Ninca[48], G. Ninio[157], A. Nisati[75a], R. Nisius[112], N. Nitika[175], E.K. Nkadimeng[34b], T. Nobe[159], D. Noll[149], T. Nommensen[153], M.B. Norfolk[145], B.J. Norman[35], L.C. Nosler[18a], M. Noury[36a], J. Novak[95], T. Novak[95], R. Novotny[135], L. Nozka[125], K. Ntekas[165], D. Ntounis[149], N.M.J. Nunes De Moura Junior[83b], A.P. O'Neill[20], J. Ocariz[130], I. Ochoa[133a], A. Odella Rodriguez[13], J.T. Offermann[40], A. Ogrodnik[88], A. Oh[103], C.C. Ohm[150], H. Oide[84], M.L. Ojeda[37], Y. Okumura[159], I. Oleksiyuk[56], G. Oliveira Correa[13], D. Oliveira Damazio[30], J.L. Oliver[1], R. Omar[68], Ö.O. Öncel[54], Y. Onoda[141], A. Onofre[133a,133e,ag], P.U.E. Onyisi[11], S. Oerdek[48,ah], M.J. Oreglia[40], D. Orestano[77a,77b], R. Orlandini[77a,77b], R.S. Orr[161], L.M. Osojnak[42], Y. Osumi[113], G. Otero y Garzón[31], H. Otono[90], M. Ouchrif[36d], F. Ould-Saada[128], T. Ovsiannikova[142], M. Owen[59], R.E. Owen[137], V.E. Ozcan[22a], F. Ozturk[88], N. Ozturk[8], S. Ozturk[82], H.A. Pacey[129], K. Pachal[162a], A. Pacheco Pages[13], C. Padilla Aranda[13], G. Padovano[75a,75b], S. Pagan Griso[18a], J. Pampel[25], J. Pan[178], D.K. Panchal[11], C.E. Pandini[60], J.G. Panduro Vazquez[137], H.D. Pandya[1], H. Pang[138], P. Pani[48], G. Panizzo[69a,69c], L. Panwar[130], L. Paolozzi[56], S. Parajuli[168], A. Paramonov[6], C. Paraskevopoulos[53], D. Paredes Hernandez[64b], S.R. Paredes Saenz[52], A. Pareti[73a,73b], K.R. Park[42], T.H. Park[112], F. Parodi[57b,57a], J.A. Parsons[42], U. Parzefall[54], B. Pascual Dias[41], L. Pascual Dominguez[101], E. Pasqualucci[75a], S. Passaggio[57b], F. Pastore[97], P. Patel[88], U.M. Patel[51], J.R. Pater[103], T. Pauly[37], F. Pauwels[136], C.I. Pazos[164], M. Pedersen[128], R. Pedro[133a], A.P. Pereira Peixoto[142], S.V. Peleganchuk[38], O. Penc[134], S. Peng[15], G. D. Penn[178], K.E. Penski[111], M. Penzin[38], B.C. Pinheiro Pereira[133a], L. Pereira Sanchez[149], D.V. Perepelitsa[30,ae], G. Perera[105], E. Perez Codina[37], M. Perganti[10], H. Pernegger[37], S. Perrella[75a,75b], K. Peters[48], R.F.Y. Peters[103], B.A. Petersen[37], T.C. Petersen[43], E. Petit[104], V. Petousis[135], A. R. Petri[71a,71b], C. Petridou[158,z], T. Petru[136], M. Pettee[18a], A. Petukhov[82], R. Pezoa[140g], L. Pezzotti[24b,24a], G. Pezzullo[178], L. Pfaffenbichler[37], A. J. Pfleger[79], T.M. Pham[176], T. Pham[107], P.W. Phillips[137], G. Piacquadio[151], E. Pianori[18a], F. Piazza[126], R. Piegaia[31], D. Pietreanu[28b], A.D. Pilkington[103], M. Pinamonti[69a,69c], J.L. Pinfold[2], J. Pinol Bel[13], A. E. Pinto Pinoargote[130], L. Pintucci[69a,69c], K. M. Piper[152], A. Pirttikoski[56], D.A. Pizzi[35], L. Pizzimento[64b], A. Plebani[33], M.-A. Pleier[30], V. Pleskot[136], E. Plotnikova[39], G. Poddar[96], L. Poggioli[130], S. Polacek[136], G. Polesello[73a], A. Poley[148], A. Polini[24b], C.S. Pollard[173], Z.B. Pollock[122], E. Pompa Pacchi[123], N. I. Pond[98], D. Ponomarenko[68], L. Pontecorvo[37], S. Popa[28a], G.A. Popeneciu[28d], A. Poreba[37], D.M. Portillo Quintero[162a], S. Pospisil[135], M. A. Postill[145], P. Postolache[28c], K. Potamianos[173], P.A. Potepa[87a], I.N. Potrap[39], C.J. Potter[33], R. Poettgen[100], H. Potti[153], J. Poveda[169], M.E. Pozo Astigarraga[37], R. Pozzi[37], A. Prades Ibanez[76a,76b], S.R. Pradhan[145], J. Pretel[171], D. Price[103], M. Primavera[70a], L. Primomo[69a,69c], M.A. Principe Martin[101], R. Privara[125], T. Procter[87b], M.L. Proffitt[142], N. Proklova[131], K. Prokofiev[64c], G. Proto[112], J. Proudfoot[6], M. Przybycien[87a], W.W. Przygoda[87b], A. Psallidas[46], J.E. Puddefoot[145], D. Pudzha[53], E. Egidio Purcino De Souza[83e], H. I. Purnell[1], D. Pyatiizbyantseva[116], J. Qian[108], R. Qian[109], Y. Qin[13], T. Qiu[52], A. Quadt[55], M. Queitsch-Maitland[103], G. Quetant[56], R.P. Quinn[170], G. Rabanal Bolanos[61], D. Rafanoharana[112], F. Raffaeli[76a,76b], F. Ragusa[71a,71b], J.L. Rainbolt[40], S. Rajagopalan[30], E. Ramakoti[39], L. Rambelli[57b,57a], I.A. Ramirez-Berend[35], K. Ran[108,114c], D. S. Rankin[131], N.P. Rapheeha[34j], H. Rasheed[28b], A. Rastogi[18a], S. Rave[102], S. Ravera[57b,57a], B. Ravina[37], I. Ravinovich[175], M. Raymond[37], A.L. Read[128], N.P. Readioff[145], D.M. Rebuzzi[73a,73b], A. S. Reed[59], K. Reeves[27], D. Reikher[37], A. Rej[49], C. Rembser[37], H. Ren[62], M. Renda[28b], F. Renner[48], A.G. Rennie[59], M. Repik[56], A.L. Rescia[57b,57a], S. Resconi[71a], M. Ressegotti[57b], S. Rettie[117], W.F. Rettie[35], M. M. Revering[33], E. Reynolds[18a], O.L. Rezanova[39], P. Reznicek[136], H. Riani[36d], N. Ribaric[51], B. Ricci[69a,69c], E. Ricci[78a,78b], R. Richter[112], S. Richter[47a,47b], E. Richter-Was[87b], M. Ridel[130], S. Ridouani[36d], P. Rieck[120], P. Riedler[37], E.M. Riefel[47a,47b], J. O. Rieger[117], M. Rijssenbeek[151], M. Rimoldi[37], L. Rinaldi[24b,24a], P. Rincke[167,55], G. Ripellino[167], I. Riu[13], J.C. Rivera Vergara[171], F. Rizatdinova[124], E. Rizvi[96], B.R. Roberts[18a], S.S. Roberts[139], D. Robinson[33], A. Robson[59], A. Rocchi[76a,76b], C. Roda[74a,74b], F.A. Rodriguez[118], S. Rodriguez Bosca[37], Y. Rodriguez Garcia[23a], A.M. Rodríguez Vera[118], S. Roe[37], J.T. Roemer[37], O. Røhne[128], R.A. Rojas[37], C.P.A. Roland[130], A. Romaniouk[79], E. Romano[73a,73b], M. Romano[24b], A.C. Romero Hernandez[168], N. Rompotis[94], L. Roos[130], S. Rosati[75a], B.J. Rosser[40], E. Rossi[129], E. Rossi[72a,72b], L.P. Rossi[61], L. Rossini[54], R. Rosten[122], M. Rotaru[28b], R. Roth[37], D. Rousseau[66], D. Rousso[48], S. Roy-Garand[161], A. Rozanov[104], Z. M. A. Rozario[59], Y. Rozen[156], A. Rubio Jimenez[169], V.H. Ruelas Rivera[19], T.A. Ruggeri[1], A. Ruggiero[129], A. Ruiz-Martinez[169], A. Rummler[37], G.B. Rupnik Boero[37], Z. Rurikova[54], N.A. Rusakovich[39], S. Ruscelli[49], H.L. Russell[171], G. Russo[75a,75b], J.P. Rutherfoord[7], S. Rutherford Colmenares[33], M. Rybar[136], P. Rybczynski[87a], A. Ryzhov[45], J.A. Sabater Iglesias[56], H.F-W. Sadrozinski[139], F. Safai Tehrani[75a], S. Saha[1], M. Sahinsoy[82], B. Sahoo[175], A. Saibel[169], B. T. Saifuddin[123], M. Saimpert[138], G.T. Saito[83c], M. Saito[159], T. Saito[159], A. Sala[71a,71b], A. Salnikov[149], J. Salt[169], A. Salvador Salas[157], F. Salvatore[152], A. Salzburger[37], D. Sammel[54], E. Sampson[93], D. Sampsonidis[158,z], D. Sampsonidou[126], M.A.A. Samy[59], J. Sánchez[169], V. Sanchez Sebastian[169], H. Sandaker[128], C.O. Sander[48], J.A. Sandesara[176], M. Sandhoff[177], C. Sandoval[23b], L. Sanfilippo[63a], D.P.C. Sankey[137], T. Sano[89], A. Sansoni[53], M. Santana Queiroz[18b], L. Santi[37], A.S. Cerqueira[83a], C. Santoni[41], H. Santos[133a,133b], A. Santra[175], E. Sanzani[24b,24a], K.A. Saoucha[85b], J. Sardain[7], A.M. Cooper-Sarkar[129], O. Sasaki[84], K. Sato[163], C. Sauer[37], E. Sauvan[4], P. Savard[161,t], R. Sawada[159], C. Sawyer[137], L. Sawyer[99], A. M. Sayed[27], C. Sbarra[24b], A. Sbrizzi[24b,24a], T. Scanlon[98], J. Schaarschmidt[142], U. Schäfer[102], A.C. Schaffer[66,45], D. Schaile[111], R.D. Schamberger[151], C. Scharf[19], M.M. Schefer[20], D. Scheirich[136], M. Schernau[140f], C. Scheulen[56], C. Schiavi[57b,57a], R. Brener[175], M. Schioppa[44b,44a], B. Schlag[149], S. Schlenker[37], J. Schmeing[177], E. Schmidt[112], M. A. Schmidt[177], K. Schmieden[25], C. Schmitt[102], N. Schmitt[102], S. Schmitt[48], N.A. Schneider[111], L. Schoeffel[138], A. Schoening[63b], P.G. Scholer[35], E. Schopf[147], M. Schott[25], S. Schramm[56], T. Schroer[56], H-C. Schultz-Coulon[63a], M. Schumacher[54], B.A. Schumm[139], Ph. Schune[138], H.R. Schwartz[7], A. Schwartzman[149], T.A. Schwarz[108], Ph. Schwemling[138], R. Schwienhorst[109], F.G. Sciacca[20], A. Sciandra[30], G. Sciolla[27], F. Scuri[74a], L.F. Oleiro Seabra[133a], C.D. Sebastiani[37], K. Sedlaczek[118], S.C. Seidel[115], A. Seiden[139], B.D. Seidlitz[42], C. Seitz[48], J.M. Seixas[83b], G. Sekhniaidze[72a], L. Selem[60], N. Semprini-Cesari[24b,24a], A. Semushin[179], D. Sengupta[56], V. Senthilkumar[169], L. Serin[66], M. Sessa[72a,72b], H. Severini[123], F. Sforza[57b,57a], A. Sfyrla[56], Q. Sha[14], H. Shaddix[118], A.H. Shah[33], R. Shaheen[150], J.D. Shahinian[131], M. Shamim[37], L.Y. Shan[14], M. Shapiro[18a], A. Sharma[37], A.S. Sharma[170], P. Sharma[30], P.B. Shatalov[38], K. Shaw[152], S.M. Shaw[103], G.A. Chelkov[39,p], Q. Shen[14], D.J. Sheppard[148], P. Sherwood[98], L. Shi[98], X. Shi[14], S. Shimizu[84], I.P.J. Shipsey[129,†], S. Shirabe[90], M. Shiyakova[39,ai], M.J. Shochet[40], D.R. Shope[128], B. Shrestha[123], S. Shrestha[122,aj], I. Shreyber[39], M.J. Shroff[171], P. Sicho[134], A.M. Sickles[168], E. Sideras Haddad[34j,166], A. C. Sidley[117], A. Sidoti[24b], F. Siegert[50], Dj. Sijacki[16], F. Sili[62], I. Silva Ferreira[83b], M.V. Silva Oliveira[30], S.B. Silverstein[47a], E. Furtado De Simas Filho[83e], S. Simion[66], R. Simoniello[37], E.L. Simpson[103], H. Simpson[152], L.R. Simpson[6], S. Simsek[82], S. Sindhu[55], P. Sinervo[161], S. N. Singh[27], S. Singh[30], S. Sinha[48], S. Sinha[103], M. Sioli[24b,24a], K. Sioulas[9], I. Siral[37], E. Sitnikova[48], J. Sjölin[47a,47b], A. Skaf[55], E. Skorda[21], P. Skubic[123], M. Slawinska[88], I. Slazyk[17], I. Sliusar[128], V. Smakhtin[175], B.H. Smart[137], S.Yu. Smirnov[140b], Y. Smirnov[82], L.N. Smirnova[38,p], O. Smirnova[100], A.C. Smith[42], D.R. Smith[165], J.L. Smith[103], M. B. Smith[35], R. Smith[149], H. Smitmanns[102], M. Smizanska[93], K. Smolek[135], P. Smolyanskiy[135], A.A. Snesarev[39], H.L. Snoek[117], S. Snyder[30], M.F. Mohd Soberi[52], R. Sobie[171,n], A. Soffer[157], C.A. Solans Sanchez[37], E.Yu. Soldatov[39], U. Soldevila[169], A.A. Solodkov[34j], S. Solomon[27], A. Soloshenko[39], K. Solovieva[54], O.V. Solovyanov[41], P. Sommer[50], A. Sonay[13], A. Sopczak[135], A.L. Sopio[52], F. Sopkova[29b], J. D. Sorenson[115], I.R. Sotarriva Alvarez[141], V. Sothilingam[63a], O. J. Soto Sandoval[140c,140b], B.S. Peralva[83d], S. Sottocornola[68], R. Soualah[85a], Z. Soumaimi[36e], M.J. Da Cunha Sargedas De Sousa[57b,57a], D. South[48], N. Soybelman[175], S. Spagnolo[70a,70b], M. Spalla[112], D. Sperlich[54], B. Spisso[72a,72b], D.P. Spiteri[59], L. Splendori[104], M. Spousta[136], E.J. Staats[35], R. Stamen[63a], E. Stanecka[88], W. Stanek-Maslouska[48], M.V. Stange[50], B. Stanislaus[18a], M.M. Stanitzki[48], E.A. Starchenko[38], G.H. Stark[139], J. Stark[91], P. Staroba[134], P. Starovoitov[85b],

R. Staszewski[88], C. Stauch[111], G. Stavropoulos[46], A. Stefl[37], A. Stein[102], P. Steinberg[30], B. Stelzer[148,162a], H.J. Stelzer[132], O. Stelzer[162a], H. Stenzel[58], T.J. Stevenson[152], G.A. Stewart[37], J.R. Stewart[124], G. Stoicea[28b], M. Stolarski[133a], S. Stonjek[112], A. Straessner[50], J. Strandberg[150], S. Strandberg[47a,47b], M. Stratmann[177], M. Strauss[123], T. Strebler[104], P. Strizenec[29b], R. Ströhmer[172], D.M. Strom[126], R. Stroynowski[45], A. Strubig[47a,47b], S.A. Stucci[30], B. Stugu[17], J. Stupak[123], N.A. Styles[48], D. Su[149], S. Su[62], X. Su[62], D. Suchy[29a], A. D. Sudhakar Ponnu[55], K. Sugizaki[131], V.V. Sulin[38], D.M.S. Sultan[129], L. Sultanaliyeva[25], S. Sultansoy[3b], S. Sun[176], W. Sun[14], N. Sur[100], M.R. Sutton[152], M. Svatos[134], P. N. Swallow[33], M. Swiatlowski[162a], A. Swoboda[37], I. Sykora[29a], M. Sykora[136], T. Sykora[136], D. Ta[102], K. Tackmann[48,ah], A. Taffard[165], R. Tafirout[162a], Y. Takubo[84], N. Hod[175], M. Talby[104], A.A. Talyshev[38], K.C. Tam[64b], N.M. Tamir[157], A. Tanaka[159], J. Tanaka[159], R. Tanaka[66], M. Tanasini[151], Z. Tao[170], S. Tapia Araya[140g], S. Tapprogge[102], A. Tarek Abouelfadl Mohamed[37], S. Tarem[156], K. Tariq[14], G. Tarna[37], G.F. Tartarelli[71a], M. J. Tartarin[91], P. Tas[136], M. Tasevsky[134], E. Tassi[44b,44a], A.C. Tate[168], Y. Tayalati[36e,ak], G.N. Taylor[107], W. Taylor[162b], R.J. Taylor Vara[169], A.S. Tegetmeier[91], P. Teixeira-Dias[97], J.J. Teoh[161], K. Terashi[159], J. Terron[101], S. Terzo[13], M. Testa[53], R.J. Teuscher[161,n], A. Thaler[79], O. Theiner[56], T. Theveneaux-Pelzer[104], D.W. Thomas[97], J.P. Thomas[21], E.A. Thompson[18a], P.D. Thompson[21], E. Thomson[131], R. E. Thornberry[45], C. Tian[62], Y. Tian[56], V. Tikhomirov[82], Yu.A. Tikhonov[39], S. Timoshenko[38], D. Timoshyn[136], E.X.L. Ting[1], P. Tipton[178], A. Tishelman-Charny[30], K. Todome[141], S. Todorova-Nova[136], L. Toffolin[69a,69c], M. Togawa[84], J. Tojo[90], S. Tokár[29a], O. Toldaiev[68], G. Tolkachev[104], M. Tomoto[84], L. Tompkins[149,al], E. Torrence[126], H. Torres[91], D. I. Torres Arza[140g], E. Torró Pastor[169], M. Toscani[31], C. Tosciri[40], M. Tost[11], D.R. Tovey[145], T. Trefzger[172], P.M. Tricarico[13], A. Tricoli[30], I.M. Trigger[162a], S. Trincaz-Duvoid[130], D.A. Trischuk[171], A. Tropina[39], D. Truncali[76a,76b], L. Truong[34c], M. Trzebinski[88], A. Trzupek[88], F. Tsai[151], M. Tsai[108], A. Tsiamis[158], P.V. Tsiareshka[39], S. Tsigaridas[162a], A. Tsirigotis[158,aa], V. Tsiskaridze[155a], E.G. Tskhadadze[155a], Y. Tsujikawa[89], I.I. Tsukerman[38], V. Tsulaia[18a], S. Tsuno[84], K. Tsuri[121], D. Tsybychev[151], Y. Tu[64b], A. Tudorache[28b], V. Tudorache[28b], S. B. Tuncay[129], S. Turchikhin[57b,57a], I. Turk Cakir[3a], R. Turra[71a], T. Turtuvshin[39,am], P.M. Tuts[42], S. Tzamarias[158,z], Y. Uematsu[84], F. Ukegawa[163], P.A. Ulloa Poblete[140c,140b], E.N. Umaka[30], G. Unal[37], A. Undrus[30], G. Unel[165], J. Urban[29b], P. Urrejola[140e], G. Usai[8], R. Ushioda[160], M. Usman[110], F. Ustuner[52], Z. Uysal[82], V. Vacek[135], B. Vachon[106], T. Vafeiadis[37], A. Vaitkus[98], C. Valderanis[111], E. Valdes Santurio[47a,47b], M. Valente[37], S. Valentinetti[24b,24a], A. Valero[169], E. Valiente Moreno[169], A. Vallier[91], J.A. Valls Ferrer[169], D. R. Van Arneman[117], E.R. Vandewall[149], A. Van Der Graaf[49], H. Z. Van Der Schyf[34j], P. Van Gemmeren[6], M. Van Rijnbach[37], S. Van Stroud[98], I. Van Vulpen[117], P. Vana[136], M. Vanadia[76a,76b], U. M. Vande Voorde[150], W. Vandelli[37], D. Vannicola[157], L. Vannoli[53], R. Vari[75a], M. Varma[178], E.W. Varnes[7], C. Varni[118], D. Varouchas[66], L. Varriale[169], K.E. Varvell[153], M.E. Vasile[28b], L. Vaslin[84], M. D. Vassilev[149], A. Vasyukov[39], L. M. Vaughan[124], R. Vavricka[136], T. Vazquez Schroeder[13], J. Veatch[32], V. Vecchio[103], M.J. Veen[105], I. Veliscek[30], I. Velkovska[95], L.M. Veloce[161], F. Veloso[133a,133c], A.G. Veltman[52], S. Veneziano[75a],

JHEP04(2026)099

A. Ventura[70a,70b], A. Verbytskyi[112], M. Verducci[74a,74b], C. Vergis[96], M. Verissimo De Araujo[83b], W. Verkerke[117], J.C. Vermeulen[117], C. Vernieri[149], M. Vessella[165], M.C. Vetterli[148,t], A. Vgenopoulos[102], N. Viaux Maira[140g,an], T. Vickey[145], O.E. Vickey Boeriu[145], G.H.A. Viehhauser[129], L. Vigani[63b], M. Vigl[112], M. Villa[24b,24a], M. Villaplana Perez[169], E.M. Villhauer[40], E. Vilucchi[53], M. Vincent[169], M.G. Vincter[35], A. Visibile[117], A. Visive[117], C. Vittori[37], I. Vivarelli[24b,24a], M.I. Vivas Albornoz[48], E. Voevodina[112], F. Vogel[111], J.C. Voigt[50], P. Vokac[135], Yu. Volkotrub[87b], L. Vomberg[25], E. Von Toerne[25], B. Vormwald[37], K. Vorobev[51], M. Vos[169], K. Voss[147], M. Vozak[37], L. Vozdecky[123], N. Vranjes[16], M. Vranjes Milosavljevic[16], M. Vreeswijk[117], N.K. Vu[144b,144a], R. Vuillermet[37], O. Vujinovic[102], I. Vukotic[40], I. K. Vyas[35], J.F. Wack[33], S. Wada[163], C. Wagner[149], J.M. Wagner[18a], W. Wagner[177], S. Wahdan[177], H. Wahlberg[92], C. H. Waits[123], J. Walder[137], R. Walker[111], K. Walkingshaw Pass[59], W. Walkowiak[147], A. Wall[131], E.J. Wallin[100], T. Wamorkar[18a], K. Wandall-Christensen[169], A. Wang[62], A.Z. Wang[139], C. Wang[102], C. Wang[11], H. Wang[18a], J. Wang[64c], P. Wang[103], P. Wang[98], R. Wang[61], R. Wang[6], S.M. Wang[154], S. Wang[14], T. Wang[116], T. Wang[62], W.T. Wang[129], W. Wang[14], X. Wang[168], X. Wang[144a], X. Wang[48], Y. Wang[151], Y. Wang[62], Z. Wang[108], Z. Wang[144b], Z. Wang[108], C. Wanotayaroj[84], A. Warburton[106], A.L. Warnerbring[147], S. Waterhouse[97], A.T. Watson[21], H. Watson[52], M.F. Watson[21], E. Watton[37], G. Watts[142], B.M. Waugh[98], J. M. Webb[54], C. Weber[30], H. A. Weber[19], M.S. Weber[20], S.M. Weber[63a], C. Wei[62], Y. Wei[54], A.R. Weidberg[129], E.J. Weik[120], J. Weingarten[49], C. Weiser[54], C.J. Wells[48], T. Wenaus[30], T. Wengler[37], N.S. Wenke[112], N. Wermes[25], M. Wessels[63a], A.M. Wharton[93], A.S. White[61], A. White[8], M.J. White[1], D. Whiteson[165], L. Wickremasinghe[127], W. Wiedenmann[176], M. Wielers[137], R. Wierda[150], C. Wiglesworth[43], H.G. Wilkens[37], J. J. H. Wilkinson[33], D.M. Williams[42], H.H. Williams[131], S. Williams[33], S. Willocq[105], B.J. Wilson[103], D.J. Wilson[103], P.J. Windischhofer[40], F.I. Winkel[31], F. Winklmeier[126], B.T. Winter[54], M. Wittgen[149], M. Wobisch[99], T. Wojtkowski[60], Z. Wolffs[117], J. Wollrath[37], M.W. Wolter[88], H. Wolters[133a,133c], M.C. Wong[139], E.L. Woodward[42], S.D. Worm[48], B.K. Wosiek[88], K.W. Woźniak[88], S. Wozniewski[55], K. Wraight[59], C. Wu[161], C. Wu[21], J. Wu[159], M. Wu[114b], M. Wu[116], S.L. Wu[176], S. Wu[14,ao], X. Wu[62], Y.Q. Wu[161], Y. Wu[62], Z. Wu[4], Z. Wu[114a], J. Wuerzinger[112], T.R. Wyatt[103], B.M. Wynne[52], S. Xella[43], L. Xia[114a], M. Xie[62], A. Xiong[126], D. Xu[14], H. Xu[62], L. Xu[62], R. Xu[131], T. Xu[108], Y. Xu[142], Z. Xu[52], R. Xue[132], B. Yabsley[153], S. Yacoob[34a], Y. Yamaguchi[84], E. Yamashita[159], H. Yamauchi[163], T. Yamazaki[18a], Y. Yamazaki[86], S. Yan[59], Z. Yan[105], H.J. Yang[144a,144b], H.T. Yang[62], S. Yang[62], T. Yang[64c], X. Yang[37], X. Yang[14], Y. Yang[159], Y. Yang[62], W-M. Yao[18a], C. L. Yardley[152], J. Ye[14], S. Ye[30], X. Ye[62], Y. Yeh[98], I. Yeletskikh[39], B. Yeo[18b], M.R. Yexley[98], T. P. Yildirim[129], H. Duran Yildiz[3a], K. Yorita[174], C.J.S. Young[37], C. Young[149], N.D. Young[126], Y. Yu[62], J. Yuan[14,114c,ao], M. Yuan[108], R. Yuan[144b], L. Yue[98], M. Zaazoua[62], B. Zabinski[88], I. Zahir[36a], A. Zaio[57b,57a], Z.K. Zak[88], T. Zakareishvili[169], S. Zambito[56], J.A. Zamora Saa[140d], J. Zang[159], R. Zanzottera[71a,71b], O. Zaplatilek[135], C. Zeitnitz[177], H. Zeng[14], D.T. Zenger Jr[27], O. Zenin[38], T. Ženiš[29a], S. Zenz[96], D. Zerwas[66], M. Zhai[14,114c], D.F. Zhang[145], G. Zhang[14,ao], J. Zhang[143a], J. Zhang[6], L. Zhang[62],

L. Zhang[114a], P. Zhang[14,114c], R. Zhang[114a], S. Zhang[91], T. Zhang[159], Y. Zhang[142], Y. Zhang[98], Y. Zhang[62], Y. Zhang[114a], Z. Zhang[18a], Z. Zhang[143a], Z. Zhang[66], H. Zhao[142], T. Zhao[143a], Y. Zhao[35], Z. Zhao[62], Z. Zhao[62], A. Zhemchugov[39], J. Zheng[114a], K. Zheng[168], X. Zheng[62], Z. Zheng[149], D. Zhong[168], B. Zhou[108], H. Zhou[7], N. Zhou[144a], Y. Zhou[15], Y. Zhou[114a], Y. Zhou[7], J. Zhu[108], X. Zhu[144b], Y. Zhu[144a], Y. Zhu[62], X. Zhuang[14], K. Zhukov[68], N.I. Zimine[39], J. Zinsser[63b], M. Ziolkowski[147], L. Živković[16], A. Zoccoli[24b,24a], K. Zoch[61], A. Zografos[37], T.G. Zorbas[145], O. Zormpa[46], L. Zwalinski[37]

[1] *Department of Physics, University of Adelaide, Adelaide, Australia*
[2] *Department of Physics, University of Alberta, Edmonton AB, Canada*
[3a] *Department of Physics, Ankara University, Ankara, Türkiye*
[3b] *Division of Physics, TOBB University of Economics and Technology, Ankara, Türkiye*
[4] *LAPP, Université Savoie Mont Blanc, CNRS/IN2P3, Annecy, France*
[5] *APC, Université Paris Cité, CNRS/IN2P3, Paris, France*
[6] *High Energy Physics Division, Argonne National Laboratory, Argonne IL, U.S.A.*
[7] *Department of Physics, University of Arizona, Tucson AZ, U.S.A.*
[8] *Department of Physics, University of Texas at Arlington, Arlington TX, U.S.A.*
[9] *Physics Department, National and Kapodistrian University of Athens, Athens, Greece*
[10] *Physics Department, National Technical University of Athens, Zografou, Greece*
[11] *Department of Physics, University of Texas at Austin, Austin TX, U.S.A.*
[12] *Institute of Physics, Azerbaijan Academy of Sciences, Baku, Azerbaijan*
[13] *Institut de Física d'Altes Energies (IFAE), Barcelona Institute of Science and Technology, Barcelona, Spain*
[14] *Institute of High Energy Physics, Chinese Academy of Sciences, Beijing, China*
[15] *Physics Department, Tsinghua University, Beijing, China*
[16] *Institute of Physics, University of Belgrade, Belgrade, Serbia*
[17] *Department for Physics and Technology, University of Bergen, Bergen, Norway*
[18a] *Physics Division, Lawrence Berkeley National Laboratory, Berkeley CA, U.S.A.*
[18b] *University of California, Berkeley CA, U.S.A.*
[19] *Institut für Physik, Humboldt Universität zu Berlin, Berlin, Germany*
[20] *Albert Einstein Center for Fundamental Physics and Laboratory for High Energy Physics, University of Bern, Bern, Switzerland*
[21] *School of Physics and Astronomy, University of Birmingham, Birmingham, U.K.*
[22a] *Department of Physics, Bogazici University, Istanbul, Türkiye*
[22b] *Department of Physics Engineering, Gaziantep University, Gaziantep, Türkiye*
[22c] *Department of Physics, Istanbul University, Istanbul, Türkiye*
[23a] *Facultad de Ciencias y Centro de Investigaciónes, Universidad Antonio Nariño, Bogotá, Colombia*
[23b] *Departamento de Física, Universidad Nacional de Colombia, Bogotá, Colombia*
[24a] *Dipartimento di Fisica e Astronomia A. Righi, Università di Bologna, Bologna, Italy*
[24b] *INFN Sezione di Bologna, Italy*
[25] *Physikalisches Institut, Universität Bonn, Bonn, Germany*
[26] *Department of Physics, Boston University, Boston MA, U.S.A.*
[27] *Department of Physics, Brandeis University, Waltham MA, U.S.A.*
[28a] *Transilvania University of Brasov, Brasov, Romania*
[28b] *Horia Hulubei National Institute of Physics and Nuclear Engineering, Bucharest, Romania*
[28c] *Department of Physics, Alexandru Ioan Cuza University of Iasi, Iasi, Romania*
[28d] *National Institute for Research and Development of Isotopic and Molecular Technologies, Physics Department, Cluj-Napoca, Romania*
[28e] *National University of Science and Technology Politechnica, Bucharest, Romania*
[28f] *West University in Timisoara, Timisoara, Romania*
[28g] *Faculty of Physics, University of Bucharest, Bucharest, Romania*

JHEP04(2026)099

[29a] *Faculty of Mathematics, Physics and Informatics, Comenius University, Bratislava, Slovak Republic*
[29b] *Department of Subnuclear Physics, Institute of Experimental Physics of the Slovak Academy of Sciences, Kosice, Slovak Republic*
[30] *Physics Department, Brookhaven National Laboratory, Upton NY, U.S.A.*
[31] *Universidad de Buenos Aires, Facultad de Ciencias Exactas y Naturales, Departamento de Física, y CONICET, Instituto de Física de Buenos Aires (IFIBA), Buenos Aires, Argentina*
[32] *California State University, CA, U.S.A.*
[33] *Cavendish Laboratory, University of Cambridge, Cambridge, U.K.*
[34a] *Department of Physics, University of Cape Town, Cape Town, South Africa*
[34b] *iThemba Labs, Western Cape, South Africa*
[34c] *Department of Mechanical Engineering Science, University of Johannesburg, Johannesburg, South Africa*
[34d] *National Institute of Physics, University of the Philippines Diliman (Philippines), Philippines*
[34e] *Department of Physics, Stellenbosch University, Matieland, South Africa*
[34f] *University of KwaZulu-Natal, School of Agriculture and Science, Mathematics, Westville, South Africa*
[34g] *University of South Africa, Department of Physics, Pretoria, South Africa*
[34h] *University of Pretoria, Department of Mechanical and Aeronautical Engineering, Pretoria, South Africa*
[34i] *University of Zululand, KwaDlangezwa, South Africa*
[34j] *School of Physics, University of the Witwatersrand, Johannesburg, South Africa*
[35] *Department of Physics, Carleton University, Ottawa ON, Canada*
[36a] *Faculté des Sciences Ain Chock, Université Hassan II de Casablanca, Morocco*
[36b] *Faculté des Sciences, Université Ibn-Tofail, Kénitra, Morocco*
[36c] *Faculté des Sciences Semlalia, Université Cadi Ayyad, LPHEA-Marrakech, Morocco*
[36d] *LPMR, Faculté des Sciences, Université Mohamed Premier, Oujda, Morocco*
[36e] *Faculté des sciences, Université Mohammed V, Rabat, Morocco*
[36f] *Institute of Applied Physics, Mohammed VI Polytechnic University, Ben Guerir, Morocco*
[37] *CERN, Geneva, Switzerland*
[38] *Affiliated with an institute formerly covered by a cooperation agreement with CERN*
[39] *Affiliated with an international laboratory covered by a cooperation agreement with CERN*
[40] *Enrico Fermi Institute, University of Chicago, Chicago IL, U.S.A.*
[41] *LPC, Université Clermont Auvergne, CNRS/IN2P3, Clermont-Ferrand, France*
[42] *Nevis Laboratory, Columbia University, Irvington NY, U.S.A.*
[43] *Niels Bohr Institute, University of Copenhagen, Copenhagen, Denmark*
[44a] *Dipartimento di Fisica, Università della Calabria, Rende, Italy*
[44b] *INFN Gruppo Collegato di Cosenza, Laboratori Nazionali di Frascati, Italy*
[45] *Physics Department, Southern Methodist University, Dallas TX, U.S.A.*
[46] *National Centre for Scientific Research "Demokritos", Agia Paraskevi, Greece*
[47a] *Department of Physics, Stockholm University, Sweden*
[47b] *Oskar Klein Centre, Stockholm, Sweden*
[48] *Deutsches Elektronen-Synchrotron DESY, Hamburg and Zeuthen, Germany*
[49] *Fakultät Physik, Technische Universität Dortmund, Dortmund, Germany*
[50] *Institut für Kern- und Teilchenphysik, Technische Universität Dresden, Dresden, Germany*
[51] *Department of Physics, Duke University, Durham NC, U.S.A.*
[52] *SUPA — School of Physics and Astronomy, University of Edinburgh, Edinburgh, U.K.*
[53] *INFN e Laboratori Nazionali di Frascati, Frascati, Italy*
[54] *Physikalisches Institut, Albert-Ludwigs-Universität Freiburg, Freiburg, Germany*
[55] *II. Physikalisches Institut, Georg-August-Universität Göttingen, Göttingen, Germany*
[56] *Département de Physique Nucléaire et Corpusculaire, Université de Genève, Genève, Switzerland*
[57a] *Dipartimento di Fisica, Università di Genova, Genova, Italy*
[57b] *INFN Sezione di Genova, Italy*
[58] *II. Physikalisches Institut, Justus-Liebig-Universität Giessen, Giessen, Germany*
[59] *SUPA — School of Physics and Astronomy, University of Glasgow, Glasgow, U.K.*
[60] *LPSC, Université Grenoble Alpes, CNRS/IN2P3, Grenoble INP, Grenoble, France*
[61] *Laboratory for Particle Physics and Cosmology, Harvard University, Cambridge MA, U.S.A.*

JHEP04(2026)099

[62] *Department of Modern Physics and State Key Laboratory of Particle Detection and Electronics, University of Science and Technology of China, Hefei, China*
[63a] *Kirchhoff-Institut für Physik, Ruprecht-Karls-Universität Heidelberg, Heidelberg, Germany*
[63b] *Physikalisches Institut, Ruprecht-Karls-Universität Heidelberg, Heidelberg, Germany*
[64a] *Department of Physics, Chinese University of Hong Kong, Shatin, N.T., Hong Kong, China*
[64b] *Department of Physics, University of Hong Kong, Hong Kong, China*
[64c] *Department of Physics and Institute for Advanced Study, Hong Kong University of Science and Technology, Clear Water Bay, Kowloon, Hong Kong, China*
[65] *Department of Physics, National Tsing Hua University, Hsinchu, Taiwan*
[66] *IJCLab, Université Paris-Saclay, CNRS/IN2P3, 91405, Orsay, France*
[67] *Centro Nacional de Microelectrónica (IMB-CNM-CSIC), Barcelona, Spain*
[68] *Department of Physics, Indiana University, Bloomington IN, U.S.A.*
[69a] *INFN Gruppo Collegato di Udine, Sezione di Trieste, Udine, Italy*
[69b] *ICTP, Trieste, Italy*
[69c] *Dipartimento Politecnico di Ingegneria e Architettura, Università di Udine, Udine, Italy*
[70a] *INFN Sezione di Lecce, Italy*
[70b] *Dipartimento di Matematica e Fisica, Università del Salento, Lecce, Italy*
[71a] *INFN Sezione di Milano, Italy*
[71b] *Dipartimento di Fisica, Università di Milano, Milano, Italy*
[72a] *INFN Sezione di Napoli, Italy*
[72b] *Dipartimento di Fisica, Università di Napoli, Napoli, Italy*
[73a] *INFN Sezione di Pavia, Italy*
[73b] *Dipartimento di Fisica, Università di Pavia, Pavia, Italy*
[74a] *INFN Sezione di Pisa, Italy*
[74b] *Dipartimento di Fisica E. Fermi, Università di Pisa, Pisa, Italy*
[75a] *INFN Sezione di Roma, Italy*
[75b] *Dipartimento di Fisica, Sapienza Università di Roma, Roma, Italy*
[76a] *INFN Sezione di Roma Tor Vergata, Italy*
[76b] *Dipartimento di Fisica, Università di Roma Tor Vergata, Roma, Italy*
[77a] *INFN Sezione di Roma Tre, Italy*
[77b] *Dipartimento di Matematica e Fisica, Università Roma Tre, Roma, Italy*
[78a] *INFN-TIFPA, Italy*
[78b] *Università degli Studi di Trento, Trento, Italy*
[79] *Universität Innsbruck, Department of Astro and Particle Physics, Innsbruck, Austria*
[80] *University of Iowa, Iowa City IA, U.S.A.*
[81] *Department of Physics and Astronomy, Iowa State University, Ames IA, U.S.A.*
[82] *Istinye University, Sariyer, Istanbul, Türkiye*
[83a] *Departamento de Engenharia Elétrica, Universidade Federal de Juiz de Fora (UFJF), Juiz de Fora, Brazil*
[83b] *Universidade Federal do Rio De Janeiro COPPE/EE/IF, Rio de Janeiro, Brazil*
[83c] *Instituto de Física, Universidade de São Paulo, São Paulo, Brazil*
[83d] *Rio de Janeiro State University, Rio de Janeiro, Brazil*
[83e] *Federal University of Bahia, Bahia, Brazil*
[84] *KEK, High Energy Accelerator Research Organization, Tsukuba, Japan*
[85a] *Khalifa University of Science and Technology, Abu Dhabi, United Arab Emirates*
[85b] *University of Sharjah, Sharjah, United Arab Emirates*
[86] *Graduate School of Science, Kobe University, Kobe, Japan*
[87a] *AGH University of Krakow, Faculty of Physics and Applied Computer Science, Krakow, Poland*
[87b] *Marian Smoluchowski Institute of Physics, Jagiellonian University, Krakow, Poland*
[88] *Institute of Nuclear Physics Polish Academy of Sciences, Krakow, Poland*
[89] *Faculty of Science, Kyoto University, Kyoto, Japan*
[90] *Research Center for Advanced Particle Physics and Department of Physics, Kyushu University, Fukuoka, Japan*
[91] *L2IT, Université de Toulouse, CNRS/IN2P3, UPS, Toulouse, France*

JHEP04(2026)099

[92] *Instituto de Física La Plata, Universidad Nacional de La Plata and CONICET, La Plata, Argentina*
[93] *Physics Department, Lancaster University, Lancaster, U.K.*
[94] *Oliver Lodge Laboratory, University of Liverpool, Liverpool, U.K.*
[95] *Department of Experimental Particle Physics, Jožef Stefan Institute and Department of Physics, University of Ljubljana, Ljubljana, Slovenia*
[96] *Department of Physics and Astronomy, Queen Mary University of London, London, U.K.*
[97] *Department of Physics, Royal Holloway University of London, Egham, U.K.*
[98] *Department of Physics and Astronomy, University College London, London, U.K.*
[99] *Louisiana Tech University, Ruston LA, U.S.A.*
[100] *Fysiska institutionen, Lunds universitet, Lund, Sweden*
[101] *Departamento de Física Teorica C-15 and CIAFF, Universidad Autónoma de Madrid, Madrid, Spain*
[102] *Institut für Physik, Universität Mainz, Mainz, Germany*
[103] *School of Physics and Astronomy, University of Manchester, Manchester, U.K.*
[104] *CPPM, Aix-Marseille Université, CNRS/IN2P3, Marseille, France*
[105] *Department of Physics, University of Massachusetts, Amherst MA, U.S.A.*
[106] *Department of Physics, McGill University, Montreal QC, Canada*
[107] *School of Physics, University of Melbourne, Victoria, Australia*
[108] *Department of Physics, University of Michigan, Ann Arbor MI, U.S.A.*
[109] *Department of Physics and Astronomy, Michigan State University, East Lansing MI, U.S.A.*
[110] *Group of Particle Physics, University of Montreal, Montreal QC, Canada*
[111] *Fakultät für Physik, Ludwig-Maximilians-Universität München, München, Germany*
[112] *Max-Planck-Institut für Physik (Werner-Heisenberg-Institut), München, Germany*
[113] *Graduate School of Science and Kobayashi-Maskawa Institute, Nagoya University, Nagoya, Japan*
[114a] *Department of Physics, Nanjing University, Nanjing, China*
[114b] *School of Science, Shenzhen Campus of Sun Yat-sen University, China*
[114c] *University of Chinese Academy of Science (UCAS), Beijing, China*
[115] *Department of Physics and Astronomy, University of New Mexico, Albuquerque NM, U.S.A.*
[116] *Institute for Mathematics, Astrophysics and Particle Physics, Radboud University/Nikhef, Nijmegen, Netherlands*
[117] *Nikhef National Institute for Subatomic Physics and University of Amsterdam, Amsterdam, Netherlands*
[118] *Department of Physics, Northern Illinois University, DeKalb IL, U.S.A.*
[119a] *New York University Abu Dhabi, Abu Dhabi, United Arab Emirates*
[119b] *United Arab Emirates University, Al Ain, United Arab Emirates*
[120] *Department of Physics, New York University, New York NY, U.S.A.*
[121] *Ochanomizu University, Otsuka, Bunkyo-ku, Tokyo, Japan*
[122] *Ohio State University, Columbus OH, U.S.A.*
[123] *Homer L. Dodge Department of Physics and Astronomy, University of Oklahoma, Norman OK, U.S.A.*
[124] *Department of Physics, Oklahoma State University, Stillwater OK, U.S.A.*
[125] *Palacký University, Joint Laboratory of Optics, Olomouc, Czech Republic*
[126] *Institute for Fundamental Science, University of Oregon, Eugene, OR, U.S.A.*
[127] *Graduate School of Science, University of Osaka, Osaka, Japan*
[128] *Department of Physics, University of Oslo, Oslo, Norway*
[129] *Department of Physics, Oxford University, Oxford, U.K.*
[130] *LPNHE, Sorbonne Université, Université Paris Cité, CNRS/IN2P3, Paris, France*
[131] *Department of Physics, University of Pennsylvania, Philadelphia PA, U.S.A.*
[132] *Department of Physics and Astronomy, University of Pittsburgh, Pittsburgh PA, U.S.A.*
[133a] *Laboratório de Instrumentação e Física Experimental de Partículas — LIP, Lisboa, Portugal*
[133b] *Departamento de Física, Faculdade de Ciências, Universidade de Lisboa, Lisboa, Portugal*
[133c] *Departamento de Física, Universidade de Coimbra, Coimbra, Portugal*
[133d] *Centro de Física Nuclear da Universidade de Lisboa, Lisboa, Portugal*
[133e] *Departamento de Física, Escola de Ciências, Universidade do Minho, Braga, Portugal*
[133f] *Departamento de Física Teórica y del Cosmos, Universidad de Granada, Granada (Spain), Spain*
[133g] *Departamento de Física, Instituto Superior Técnico, Universidade de Lisboa, Lisboa, Portugal*

JHEP04(2026)099

[134] *Institute of Physics of the Czech Academy of Sciences, Prague, Czech Republic*
[135] *Czech Technical University in Prague, Prague, Czech Republic*
[136] *Charles University, Faculty of Mathematics and Physics, Prague, Czech Republic*
[137] *Particle Physics Department, Rutherford Appleton Laboratory, Didcot, U.K.*
[138] *IRFU, CEA, Université Paris-Saclay, Gif-sur-Yvette, France*
[139] *Santa Cruz Institute for Particle Physics, University of California Santa Cruz, Santa Cruz CA, U.S.A.*
[140a] *Departamento de Física, Pontificia Universidad Católica de Chile, Santiago, Chile*
[140b] *Millennium Institute for Subatomic physics at high energy frontier (SAPHIR), Santiago, Chile*
[140c] *Instituto de Investigación Multidisciplinario en Ciencia y Tecnología, y Departamento de Física, Universidad de La Serena, Chile*
[140d] *Universidad Andres Bello, Department of Physics, Santiago, Chile*
[140e] *Universidad San Sebastian, Recoleta, Chile*
[140f] *Instituto de Alta Investigación, Universidad de Tarapacá, Arica, Chile*
[140g] *Departamento de Física, Universidad Técnica Federico Santa María, Valparaíso, Chile*
[141] *Department of Physics, Institute of Science, Tokyo, Japan*
[142] *Department of Physics, University of Washington, Seattle WA, U.S.A.*
[143a] *Institute of Frontier and Interdisciplinary Science and Key Laboratory of Particle Physics and Particle Irradiation (MOE), Shandong University, Qingdao, China*
[143b] *School of Physics, Zhengzhou University, China*
[144a] *State Key Laboratory of Dark Matter Physics, School of Physics and Astronomy, Shanghai Jiao Tong University, Key Laboratory for Particle Astrophysics and Cosmology (MOE), SKLPPC, Shanghai, China*
[144b] *State Key Laboratory of Dark Matter Physics, Tsung-Dao Lee Institute, Shanghai Jiao Tong University, Shanghai, China*
[145] *Department of Physics and Astronomy, University of Sheffield, Sheffield, U.K.*
[146] *Department of Physics, Shinshu University, Nagano, Japan*
[147] *Department Physik, Universität Siegen, Siegen, Germany*
[148] *Department of Physics, Simon Fraser University, Burnaby BC, Canada*
[149] *SLAC National Accelerator Laboratory, Stanford CA, U.S.A.*
[150] *Department of Physics, Royal Institute of Technology, Stockholm, Sweden*
[151] *Departments of Physics and Astronomy, Stony Brook University, Stony Brook NY, U.S.A.*
[152] *Department of Physics and Astronomy, University of Sussex, Brighton, U.K.*
[153] *School of Physics, University of Sydney, Sydney, Australia*
[154] *Institute of Physics, Academia Sinica, Taipei, Taiwan*
[155a] *E. Andronikashvili Institute of Physics, Iv. Javakhishvili Tbilisi State University, Tbilisi, Georgia*
[155b] *High Energy Physics Institute, Tbilisi State University, Tbilisi, Georgia*
[155c] *University of Georgia, Tbilisi, Georgia*
[156] *Department of Physics, Technion, Israel Institute of Technology, Haifa, Israel*
[157] *Raymond and Beverly Sackler School of Physics and Astronomy, Tel Aviv University, Tel Aviv, Israel*
[158] *Department of Physics, Aristotle University of Thessaloniki, Thessaloniki, Greece*
[159] *International Center for Elementary Particle Physics and Department of Physics, University of Tokyo, Tokyo, Japan*
[160] *Graduate School of Science and Technology, Tokyo Metropolitan University, Tokyo, Japan*
[161] *Department of Physics, University of Toronto, Toronto ON, Canada*
[162a] *TRIUMF, Vancouver BC, Canada*
[162b] *Department of Physics and Astronomy, York University, Toronto ON, Canada*
[163] *Division of Physics and Tomonaga Center for the History of the Universe, Faculty of Pure and Applied Sciences, University of Tsukuba, Tsukuba, Japan*
[164] *Department of Physics and Astronomy, Tufts University, Medford MA, U.S.A.*
[165] *Department of Physics and Astronomy, University of California Irvine, Irvine CA, U.S.A.*
[166] *University of West Attica, Athens, Greece*
[167] *Department of Physics and Astronomy, University of Uppsala, Uppsala, Sweden*
[168] *Department of Physics, University of Illinois, Urbana IL, U.S.A.*
[169] *Instituto de Física Corpuscular (IFIC), Centro Mixto Universidad de Valencia — CSIC, Valencia, Spain*

JHEP04(2026)099

[170] Department of Physics, University of British Columbia, Vancouver BC, Canada
[171] Department of Physics and Astronomy, University of Victoria, Victoria BC, Canada
[172] Fakultät für Physik und Astronomie, Julius-Maximilians-Universität Würzburg, Würzburg, Germany
[173] Department of Physics, University of Warwick, Coventry, U.K.
[174] Waseda University, Tokyo, Japan
[175] Department of Particle Physics and Astrophysics, Weizmann Institute of Science, Rehovot, Israel
[176] Department of Physics, University of Wisconsin, Madison WI, U.S.A.
[177] Fakultät für Mathematik und Naturwissenschaften, Fachgruppe Physik, Bergische Universität Wuppertal, Wuppertal, Germany
[178] Department of Physics, Yale University, New Haven CT, U.S.A.
[179] Yerevan Physics Institute, Yerevan, Armenia

[a] Also at Department of Physics, King's College London, London, U.K.
[b] Also at Institute of Physics, Azerbaijan Academy of Sciences, Baku, Azerbaijan
[c] Also at Imam Mohammad Ibn Saud Islamic University, Saudi Arabia
[d] Also at Department of Physics, University of Thessaly, Greece
[e] Also at An-Najah National University, Nablus, Palestine
[f] Also at Department of Physics, University of Fribourg, Fribourg, Switzerland
[g] Also at Department of Physics, Westmont College, Santa Barbara, U.S.A.
[h] Also at Departament de Fisica de la Universitat Autonoma de Barcelona, Barcelona, Spain
[i] Also at Borough of Manhattan Community College, City University of New York, New York NY, U.S.A.
[j] Also at University of Siena, Italy
[k] Also at The Collaborative Innovation Center of Quantum Matter (CICQM), Beijing, China
[l] Also at Faculty of Physics, Sofia University, 'St. Kliment Ohridski', Sofia, Bulgaria
[m] Also at Università di Napoli Parthenope, Napoli, Italy
[n] Also at Institute of Particle Physics (IPP), Canada
[o] Also at Department of Physics, Bolu Abant Izzet Baysal University, Bolu, Türkiye
[p] Also at Affiliated with an institute formerly covered by a cooperation agreement with CERN
[q] Also at Faculty of Physics, University of Bucharest, Romania
[r] Also at National Institute of Physics, University of the Philippines Diliman (Philippines), Philippines
[s] Also at Department of Financial and Management Engineering, University of the Aegean, Chios, Greece
[t] Also at TRIUMF, Vancouver BC, Canada
[u] Also at Institucio Catalana de Recerca i Estudis Avancats, ICREA, Barcelona, Spain
[v] Also at Henan University, China
[w] Also at Yeditepe University, Physics Department, Istanbul, Türkiye
[x] Also at Institute of Theoretical Physics, Ilia State University, Tbilisi, Georgia
[y] Also at CERN, Geneva, Switzerland
[z] Also at Center for Interdisciplinary Research and Innovation (CIRI-AUTH), Thessaloniki, Greece
[aa] Also at Hellenic Open University, Patras, Greece
[ab] Also at Department of Modern Physics and State Key Laboratory of Particle Detection and Electronics, University of Science and Technology of China, Hefei, China
[ac] Also at Department of Mathematical Sciences, University of South Africa, Johannesburg, South Africa
[ad] Also at Department of Physics, Stellenbosch University, South Africa
[ae] Also at University of Colorado Boulder, Department of Physics, Colorado, U.S.A.
[af] Also at Département de Physique Nucléaire et Corpusculaire, Université de Genève, Genève, Switzerland
[ag] Also at Centre of Physics of the Universities of Minho and Porto (CF-UM-UP), Portugal
[ah] Also at Institut für Experimentalphysik, Universität Hamburg, Hamburg, Germany
[ai] Also at Institute for Nuclear Research and Nuclear Energy (INRNE) of the Bulgarian Academy of Sciences, Sofia, Bulgaria
[aj] Also at Washington College, Chestertown, MD, U.S.A.
[ak] Also at Institute of Applied Physics, Mohammed VI Polytechnic University, Ben Guerir, Morocco
[al] Also at Department of Physics, Stanford University, Stanford CA, U.S.A.
[am] Also at Institute of Physics and Technology, Mongolian Academy of Sciences, Ulaanbaatar, Mongolia

JHEP04(2026)099

[an] *Also at Millennium Institute for Subatomic physics at high energy frontier (SAPHIR), Santiago, Chile*
[ao] *Also at University of Chinese Academy of Sciences (UCAS), Beijing, China*
[†] *Deceased*